

2013-05-06

Mechanobiology of the Intervertebral Disc: Influences of Static and Dynamic Compressions on Energy Metabolism

Chong Wang

University of Miami, c.wang14@umiami.edu

Follow this and additional works at: https://scholarlyrepository.miami.edu/oa_dissertations

Recommended Citation

Wang, Chong, "Mechanobiology of the Intervertebral Disc: Influences of Static and Dynamic Compressions on Energy Metabolism" (2013). *Open Access Dissertations*. 1003.

https://scholarlyrepository.miami.edu/oa_dissertations/1003

This Open access is brought to you for free and open access by the Electronic Theses and Dissertations at Scholarly Repository. It has been accepted for inclusion in Open Access Dissertations by an authorized administrator of Scholarly Repository. For more information, please contact repository.library@miami.edu.

UNIVERSITY OF MIAMI

MECHANOBIOLOGY OF THE INTERVERTEBRAL DISC: INFLUENCES OF
STATIC AND DYNAMIC COMPRESSIONS ON ENERGY METABOLISM

By

Chong Wang

A DISSERTATION

Submitted to the Faculty
of the University of Miami
in partial fulfillment of the requirements for
the degree of Doctor of Philosophy

Coral Gables, Florida

May 2013

©2013

Chong Wang

All Rights Reserved

UNIVERSITY OF MIAMI

A dissertation submitted in partial fulfillment of
the requirements for the degree of
Doctor of Philosophy

MECHANOBIOLOGY OF THE INTERVERTEBRAL DISC: INFLUENCES OF
STATIC AND DYNAMIC COMPRESSIONS ON ENERGY METABOLISM

Chong Wang

Approved:

Charles Chun-Yuh Huang, Ph.D.
Assistant Professor of Biomedical
Engineering

M. Brian Blake, Ph.D.
Dean of the Graduate School

Weiyong Gu, Ph.D.
Professor, Chair of Mechanical
Engineering

Herman S. Cheung, Ph.D.
Professor of Biomedical
Engineering

Alicia R. Jackson, Ph.D.
Assistant Professor of Biomedical
Engineering

Howard B. Levene, M.D., Ph.D.
Assistant Professor of Clinical
Neurological Surgery

WANG, CHONG
Mechanobiology of the Intervertebral Disc:
Influences of Static and Dynamic Compressions
on Energy Metabolism

(Ph.D., Biomedical Engineering)
(May 2013)

Abstract of a dissertation at the University of Miami.
Dissertation supervised by Assistant Professor Charles Chun-Yuh Huang
No. of pages in text. (116)

Low back pain (LBP) is the leading reason for people to miss work and chief complaint of 5% people who visit doctors. Although it has a high impact in society, the causes of LBP cannot always be clarified. However, intervertebral disc (IVD) degeneration has been reported to be a possible leading source for LBP. Since IVD is the biggest avascular tissue in human body, nutrition supply plays very important role for IVD degeneration. IVDs are under mechanical load all the time *in vivo*, it is also been revealed by *in vitro* studies that mechanical loadings can alter cellular activities including metabolism. However, how mechanical loadings affect IVD metabolism has not been elucidated yet. Therefore, the purpose of this dissertation is to study the energy metabolism of IVD under compressive loadings.

A bioreactor system was built to apply static and dynamic mechanical loadings to IVD. A pump was utilized to maintain culture medium circulation during tissue culture and loading experiments; a load cell and a data acquisition device were also included in the system to record loading forces.

Adenosine-5'-triphosphate (ATP) is the "energy currency" of cell activities and extracellular ATP is an important molecule which can mediate various physiological activities by activating series of receptors. Therefore it is essential to detect

extracellular ATP contents. However, existing techniques have their drawbacks and are not ideal for *in vivo/in situ* measurement. We thus developed an optical biosensor for *in situ* measurement of extracellular ATP measurement in biological tissues. This ATP sensor utilized the technique of sol-gel coating and two layers of coatings were applied to the end of optical fibers; the first layer contained Ruthenium complex which can be excited by blue light with 465 nm of wavelength and emit red light with wavelength at 610 nm; the second layer contains two enzymes: glycerol kinase and glycerol 3-phosphate which can oxidase ATP and consume oxygen. During measurement, ATP molecules diffuse into the second layer and are oxidized thus decrease local oxygen concentration; this decrease of oxygen is detected by the first layer and is recorded by NeoFox® software; the signal detected has a linear relationship with the ATP content. This ATP sensor has a broad range of measurement at 10^{-3} mM to 1.5 mM. A compensation method was established to enable the measurement of ATP contents at different environmental oxygen concentrations. We also demonstrated that the performance of this sensor was not affected by environmental pH and derivatives of ATP such as adenosine diphosphate (ADP) and adenosine monophosphate (AMP) or adenosine.

From static and dynamic compression experiments of porcine IVDs it was found that under both static and dynamic compressive compressions, pH decreased and the contents of lactate and ATP increased significantly in both annulus fibrosus (AF) and nucleus pulposus (NP) regions, suggesting that compressive loading can promote ATP production via glycolysis and reduce pH by increasing lactate accumulation. We also detected high level of extracellular ATP contents in the NP region and compressive loadings significantly decrease extracellular ATP contents. Since ATP

can be utilized as intracellular energy currency and regulate a variety of extracellular activities through the purinergic signaling pathway, the findings of this dissertation suggest that compression mediated ATP metabolism could be a novel mechanobiological pathway for regulating IVD metabolism.

ACKNOWLEDGEMENTS

There are so many people I would like to give my sincere appreciation to for their guidance, help, and assistance over the years. Without them, I would never have achieved this milestone.

Firstly I am grateful to Dr. Charles Chun-Yuh Huang, my supervisor, who guided me not just academically, but personally as well. You provided me with all kinds of great advice and support, confidence, and encouragement. The experience of working in your lab was invaluable.

I must also thank my other committee members: Dr. Weiyong Gu, Dr. Herman S. Cheung, Dr. Howard Levene, and Dr. Alicia Jackson. I appreciate your time and consideration. It was my honor to have you on my committee board! Another special person I would like to thank is my supervisor back at the University of Sydney, Dr. Qing Li, who led me into the field of research. I would also like to thank Dr. Wei-Chiang Lin from Florida International University who helped us a great deal with building the optical system.

To my other Stem Cell and Mechanobiology lab members, I would like to thank you for making my research life here at Miami a fantastic journey! Many thanks to Lauren Vernon for always being helpful when I was composing manuscripts and hosting all those phenomenal parties; to Silvia Daniela Gonzales for joking around and all those snacks from Tawantinsuyu; to Hanan Fernando, Jessica Czamanski, and Taiyi Yuan for teaching me lab skills; and to many other students for their help and assistance, including Amaris Genemaras, Jason Wang, Byron Hsu, Mike Helbig, Kristen Khoury, Chris Scanlon, and Sebastian Verne.

I would like to thank the following Tissue Biomechanics Lab members, Francesco and Alicia, for their help. Thanks to my friends in Miami: Feiran Zhong, Ye Zhou Spector, Shawn Spector and Oa Chilong Spector, Shunling Cui, Hong Wang, Bob Bo Zhang, Zhetong Chen, Peng Jin, Linwei Xu, Kay Lopate and Joel Lopate.

Work and study are circles under the big circle of life. Family is another circle that is even more important. My highest regards to my parents, for they are wonderful parents and without them I could not have become what I am now. Nobody is perfect, but they are perfect parents to me. Special thanks to my Aunt Li, you are my model for all these years and provided guidance. Thanks to my maternal grandma, you are a role model for the family. Thanks to my maternal uncle, you never left us! I thank my lovely cousin Qing Ren for all the happy memories we had since we were little kids; my maternal uncle who is always in our memory; my cute cousin Andy for playing piano for me; Uncle Yao for helping me on many issues. Thanks to my aunts for taking care of me! Thanks to my friend Ying Zhang, you are like my family all these years.

I salute my lovely wife, Zhizhen Chen. Thank you for being with me, supporting me, and encouraging me when I am down. In China, we say family is your harbor where you can rest your body and soul, so thank you for building a harmonious harbor for me. I dedicate this to you.

This is for those I love and those who love me.

[ACKNOWLEDGEMENT IN MY NATIVE LANGUAGE]

致谢

人生旅程中有很多的关口，完成博士学位无疑是其中重要的一个。一路走来一路酸甜苦辣，等了好久终于等到今天。此刻我想对很多人表达我的谢意。

首先我想对我的导师黄俊裕博士表达我最真挚的谢意!你不只是在学术上指导我，你润物细无声的为人处世也使我受益匪浅。在我攻读博士期间你的建议和支持都是我人生的宝贵财富。非常荣幸能有机会在你的实验室工作并成为你的第一个博士生。

对于我博士答辩委员会的其他成员：顾老师，Dr. Cheung, Dr. Levene 和 Dr. Jackson,非常感谢你们的指导与宝贵时间。很荣幸能有你们在我的博士论文委员会中。借此机会我还想感谢我在悉尼大学的导师李青博士。是你引导我进入研究领域。你对待学生如春风化雨，从你身上所学到的使我一生受用。

感谢干细胞与力学生物学实验室的其他成员：劳伦（Lauren），帮我修改我的文章还有你家的所有精彩派对。感谢丹尼尔娜（Daniela），开各种玩笑还有来自印加帝国的零食。谢谢汉娜（Hanan），洁西卡（Jessica）和袁台逸，在我进实验室初期教我各种实验技能。感谢组织生物力学实验室的成员：弗朗西斯科（Francesco）和艾丽西亚（Alicia）。感谢我在迈阿密的朋友们：衷斐然，周业和肖恩.斯佩克特（Shawn）夫妻还有他们可爱的儿子奥阿.赤龙.斯佩克特

(Oa Chilong Spector)，崔顺玲，汪泓，鲍勃.张波，陈哲通，金鹏，许林蔚，还有凯宜和乔伊夫妻（Kay Lopate and Joel Lopate）。

工作学习都只是生活这个大圈里的环节。在生活这个大圈里，家庭是没有那么起眼但重要性犹有过之的一环。我有幸拥有一个良好的家庭环境。非常感谢我的父母，这么多年一直支持我。虽然你们都不是完美的人，但对我来说你们就是最好最完美的父母。感谢我的小姨，多年来你都是我的人生榜样，从我呱呱坠地起人生的各个阶段都有你的指导。感谢我的外婆，你是中国女性正面形象的完美代表，是我们大家庭的模范。我亲爱的舅舅，你不曾远离我们！感谢我的表妹任劼，我们从孩提时代起的无数美好回忆是我人生的宝贵财富。感谢我可爱的表弟姚安迪，为我们弹奏动听的乐曲。感谢姚叔叔，多年来给我各种各样的帮助和指点。谢谢我的舅妈和三姨，在我人生的不同时期给予我关怀。感谢小猫，多年好友，亲如家人。

感谢我的妻子陈智珍，对我的默默支持，在我低谷的时候给我鼓励。家庭是人生的港湾，感谢你为我营造了一个温馨的港湾，积蓄在人生风浪中搏杀的力量。

谨以此献给所有我爱和爱我的人们。

TABLE OF CONTENTS

LIST OF FIGURES	IX
LIST OF TABLES	XIII
LIST OF EQUATIONS	XIV
CHAPTER 1: INTRODUCTION AND SPECIFIC AIMS	1
1.1 INTRODUCTION	1
1.2 SPECIFIC AIMS	2
1.3 CONTENT OF THIS DISSERTATION	3
1.4 SIGNIFICANCE OF THIS STUDY	4
CHAPTER 2: BACKGROUND	6
2.1 STRUCTURE OF IVD TISSUE	6
2.2 CELL TYPES IN DIFFERENT IVD REGIONS	10
2.3 NUTRITION SUPPLY AND IVD DEGENERATION	15
2.4 ENERGY METABOLISM OF IVD.....	21
2.5 EFFECTS OF MECHANICAL LOADING ON IVD CELLS.....	25
2.6 EXTRACELLULAR ATP.....	26
CHAPTER 3 BIOREACTOR	28
3.1 PRINCIPLES OF BIOREACTOR	28
3.2 VERIFYING THE BIOREACTOR SYSTEM.....	29
3.2.1 Swelling and preload.....	29
3.2.2 Verifying displacement-controlled dynamic loading.....	33
CHAPTER 4 OPTICAL BIOSENSORS	36
4.1 INTRODUCTORY REMARKS.....	36
4.2 EXPERIMENTS	38
4.2.1 Materials	38
4.2.2 Fabrication of ATP optical sensor	38
4.2.3 Calibration test of the ATP sensor	41

4.2.4	Examination of the effects of pH on the ATP biosensor	44
4.2.7	In situ measurement of extracellular ATP in porcine intervertebral disc	47
4.3	RESULTS	48
4.3.1	Calibration test of the ATP biosensor	48
4.3.2	The effects of ADP, AMP, adenosine, ascorbate and pH on the ATP biosensor	51
4.3.3	Compensation of the ATP biosensor under different oxygen levels	52
4.3.4	Sensor stability	52
4.3.5	Measurement of extracellular ATP in porcine intervertebral disc	58
4.4	DISCUSSION	60
4.5	OTHER OPTICAL SENSORS	62
CHAPTER 5 ENERGY METABOLISM OF IVD UNDER COMPRESSIONS.		66
5.1	INTRODUCTORY REMARKS	66
5.2	MATERIALS AND METHODS	68
5.3	RESULTS	72
5.3.1	Effects of static compression	72
5.3.2	Effects of dynamic compression	77
5.3.3	Comparison between AF and NP regions	77
5.3.4	Extracellular ATP content in the NP region	77
5.4	DISCUSSION	84
5.5	OTHER MEASUREMENTS	93
CHAPTER 6 CONCLUSION AND RECOMMENDATIONS		96
6.1	SUMMARY AND CONCLUDING REMARKS	96
6.1.1	Optical fiber based ATP sensor	97
6.1.2	Effects of static and dynamic compressions on IVD energy metabolism ...	98
6.2	RECOMMENDATION FOR FUTURE STUDIES	99
REFERENCES		102

LIST OF FIGURES

Figure 2-1: Anatomy of the Intervertebral Disc.....	7
Figure 2-2: Scanning electron microscopy of cartilage endplate from A) 30 years old and B) 80 years old human beings (Benneker, Heini et al. 2005).	9
Figure 2-3: Cross-section view of a porcine lumbar disc. Three distinct regions can be seen from the Figure: Annulus Fibrosis (AF), Nucleus Pulposus (NP) and Transition Zone (TZ).	12
Figure 2-4: AF cells from 6-month old porcine lumbar disc.....	13
Figure 2-5: 6-month old porcine lumbar disc NP cells.....	14
Figure 2-6: Sagittal views of human IVDs. Left: healthy from 20-30 year-old disc. Right: degenerated from 50-60 year-old disc (Adams, Stefanakis et al. 2010).	19
Figure 2-7: Different stages of human lumbar region disc degeneration obtained with Magnetic Resonance Images (MRI) (A) Shows a healthy disc with distinct NP and AF regions; (B) A disc in early stage of degeneration with slightly decreased disc height and reduced signal density of NP region. * indicates AF bulging inward. (C) A severe degenerated disc showing largely decreased height, * indicates large cleft (Smith, Nerurkar et al. 2011).	20
Figure 2-8: Schematic representation of ATP production in cells (Siegel 1999).....	22
Figure 2-9: Simplified flow of glycolysis (Lodish 2013).	23
Figure 3-1: Bioreactor system.....	30
Figure 3-2: Bioreactor in incubator.....	31
Figure 3-3: Bioreactor chamber with lid closed (up) and open (down).....	32
Figure 3-4: Schematic diagram of displacement-controlled dynamic loading.	34

Figure 3-5: 10 seconds of loading force-time recorded for 1 Hz dynamic compression.....	35
Figure 4-1: Cross sectional view of the ATP sensor	42
Figure 4-2: Mechanism of optical biosensor system.	45
Figure 4-3: (a) A typical decay time curve of the ATP sensor in response to the ATP concentrations of 50, 100, 200, and 300 μM and (b) the corresponding calibration curve (mean values \pm standard deviation).	49
Figure 4-4: (a) A typical sensor response at low ATP levels (1, 5, 10 and 20 μM) and (b) a representative calibration curve showing a linear relationship between the inverse of decay time and the ATP concentration up to 1.5 mM.	50
Figure 4-5: The typical reaction of the ATP sensor to ADP, AMP and adenosine of 200 μM compared to ATP of 100 μM	53
Figure 4-6: Normalized signal of the ATP sensor in response to 100 μM ATP at different pH conditions (n=3). The data were normalized to the response at pH 7.5 and are expressed as mean values \pm standard deviation.	54
Figure 4-7: (a) Typical calibration curves obtained at different oxygen concentration and (b) the corresponding linear relationship between the parameter k and oxygen concentration.....	55
Figure 4-8: Accuracy of the oxygen compensation method on determination of ATP concentration at 15% oxygen level using the parameters obtained from the calibration tests at 10% and 20% oxygen levels (n=3). The data were normalized to the corresponding ATP concentration and expressed as mean values \pm standard deviation.	56

Figure 4-9: Stability of the ATP biosensor. The signal strength of florescence is defined as the difference between the inverse of decay times measured at 0 and 200 μ M ATP. The data are expressed as mean values \pm standard deviation.	57
Figure 4-10: Typical responses of the oxygen and ATP sensors during the extracellular ATP measurement in the porcine intervertebral disc.	59
Figure 4-11: A typical response of glucose sensor to 0.05, 0.1, 0.15and 0.2 g/L glucose solutions.	64
Figure 4-12: A typical calibration curve of a glucose optical sensor.	65
Figure 5-1: Bioreactor system for whole disc loading experiments	70
Figure 5-2: Harvest locations of AF and NP from IVD	71
Figure 5-3: Actual harvest locations of IVD and porcine IVD dimension	71
Figure 5-4: Cell viability stain of AF (up) and NP (down) tissues. Green indicates live cells while red indicated dead cells.	73
Figure 5-5: Effects of static loadings on lactate content (n=6), *: significantly different from the control group (p<0.05);	74
Figure 5-6: Effects of static loadings on pH value (n=8), *: significantly different from the control group (p<0.05).	75
Figure 5-7: Effects of static loadings on total ATP content (n=8). *: significantly different from the control group (p<0.05); #: significantly different from the other groups (p<0.05).	76
Figure 5-8: Effects of dynamic loadings on lactate accumulation (n=6). Static compression represents as 0 Hz. *: significantly different from the control group (p<0.05); #: significantly different from the other groups (p<0.05).	78

Figure 5-9: Effects of dynamic loadings on total ATP (n=8). Static compression represents as 0 Hz. *: significantly different from the control group (p<0.05); #: significantly different from the other groups (p<0.05); & significant difference between two groups (p<0.05).79

Figure 5-10: Effects of dynamic loadings on pH value (n=8). *: significantly different from the control group (p<0.05).80

Figure 5-11: Comparison of pH between the AF and NP regions (n=7). *: significantly different from the control group (p<0.05).....81

Figure 5-12: Comparison of total ATP content between the AF and NP regions (n=8). *: significantly different from the control group (p<0.05).82

Figure 5-13: Effects of static and dynamic compression on extracellular ATP content in the NP regions (n=5). *: significantly different from the control group (p<0.05); # significant difference between two groups (p<0.05).83

Figure 5-14: Oxygen profiles measured in the IVD using a needle type optical oxygen sensor.....94

Figure 5-15: Glucose contents of AF and NP under low glucose DMEM culture.95

LIST OF TABLES

Table 2-1: Human IVD composition summarized from literature (Hendry 1958; Kraemer, Kolditz et al. 1985; Panagiotacopulos, Pope et al. 1987; Eyre 1989; Johnstone, Urban et al. 1992; Pearce 1993; Gu, Mao et al. 1999). Other matrix proteins are also found in IVDs in small amount and thus not listed here. 11

LIST OF EQUATIONS

Equation 1: Glycolysis Equation	24
Equation 2: Enzymatic Reaction 1	38
Equation 3: Enzymatic Reaction 2	38
Equation 4: Stern-Volmer equation.....	41
Equation 5: Relationship between oxygen concentration and ATP concentration.....	41
Equation 6: Ruthenium quenching in the presence of ATP	43
Equation 7: Relationship between ATP concentration and decay time.....	43
Equation 8: Relationship between k and oxygen level	46

CHAPTER 1: INTRODUCTION AND SPECIFIC AIMS

1.1 INTRODUCTION

There are many reasons for people to miss work. One of the leading contributors is low back pain (LBP), which is believed to affect 80% of the population at some point during their lifetime (Borenstein, Calin et al. 2012). Suffering from back pain is the chief complaint of 5% of people who visit the doctor in the US (2008). The total medical cost related to low back pain in the US exceeds 100 billion dollars every year (Willis 2009).

There are many factors that may cause LBP; such as spine stenosis, spinal lesions, and disc herniation. Doctors diagnose LBP through patients' histories, imaging studies and physical tests. The equipment often employed in modern diagnosis of LBP includes discography, magnetic resonance imaging (MRI), computerized tomography (CT), x-ray imaging, bone scintigraphy (bone scanning) and electrodiagnostic assessments (such as needle electromyography, nerve conduction, electromyography (EMG) and evoked potential (EP) studies) as auxiliary methods of detecting LBP. The diagnosis and treatment technologies have been extensively developed over time. However, the cause of LBP is still unclear (Deyo 1998). Other non-disc sources such as sacroiliac joints or hip joints may also mimic back pain. Doctors must also be aware of other diseases such as Parkinson's disease or Vitamin D deficiency (rickets) that can also mimic back pain.

While the exact cause of LBP remains unclear, recent studies revealed that intervertebral disc (IVD) degeneration is closely related to LBP (Luoma, Riihimaki et al. 2000; Roberts 2003). Although aging, nutrition supply, mechanical factors and

many other aspects contribute to disc degeneration, the mechanism of degeneration is not yet determined (Hadjipavlou, Tzermiadianos et al. 2008; Kandel, Roberts et al. 2008; Adams, Dolan et al. 2009).

IVD is the largest avascular tissue in human body and undergoes repeated static and dynamic loading. The structure and local mechanical environment of IVDs create energy pathways that rely on diffusion of small solutes from peripheral and vertebral blood vessels and convection (Urban, Holm et al. 1982) which are affected by many factors such as endplate calcification (Grunhagen, Shirazi-Adl et al. 2011). Nutrition supply is essential for cell activity and maintaining tissue integrity; therefore, it is important for IVD degeneration studies and regenerative methods development to elucidate the energy metabolism of IVDs under mechanical loading.

1.2 SPECIFIC AIMS

The following are the hypotheses of this study:

1. Mechanical loading affects energy metabolism of IVD;
2. Annulus fibrosus (AF) and nucleus pulposus (NP) tissues exhibit different energy metabolism.

To test these hypotheses, the following are the specific aims of this project.

Aim 1: To design and build a novel bioreactor system for whole IVD disc culture in order to perform static and dynamic compression studies.

Custom designed chambers will be fabricated, with a dialysis pump for disc culture. A bioreactor system will be built which is able to perform both static and dynamic (sinusoidal) compression experiments. Omega® load cell will be used to monitor load. Different frequencies of dynamic compression will be performed.

Aim 2: To develop novel optical sensors to detect glucose and ATP contents.

Blue LED light source, spectrometer and oxygen partial pressure monitoring software from Ocean Optics® will be used. Novel coating layers containing specific enzymes will be developed for detecting glucose and ATP contents.

Aim 3: To investigate the effects of static and dynamic compressions on energy metabolism of IVD.

In the static compression experiment, 10% strain will be applied to the IVD for 1 hour and 2 hours. In the dynamic compression experiment, IVD will be subjected to sinusoidal compressive strain of 15% at 0.1 and 1 Hz. After compression experiments, pH and the contents of ATP, glucose, lactate, and nitric oxide in AF and NP regions will be determined.

1.3 CONTENT OF THIS DISSERTATION

The overall objective of this dissertation is to investigate the energy metabolism of IVD under static and dynamic compressions, in order to better understand the mechanism of disc degeneration and its relation with low back pain. To achieve this goal, a bioreactor system with a step motor and a moving piece to perform static and dynamic compressive loads which was attached with a culture medium circulation system and was attached to a loading recording system was built to perform compressive mechanical loadings, both static and dynamic. A fiber optic based ATP sensor was fabricated using sol-gel entrapped enzyme technique for extracellular ATP measurement. Static and dynamic compression experiments were performed on porcine IVDs and the effects of compression on energy metabolism of two anatomical regions in the IVD were analyzed.

In Chapter 3, a custom-made bioreactor system is described. This system can perform controllable static and dynamic compressive loadings. A culture medium

circulation system consisting of a pump and a reservoir was attached to this bioreactor system for maintaining viability of IVD during experiments by circulating culture medium. A data acquisition device and a load cell were used to read and record the force response of IVD during compression experiments.

In Chapter 4, a novel optical fiber based ATP sensor is presented. This sensor utilizes the sol-gel entrapped enzyme technique, detecting ATP contents in target solutions or tissues by measuring local oxygen concentration change caused by enzymatic oxidization of ATP.

In Chapter 5, the changes of pH, lactate accumulation, total ATP content and extracellular ATP concentration in the IVD caused by static and dynamic loadings are illustrated. The difference of above measurements between AF and NP regions are also presented.

Chapter 6 is the peroration of this dissertation and recommendation of future works.

1.4 SIGNIFICANCE OF THIS STUDY

Low back pain in the US is the leading cause of lost working ability. Low back pain and related ailments cost more than \$ 100 billion in the US every year (2008; Borenstein, Calin et al. 2012). Although the real causes remain to be elucidated, low back pain is closely associated with disc degeneration.

Due to the avascular nature of the IVD, nutrients are delivered via diffusion and convection over a long distance through the dense extracellular matrix to the cells. Poor nutrient supply has been considered a potential mechanism for disc degeneration (Urban and Roberts 2003; Urban, Smith et al. 2004; Stephan, Johnson et al. 2011). IVD cells consume glucose and oxygen to produce energy (i.e., ATP) which is essential for ECM biosynthesis pivotal for maintaining ECM integrity and preventing

disc degeneration (Hay 1991; Silva and Mooney 2004). Due to poor nutrient supply, ATP production may be a limiting factor for ECM biosynthesis in the IVD.

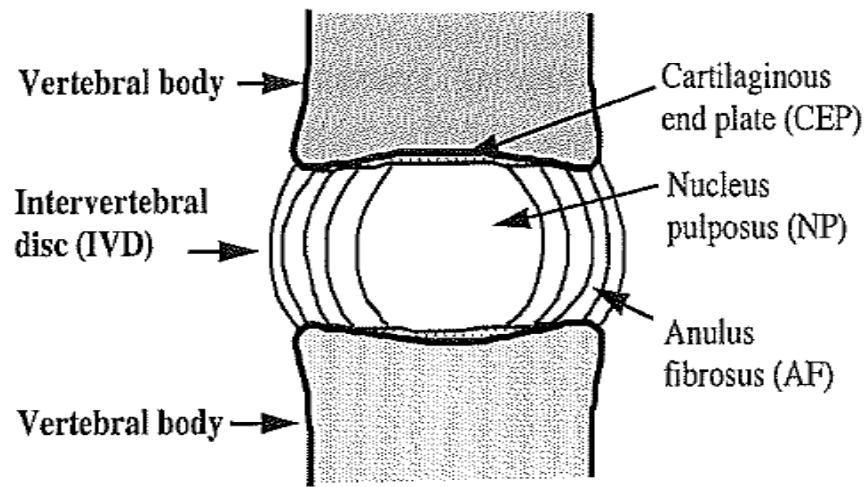
Since the main function of IVD is to support loads and to provide flexibility for the spine, IVDs are subjected to mechanical loadings frequently. Many mechanical events at high magnitude can be generated inside the IVD under mechanical loading, such as fluid flow, hydrostatic pressure, tension, deformation, shear force and streaming potential, etc. All of these have been proved to have effects on ECM synthesis of IVD cells (Ohshima, Urban et al. 1995; Ishihara, McNally et al. 1996; Handa, Ishihara et al. 1997; Hutton, Elmer et al. 1999; Iatridis, Mente et al. 1999; Lotz and Chin 2000; Chen, Yan et al. 2004; Maclean, Lee et al. 2004; Walsh and Lotz 2004). This indicates that ATP production may be affected by mechanical loading. In addition, cells constantly release ATP which can regulate a variety of cellular activities via purinergic receptors (Burnstock 2006). ATP released by IVD cells can be promoted by mechanical loading, including IVD cells (Fernando, Czamanski et al. 2011). Due to the avascular nature of IVD, ATP may accumulate extracellularly and regulate metabolic activities of IVD cells, including ECM production (Chowdhury and Knight 2006). Therefore, mechanical loading could influence biological function of the IVD by regulating intra- and extra- cellular ATP metabolism. The overall objective of the studies in this dissertation was to investigate the energy metabolism of IVD under static and dynamic compressions. Thus, the outcomes of the studies in this dissertation improve our understanding of cellular energy metabolism and nutrient transport in the IVD under mechanical loading and provide guidance for future studies which will investigate a new mechanobiological pathway to disc degeneration by governing ATP metabolism and develop new strategies to prevent or retard the degenerative process of IVD.

CHAPTER 2: BACKGROUND

2.1 STRUCTURE OF IVD TISSUE

IVD is a strong yet deformable tissue that lies between vertebrae and is important for the whole spine structure. The anatomic views of IVD are shown in Figure 2-1. IVD transfers loads and allows the spine to move through torsion, bending or compression (Hickey and Hukins 1980; Hadjipavlou, Tzermiadianos et al. 2008; Adams, Dolan et al. 2009). IVD is also one of the largest avascular cartilaginous tissues in the human body. The main methods for delivering nutrients into IVD are diffusion and convection.

There are three major anatomical parts of the IVD: the inner nucleus pulposus (NP), the outer annulus fibrosus (AF) and cartilaginous endplate (CEP) (Figure 2-1) (Kandel, Roberts et al. 2008). The composition of IVDs is not identical but differs according to different ages and locations within the spine (Pearce, Grimmer et al. 1987; Urban, Fairbank et al. 2001). However, in a healthy and normal disc, the NP is a jelly-like part which contains randomly oriented collagen fibrils suspended in a proteoglycan gel (Marchand and Ahmed 1990). The main content of NP is water; collagen (mainly type II and type VI) is randomly oriented to form a loose network and to hold proteoglycan (Wu, Eyre et al. 1987; Roberts, Ayad et al. 1991). Negatively charged glycosaminoglycan provides NP the osmotic properties, which enables NP to play an important role for distributing hydraulic pressure when mechanical loadings applied to the spine (Setton and Chen 2006).



Sagittal section

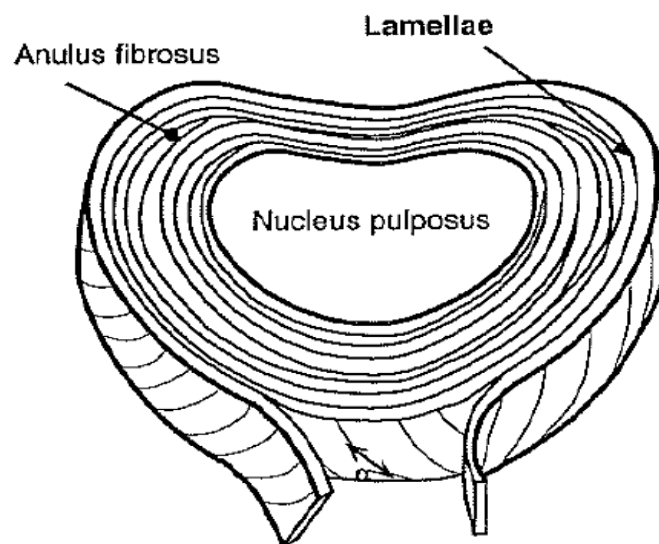


Figure 2-1: Anatomy of the Intervertebral Disc

The AF is made of 15-25 distinct layers of organized collagen fiber lamellae which form the surrounding ring around the NP (Marchand and Ahmed 1990; N. 2005). Each lamella has collagen fibers (type II) aligning the same direction but has an angle of $\sim 30^\circ$ to adjacent lamellae. Lamellae have relatively loose connections to each other and this helps the IVD to transmit movement such as flexion and torsion (Bibby, Jones et al. 2001). The AF and endplate together confine the more flexible and deformable NP (Adam and Deyl 1984; Guiot and Fessler 2000).

The vertebrae body and IVD are separated by CEP, a thin layer of hyaline cartilage (Lundon and Bolton 2001). The CEP prevents the NP from being squeezed out under compression and allows loading to be evenly transferred to vertebral bodies (Ferguson and Steffen 2003). The CEP is porous to allow solute transportation through the endplate (Grunhagen, Shirazi-Adl et al. 2011); therefore, the CEP is a very important nutrition pathway for IVD. The AF can receive nutrition supply by solute diffusion and convection from surrounding blood vessels, while the CEP is the main route of nutrition supply for the NP. However, the nutrition pathway tends to be less effective as CEP calcification due to aging occurs (Figure 2-2).

Water makes up the largest portion of the IVD. Water makes up 60-70% weight of the AF and 70-90% weight for NP (Panagiotacopoulos, Pope et al. 1987; Iatridis, MacLean et al. 2007). However, the water content varies due to age and region. Proteoglycan makes up 10-60% of dry weight of IVD tissue, collagens (all types) make up 15-65% dry weight and other matrix proteins make up 15-45% of dry weight in human IVDs (Hendry 1958; Kraemer, Kolditz et al. 1985; Panagiotacopoulos, Pope et al. 1987; Eyre 1989; Johnstone, Urban et al. 1992; Pearce 1993; Gu, Mao et al. 1999). The composition of human IVD is summarized in Table 2-1.

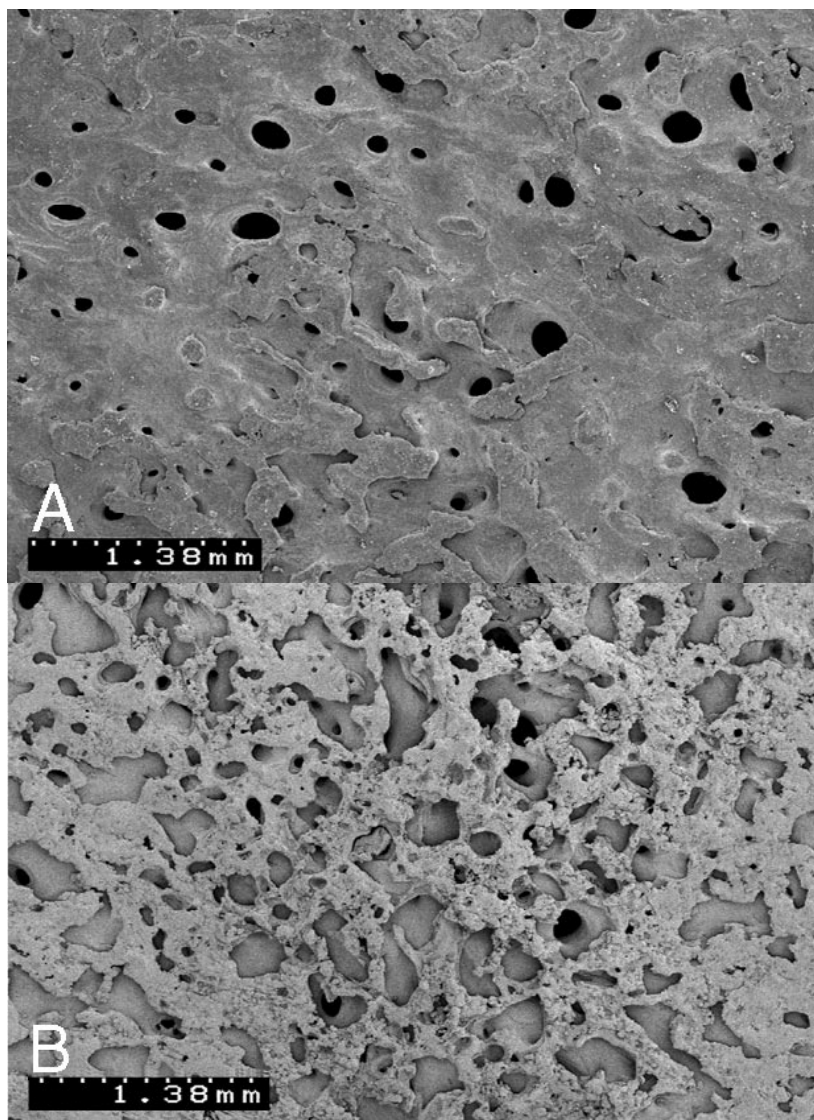


Figure 2-2: Scanning electron microscopy of cartilage endplate from A) 30 years old and B) 80 years old human beings (Benneker, Heini et al. 2005).

2.2 CELL TYPES IN DIFFERENT IVD REGIONS

In addition to morphological differences in the AF and NP, they also have different cell types. Within the AF there are different types of cells from the outer region to the inner region and in the transition zone (TZ). The AF outer region cells are mainly fibroblastic and in each lamellae they orient along the predominant direction (Figure 2-3) (O'Halloran and Pandit 2007). The cells in the AF inner region and TZ have both chondrocyte-like and fibroblastic characteristics (Walker and Anderson 2004).

NP cells are larger than AF and TZ cells (Figure 2-4 & Figure 2-5); they are spherical and surrounded by capsules (Maldonado and Oegema 1992; Oegema 1993). The cells in the NP change over an individual's lifetime. The bigger cells, which are predominant in the earlier ages, are notochordal. For human beings, mature NP cells begin to replace notochordal NP cells from the age of 10. The mature fibroblastic cells are round in shape and much smaller (Adams, Dolan et al. 2009; Guehring, Wilde et al. 2009). NP tissues containing notochordal cells usually maintain a water content between 80-88% while mature NP tissue is around 70% water (Humzah and Soames 1988). It has been suggested that the disappearance of notochordal cells is due to the insufficient nutrient supply and the change of NP cell type contributes to disc degeneration (Aguiar, Johnson et al. 1999).

The cell density in the AF is 7000 to 12,000 cells/ mm³ and higher than NP with 3,300 – 4,400 cells/ mm³ (Maroudas 1975). Cells only form 1% of the disc volume, however, they play pivotal roles in maintaining disc integrity and health by producing ECM components and the chemicals responsible for breaking down the matrix (Bibby, Jones et al. 2001).

Table 2-1: Human IVD composition summarized from literature (Hendry 1958; Kraemer, Kolditz et al. 1985; Panagiotacopulos, Pope et al. 1987; Eyre 1989; Johnstone, Urban et al. 1992; Pearce 1993; Gu, Mao et al. 1999). Other matrix proteins are also found in IVDs in small amount and thus not listed here.

	Annulus Fibrosus (AF)	Nucleus Pulposus (NP)
Cell density	~9000 cells/mm ³	~4000 cells/ mm ³
Water (% wet wt.)	60-70%	70-90%
Proteoglycan (% dry wt.)	10-20%	~50%
Collagen (% dry wt.)	50-70%	15-25%

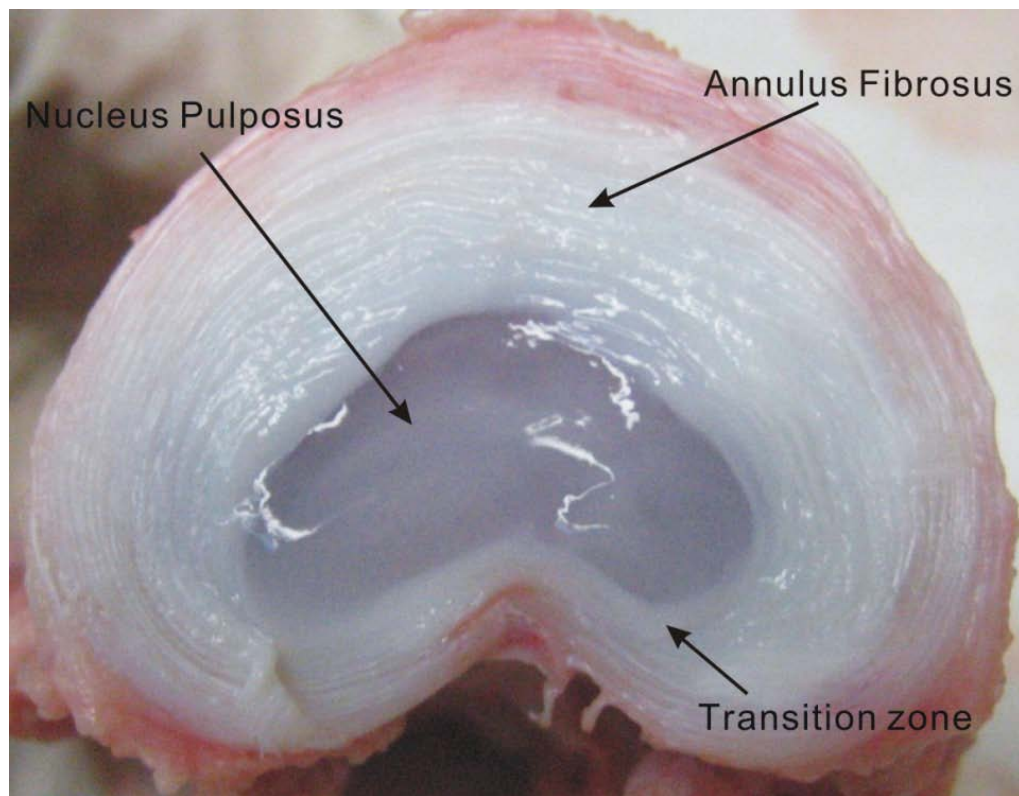


Figure 2-3: Cross-section view of a porcine lumbar disc. Three distinct regions can be seen from the Figure: Annulus Fibrosus (AF), Nucleus Pulposus (NP) and Transition Zone (TZ).

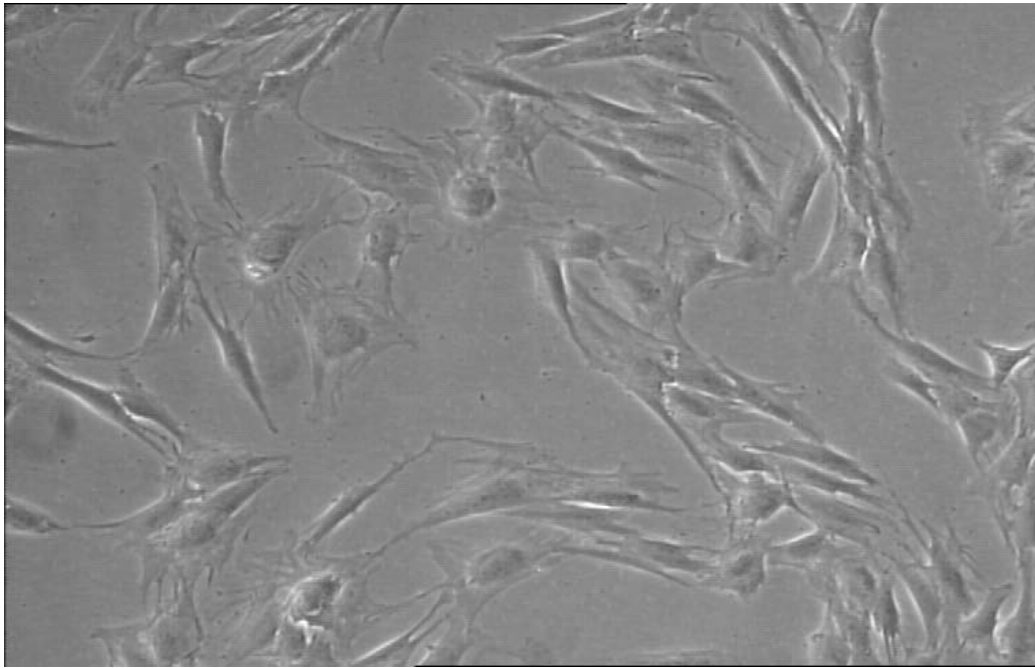


Figure 2-4: AF cells from 6-month old porcine lumbar disc.

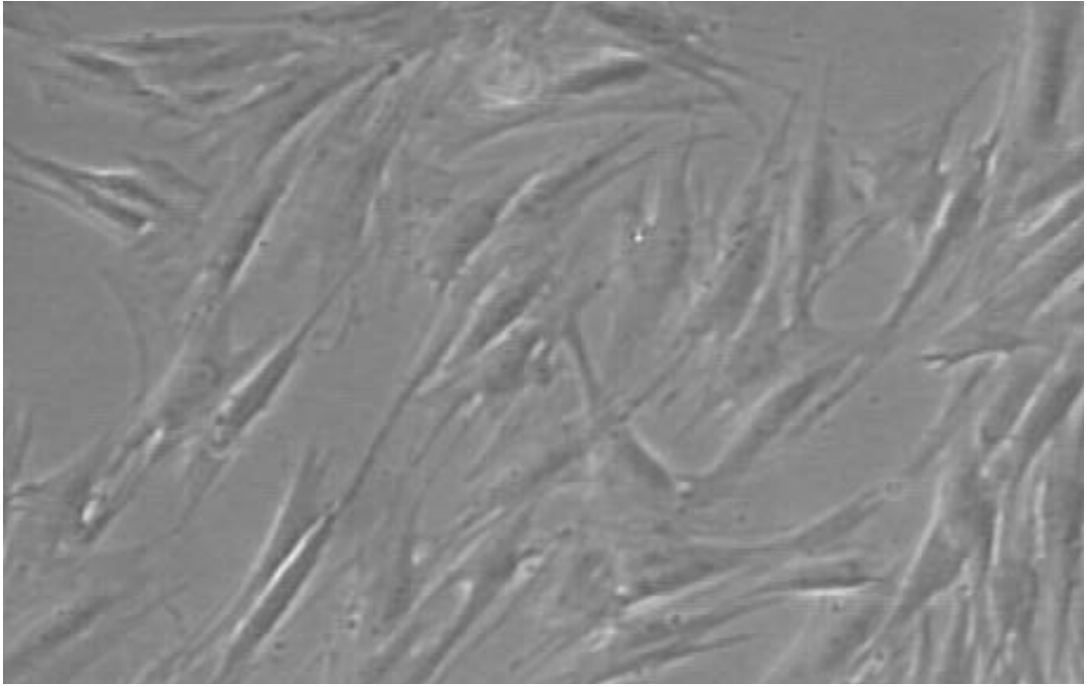


Figure 2-5: 6-month old porcine lumbar disc NP cells

These processes are highly energy demanding. Cells consume large amount of adenosine triphosphate (ATP), which is the main cell energy source and generated via glycolysis and the consumption of glucose and oxygen. IVDs are under daily cyclic mechanical loading *in vivo*; it is reported that mechanical loading can alter the consumption of oxygen and glucose, change ATP release in chondrocytes and promote ECM synthesis *in vitro* (Lee, Wilkins et al. 2002; Huang, Hagar et al. 2004; Chowdhury and Knight 2006; Fernando, Czamanski et al. 2011; Salvatierra, Yuan et al. 2011). This may indicate the change of overall energy production of the IVD cells (Urban, Smith et al. 2004). Since IVD becomes avascular a few years after the fetal stage, the nutrients supply of IVD is mainly by diffusion, which is not a very efficient pathway and can be affected by many factors (Urban, Smith et al. 2004). When this pathway is affected, the consequence is insufficient nutrient supply which causes decreased energy production and is the main contributing factor in disc degeneration.

In addition to the differences in cell type, AF has higher collagen content and lower proteoglycan content compared to NP. Due to the differences in cell type and structure, AF and NP may have different metabolism pathways (Raj 2008; Bron, Helder et al. 2009). However, research on the energy metabolism of IVD and possible relations with disc degeneration is limited. Previous studies have shown the difference in energy metabolism between AF and NP in an agarose gel model (Fernando, Czamanski et al. 2011; Salvatierra, Yuan et al. 2011). However, the *in vivo* environment involves the cell-ECM interaction and mechanical loading which can change the transport properties of the disc such as permeability and diffusivity.

2.3 NUTRITION SUPPLY AND IVD DEGENERATION

As mentioned above, IVDs are the biggest avascular tissue in the human body; the main nutrient supply pathways: diffusion and convection of solutes from periphery

blood vessels penetrated into outer lamellae and CEP are affected by factors such as diffusivity and tissue permeability. Furthermore, the number of periphery blood vessels decrease dramatically while the volume of IVDs grow rapidly around the age of three to four for human beings (Urban and Roberts 1995). Upon skeletal maturation remodeling of CEP initiates and leads to mineralization and bone eventually replaces cartilage. Change to the morphology of the CEP decrease the permeability; thereby decreasing the overall nutrient supply to the NP (Moore 2006). It has been shown theoretically and clinically that CEP calcification will significantly decrease glucose and oxygen concentration in NP region and initiate disc degeneration (Peng 2001; Jackson, Huang et al. 2011). IVDs also endure repeated mechanical loading. This loading, taken in combination with CEP calcification creates a harsh environment for IVD cells, especially NP cells (Guiot and Fessler 2000; Grunhagen, Shirazi-Adl et al. 2011). Consequently, fibro-chondrocyte-like mature cells will replace notochord cells in NP which is believed to protect NP cells from degradation and apoptosis (Erwin, Islam et al. 2011). Hence necrotic and apoptotic cells increase from about two percent of at fetal population to more than fifty percent in the adult as a result of a decrease in the number of notochord cells (Gruber and Hanley 1998).

It is believed that disc degeneration in humans starts at the beginning of second decade of life, earlier than any other musculoskeletal tissues (Miller, Schmatz et al. 1988; Boos, Wallin et al. 1993), and the severity increases along with age (Nerlich, Schleicher et al. 1997). Disc degeneration within a population increases with age: 20% of teenagers showed signs of disc degeneration, by age 50 the percentage increases to 97%. Furthermore, 10% lumbar discs are severely degenerated at age 50, compared to 60% at the age of 60 (Miller, Schmatz et al. 1988).

With age, the AF lamellae become thicker and more fibrillated. Cracks grow between lamellae and gradually disrupt the structure of the AF, decreasing the AF's load bearing ability. The NP progressively loses its water content and morphology with age. Microscopically, collagen content of the NP increases and leads to a blurring of the transition zone that lies between AF and NP. These changes together may lead to IVD fracture. The color of IVD also changes with age (Figure 2-6), from white or transparency to yellowish or brown fragments (Urban and Roberts 1995).

IVD gains its mechanical strength from two major macromolecular components: proteoglycans and collagens. The network formed by collagen (mainly type I and type II fibrils) making up around 70% and 20% of dry weight in AF and NP, respectively, provide the tensile strength for IVD. Proteoglycan has a hydrophilic property and thus helps IVD to maintain a relatively higher water content (around 70% in AF and 90% in NP for normal IVDs) to endure compressions. Unfortunately, IVD gradually loses its proteoglycan and collagen content with age and aggravation of disc degeneration. It is reported that the most significant biochemical change detected in degenerated discs is the decreased content of proteoglycan (Eyre 1977). Collagen content also changes with disc degeneration but not as significantly as proteoglycans (Urban and Roberts 2003).

Enzyme activity is also an indicator of biochemical change of IVD degeneration (Urban and Roberts 2003). IVD cells not only produce molecules to synthesize ECM, but also produce enzymes (such as MMPs and aggrecanases) to break down ECM (Urban and Roberts 2003). The balance between synthesis and break-down is well maintained in the healthy discs, but it is disrupted in degenerated IVD. In the degenerated IVD, matrix metalloproteinase (MMP) and aggrecanases show higher levels of activity than in healthy discs.

Figure 2-6 shows the conditions of healthy and degenerated IVDs: healthy disc with a more hydrated NP and white color while degenerated disc lose much of water content in the NP region and has a yellow color. Degenerated discs usually have decreased heights which can be detected by clinical imaging techniques such as MRI and CT scan (Figure 2-7).

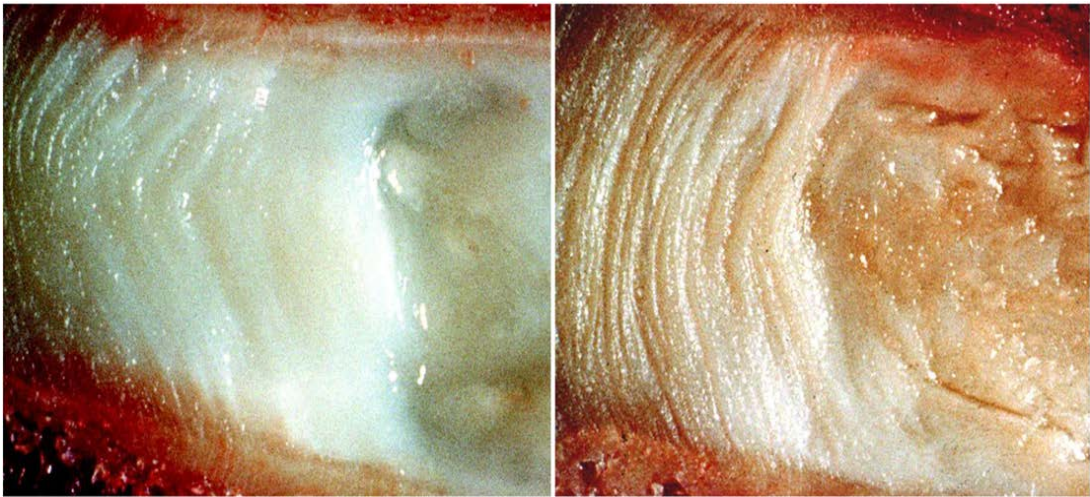


Figure 2-6: Sagittal views of human IVDs. Left: healthy from 20-30 year-old disc. Right: degenerated from 50-60 year-old disc (Adams, Stefanakis et al. 2010).

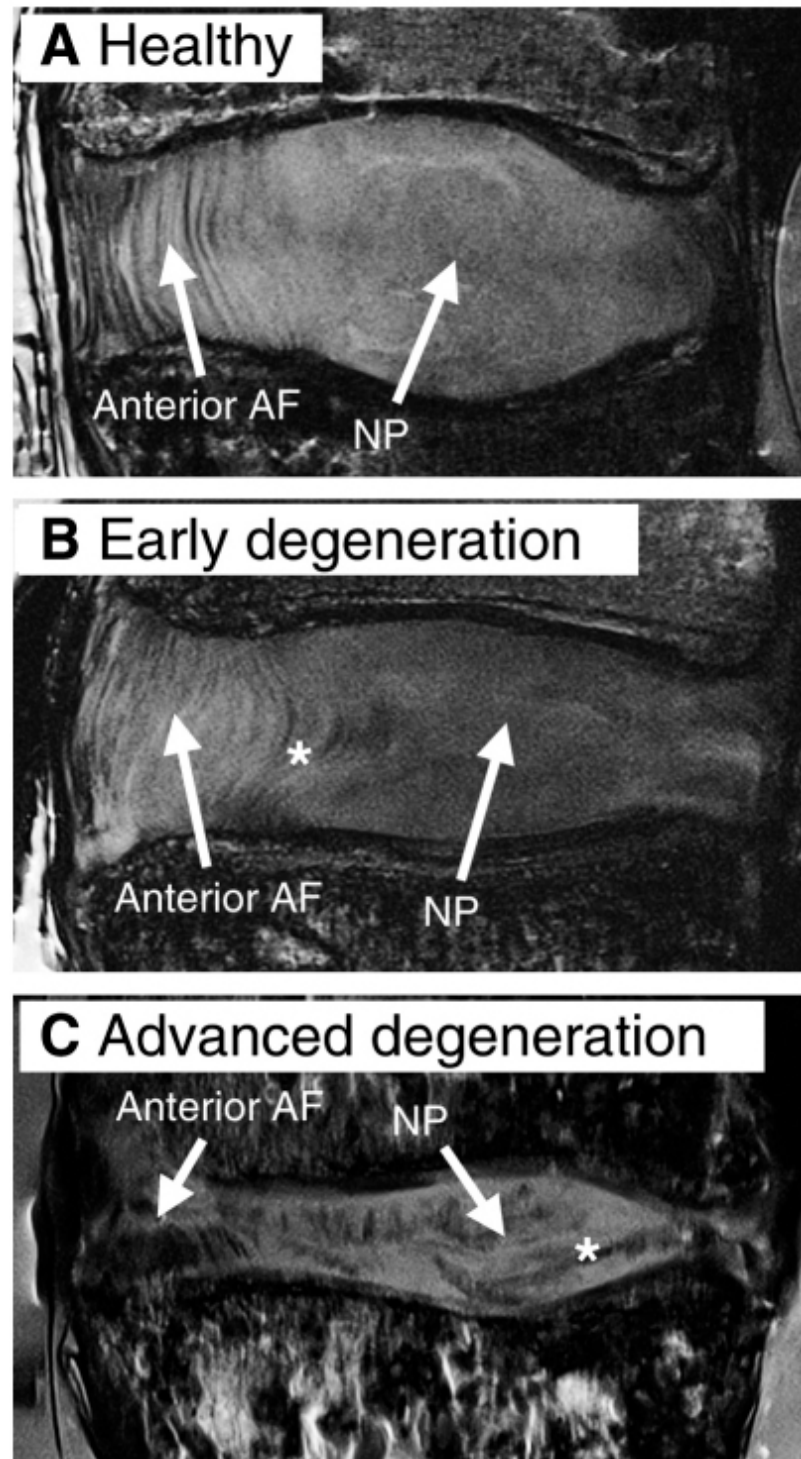


Figure 2-7: Different stages of human lumbar region disc degeneration obtained with Magnetic Resonance Images (MRI) (A) Shows a healthy disc with distinct NP and AF regions; (B) A disc in early stage of degeneration with slightly decreased disc height and reduced signal density of NP region. * indicates AF bulging inward. (C) A severe degenerated disc showing largely decreased height, * indicates large cleft (Smith, Nerurkar et al. 2011).

2.4 ENERGY METABOLISM OF IVD

Adenosine tri-phosphate (ATP) is called the “molecular unit of currency” for organism cells (Knowles 1980). Each ATP molecule contains three phosphate groups and can be hydrolyzed into adenosine di-phosphate (ADP) or into adenosine mono-phosphate (AMP).

The hydrolysis of one mole of ATP to ADP will release 30.5 kJ of free energy and hydrolysis of one mole of ATP to AMP will release 45.6 kJ of free energy (Berg, Tymoczko et al. 2012). For eukaryotic cells, many sources such as amino acids, fatty acids, carbohydrates and glucose can all be substrates for ATP production. Glucose is the most common one among all of these sources to produce ATP. However, fatty acids can be the primary energy source when high energy is required. Heart muscle is an example which utilizes fatty acids to produce the high amount of ATP required to maintain normal functions. The cell energy production process starts firstly when the substrate is transported into the cytosol where the energy metabolism is conducted; ATP is produced from a series of complex enzyme catalyzed reactions (Figure 2-8).

Two processes contribute to ATP production: aerobic respiration with adequate oxygen supply and glycolysis when oxygen is absent in the environment. Through aerobic respiration thirty-six (36) ATP will be produced per molecule of substrate; while for glycolysis three (3) net ATP will be yield per molecule of glycogen and two (2) net ATP will be produced per molecule of glucose (Lodish 2013).

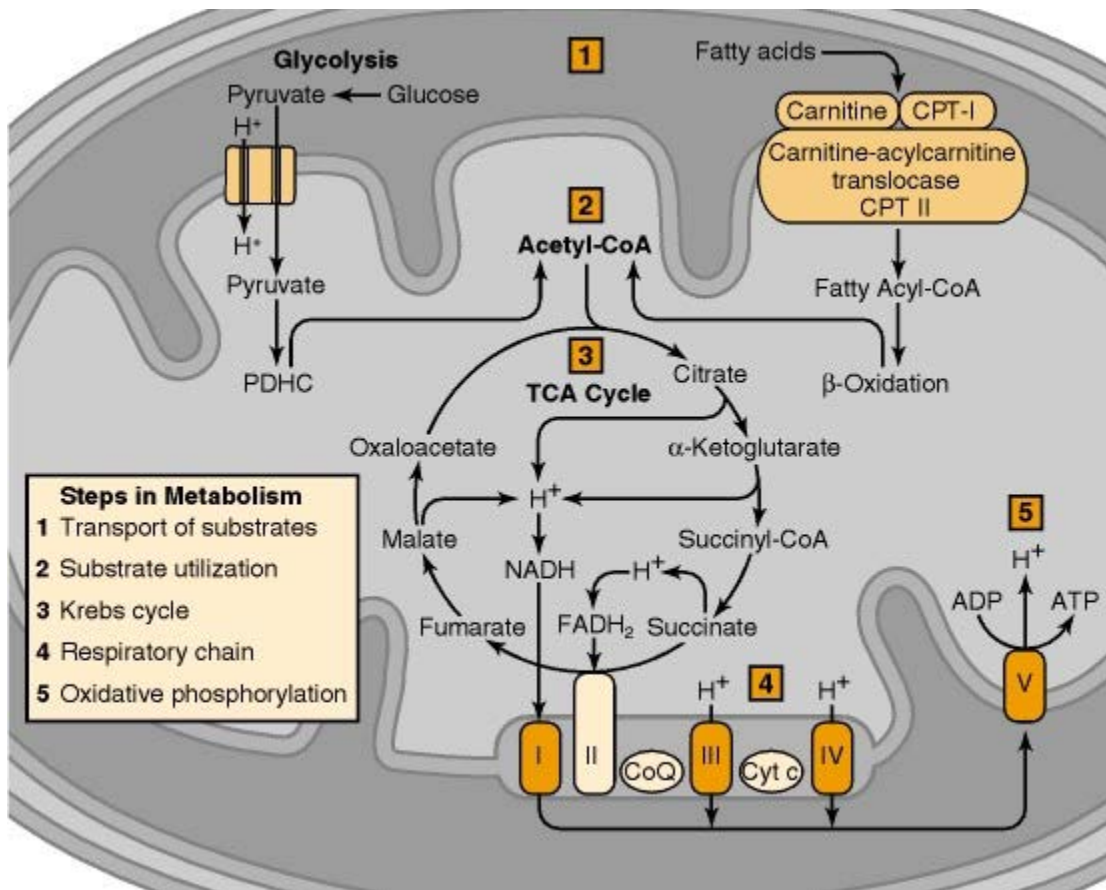


Figure 2-8: Schematic representation of ATP production in cells (Siegel 1999).

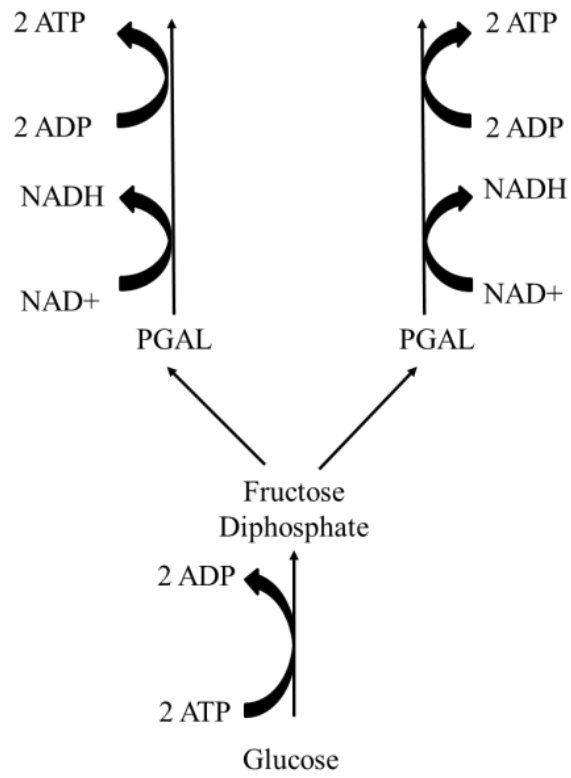
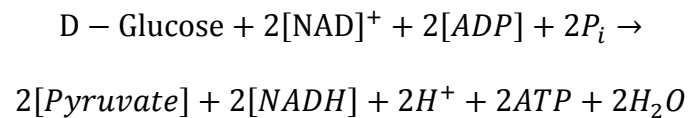


Figure 2-9: Simplified flow of glycolysis (Lodish 2013).

It is reported that some cells such as immature IVD cells and chondrocytes contain glycogen-glucose deposits (Trout, Buckwalter et al. 1982). When necessary glycogen can be broken down to glucose and can be used to produce ATP. The intermediate of glycolysis, pyruvate, can enter mitochondria to undergo respiration for the production of ATP when oxygen supply is abundant. When oxygen supply is limited, lactate will be produced and only two (2) ATP per molecule of glucose will be yield from the reaction (Berg, Tymoczko et al. 2012; Lodish 2013). The overview of glycolysis is shown in Figure 2-9; in which ten intermediates are involved in a sequence of ten steps of reactions. The overall reaction with D-glucose as the initial substrate is as following:

Equation 1: Glycolysis Equation



Pyruvate and other intermediates that have been transported into mitochondria will be converted to Acetyl-coenzyme A, which is the initiating compound for the following citric acid cycle (TCA cycle, also referred as Krebs cycle) as shown in Figure 2-8. It is known that the Krebs cycle can produce 2 ATP molecules per cycle and also yield intermediates such as NADH, which is an important compound for oxidative phosphorylation or called electron transport chain. Oxidative phosphorylation also takes place in mitochondria and the location is the inner membrane. Mitochondrial respiration can theoretically produce 36 ATP molecules per glucose molecule.

2.5 EFFECTS OF MECHANICAL LOADING ON IVD CELLS

The main function of IVD is to provide flexibility and support load of the spine. Throughout the walking cycle the IVD undergoes frequent mechanical loading. Numerous mechanical events can be produced inside IVD by mechanical loading, such as fluid flow, tensile/compressive stress, shear force, matrix deformation, stream potential, hydrostatic pressure, etc. All these mechanical events were reported to regulate ECM synthesis of IVD cells (Ohshima, Urban et al. 1995; Ishihara, McNally et al. 1996; Handa, Ishihara et al. 1997; Hutton, Elmer et al. 1999; Iatridis, Mente et al. 1999; Lotz and Chin 2000; Chen, Yan et al. 2004; Maclean, Lee et al. 2004; Walsh and Lotz 2004).

High magnitude of static compression (> 1 MPa) has been shown to be detrimental to ECM synthesis and cell viability (Iatridis, Mente et al. 1999; Lotz and Chin 2000). Moderate static compression (0.1-0.4 MPa) can promote collagen and proteoglycan synthesis in explants and increase ECM gene expression under *in vitro* three-dimensional IVD cells culture system (Ohshima, Urban et al. 1995; Chen, Yan et al. 2004). It is showed that hydrostatic pressures lower than 3.0 MPa can increase synthesis of collagen and proteoglycan of IVD cells at in vitro three-dimensional culture or tissue explants (Ishihara, McNally et al. 1996)

It is found that dynamic compression of various frequencies and amplitudes can cause different responses from IVD cells. Previous studies showed that low frequency dynamic compression (e.g. 0.01 Hz, 1 MPa) applied to rat IVDs up-regulated anabolic gene expression (aggrecan, type I and type II collagen) in NP cells (Maclean, Lee et al. 2004).

Previous studies also demonstrated that mechanical loading influences cellular energy metabolism (Lee, Wilkins et al. 2002; Fernando, Czamanski et al. 2011; Salvatierra, Yuan et al. 2011). Hydrostatic pressure can affect cellular membrane transport of solutes (Benz and Conti 1986; Hall 1999) and glycolysis by changing the rate of glucose to lactate conversion (Takagi, Ohara et al. 1995). Hydrostatic pressure at physiological level (5-15 MPa) has been shown to up-regulate ECM synthesis *in vitro* by promoting incorporation rates of ECM building blocks (Hall, Urban et al. 1991). A recent study also showed that static compression can also inhibit the rate of oxygen uptake and lactate production of chondrocytes (Lee, Wilkins et al. 2002). It is also found that static and dynamic compressions promote ATP production and release from both AF and NP cells of IVD (Fernando, Czamanski et al. 2011; Salvatierra, Yuan et al. 2011). In summary, since ECM biosynthesis is a high energy demanding process (Lee and Urban 1997), the change of cell energy production caused by mechanical loads can lead to changes of cell metabolism.

2.6 EXTRACELLULAR ATP

ATP plays very important roles in regulating cellular activities other than serving as an energy molecule when released into extracellular space. Extracellular ATP (eATP) regulates many physiological activities by activating purinergic P2 receptors (ligand-gated ion channel) (Cook, Vulchanova et al. 1997) which are widely distributed in the nervous system, muscle, bone, endothelia and epithelia (Burnstock 2000; North 2002). ATP acts as a transmitter of the senses of pain (Cook, Vulchanova et al. 1997), mechanical loading (Cockayne, Hamilton et al. 2000; Vlaskovska, Kasakov et al. 2001), and temperature (Souslova, Cesare et al. 2000) by activating P2X receptors in the nervous system. ATP also plays an essential role in diseases, such as ischemia (Bush, Keller et al. 2000) and Parkinson's disease (Przedborski and

Vila 2001). In addition, ATP can initiate and modulate calcification of cartilaginous tissues (Felix and Fleisch 1976; Hsu and Anderson 1996; Golub 2011). It was found that 1 mM of ATP can promote tissue calcification, while higher ATP concentrations (e.g., 4 mM) can inhibit calcification (Hsu, Camacho et al. 1999). Therefore, the sensing of extracellular ATP *in-vivo* has recently attracted increasing interest (Schneider, Egan et al. 1999; Brown and Dale 2002; Seminario-Vidal, Lazarowski et al. 2009; Trautmann 2009). However, the lack of efficient direct measurement techniques limits future studies of the comprehensive role of ATP. In addition, mechanical loading can promote ATP release from IVD cells (Fernando, Czamanski et al. 2011; Salvatierra, Yuan et al. 2011). Due to the avascular nature of the IVD, eATP may accumulate and has an influence on the biological function of the IVD.

CHAPTER 3 BIOREACTOR

3.1 PRINCIPLES OF BIOREACTOR

Human IVDs undergo different types of mechanical loading continuously; therefore, a bioreactor system is required to simulate these loadings to fulfill our specific aims of this study. One aim is to better simulate mechanical loadings applied to IVDs caused by human body movement. To fulfill these requirements, the design principle of this bioreactor system should cover the following points:

1. It should be able to work correctly in incubators with temperature, oxygen and carbon dioxide controls;
2. It should be able to perform both static and dynamic loadings;
3. It should be able to be connected to a culture medium circulation system.

We have designed and built a bioreactor system as shown in Figure 3-1. Figure 3-2 shows the bioreactor placed in an incubator with controlled temperature, oxygen level and carbon dioxide level. In Figure 3-3 details of a bioreactor chamber is shown.

This bioreactor system is driven by a SmartMotor® (Moog Animatics, Santa Clara, CA, USA), and SmartMotor® Interface (SMI) software was used to control the motor through a customer written program. An OMEGA® LC 402 High Accuracy Low Profile load cell (OMEGA Engineering Inc., Stamford, CT, USA) was utilized to measure the compression loadings applied to the IVD. NI USB 6590 digital data acquisition instrument (National Instruments Corporation, Austin, TX, USA) was connected to measure load response during compression; an OMEGA® (OMEGA Engineering Inc., Stamford, CT, USA) DP25P-C panel display was connected to

display the force readings. During disc compression experiments, the custom made chamber was connected with a Bio-Rad (Hercules, CA, USA) model EP1 Econo pump to maintain culture medium circulation (Figure 3-1 and Figure 3-2).

3.2 VERIFYING THE BIOREACTOR SYSTEM

3.2.1 Swelling and preload

IVDs undergo substantial mechanical loads *in vivo* and the external loads affect internal swelling pressure. The relationship of external loads to internal swelling pressure and proteoglycan contents affects fluid content of the IVD (Urban and McMullin 1988). Swelling may happen when the IVD lose weight bearing functionality *in vitro* (Urban and Maroudas 1981). Swelling of the IVD may cause leaching of proteoglycan and other components of the IVD and cause other deleterious consequences (Urban and Maroudas 1981; Holguin, Muir et al. 2007). Therefore, for *in vitro* culture of IVD, a preload is often added to the disc to balance the swelling pressure and thus prevent the IVD from swelling (Costi, Stokes et al. 2008). The effect of preload on mechanical properties of IVDs has previously been studied (Panjabi, Krag et al. 1977).

However, our preliminary study showed that porcine IVDs exhibited a very small disc heights change during overnight culture ($2.3\% \pm 0.9\%$, $n=3$). Thus no preload was applied to the IVD during overnight culture in this study.

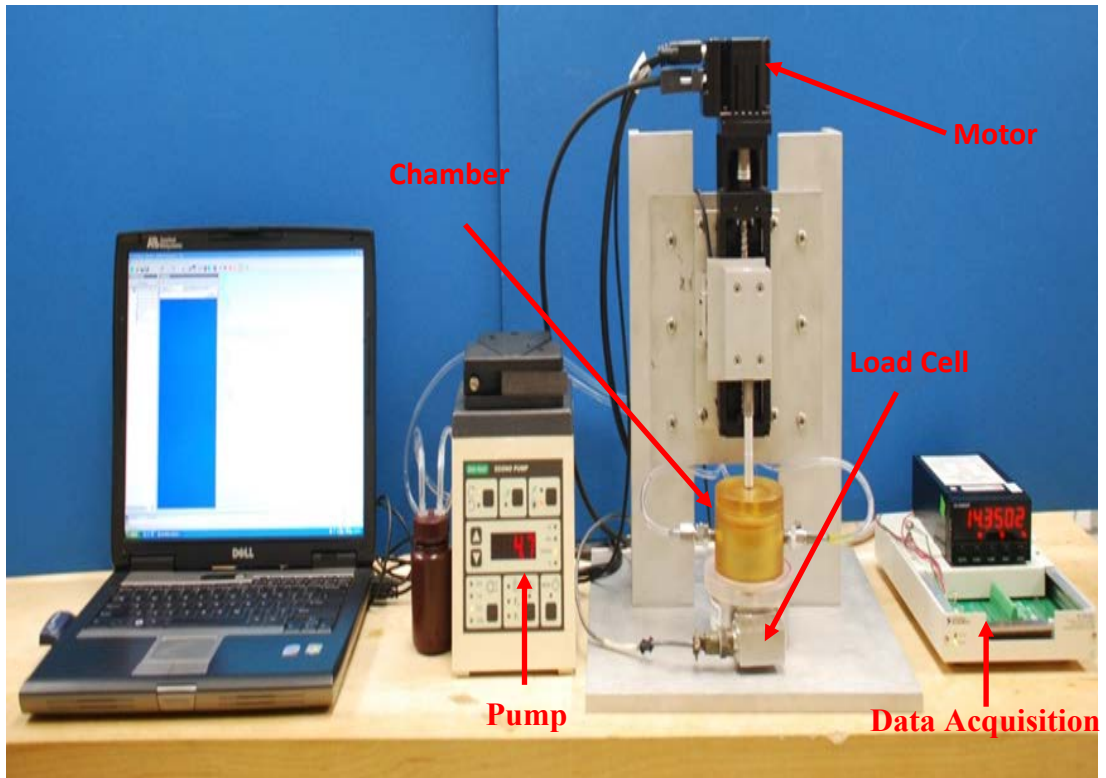


Figure 3-1: Bioreactor system.



Figure 3-2: Bioreactor in incubator



Figure 3-3: Bioreactor chamber with lid closed (up) and open (down).

3.2.2 Verifying displacement-controlled dynamic loading

The dynamic compressive loading applied in this study was displacement-controlled. An initial 10% strain was added to the disc by 10 steps with 1% per step. Then a dynamic loading with 10% strain was applied. Therefore the maximum strain applied on the disc during the experiment was 15% (Figure 3-4). The range of strain during dynamic compression experiments was 5%-15%.

IVDs have high fluid content which will be squeezed out slowly when compressive loads are applied. Therefore the IVD has a delayed response to compressive loads applied which may cause a so-called “lift off” effect. This effect indicates the status: when the moving piece that applies compression to the IVD is moved upward, the IVD is not able to follow due to the delayed response. In this short period of time, the moving piece and the IVD will be out of contact, the disc will thus not experience the next compression cycle. To verify if this effect happens on our bioreactor, we used a load cell with an attached data acquisition device, a display device and a recording program on the computer to monitoring the loading force fluctuation during the compression. A typical 10-second period of loading force approaching the end of 1-hour dynamic compression was shown in Figure 3-5. During the dynamic compression experiments, the force detected by the load cell never fell under zero (0). Therefore we have not observed any lift off effect on our bioreactor.

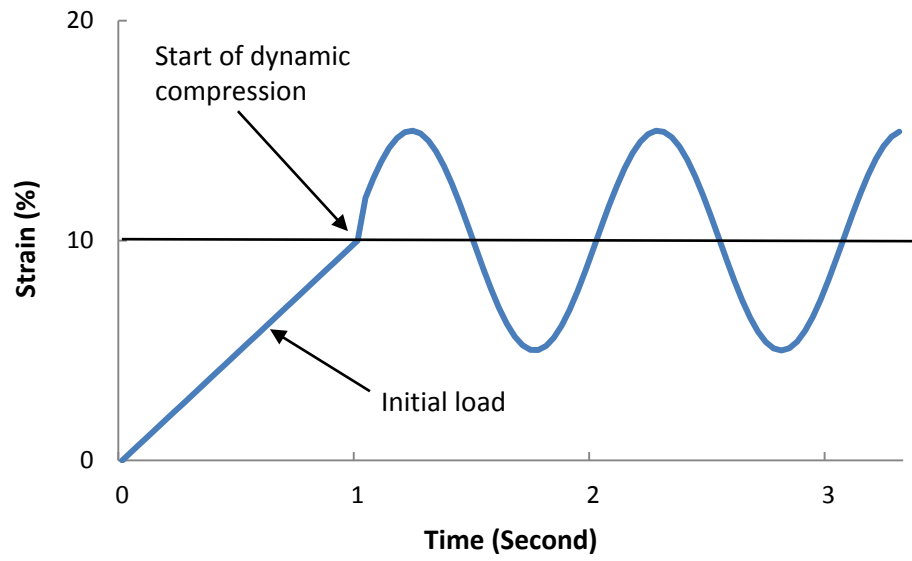


Figure 3-4: Schematic diagram of displacement-controlled dynamic loading.

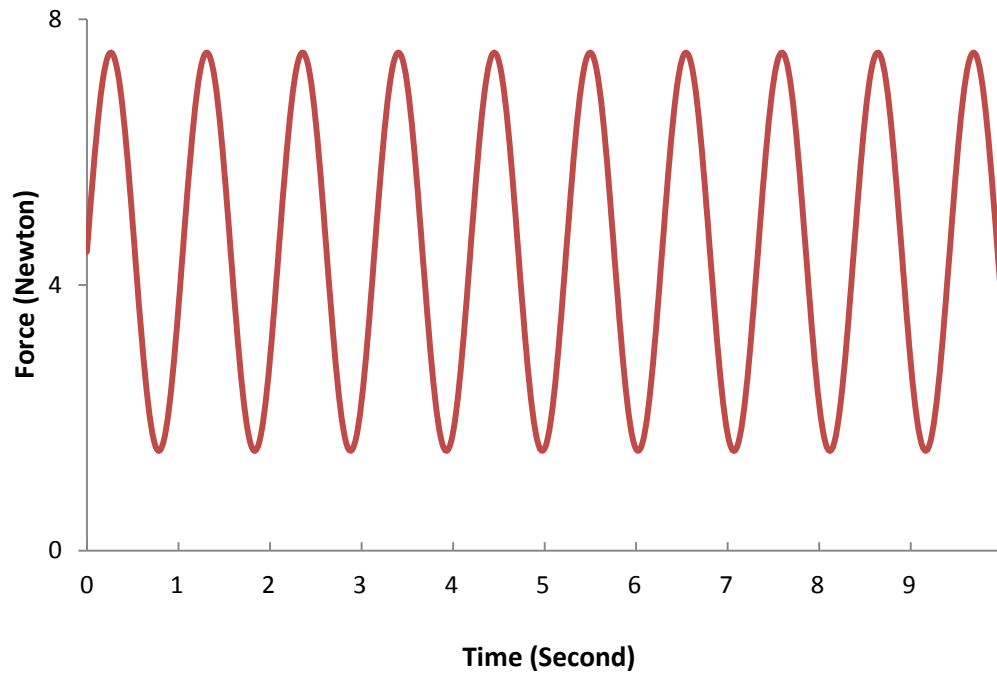


Figure 3-5: 10 seconds of loading force-time recorded for 1 Hz dynamic compression.

CHAPTER 4 OPTICAL BIOSENSORS

4.1 INTRODUCTORY REMARKS

Adenosine-5'-triphosphate (ATP) is an important multi-functional molecule which was first discovered in 1929 by Karl Lohmann and has long been recognized as “the molecular unit of currency” (Lohmann 1929; Knowles 1980). ATP has two phosphate groups which release energy when hydrolyzed, and this is the energy source for the metabolic activities of ubiquitous organisms (Knowles 1980). When it is released to the extracellular environment, ATP can mediate numerous physiological activities by activating purinergic P2 receptors (ligand-gated ion channel) (Cook, Vulchanova et al. 1997) which are widely distributed in the nervous system, muscle, bone, endothelia and epithelia (Burnstock 2000; North 2002). In the nervous system, ATP acts as a transmitter of the senses of pain (Cook, Vulchanova et al. 1997), temperature (Souslova, Cesare et al. 2000), and mechanical loading (Cockayne, Hamilton et al. 2000; Vlaskovska, Kasakov et al. 2001) by activating P2X receptors. ATP also plays an essential role in diseases, such as particular ischemia (Bush, Keller et al. 2000) and Parkinson’s disease (Przedborski and Vila 2001). In addition, ATP can initiate and modulate calcification of cartilaginous tissues (Felix and Fleisch 1976; Hsu and Anderson 1996; Golub 2011). It was found that 1 mM of ATP can promote tissue calcification, while higher ATP concentrations (e.g., 4 mM) can inhibit calcification (Hsu, Camacho et al. 1999). Therefore, the sensing of extracellular ATP *in-vivo* has recently attracted increasing interest (Schneider, Egan et al. 1999; Brown and Dale 2002; Seminario-Vidal, Lazarowski et al. 2009; Trautmann 2009). However, the lack

of efficient direct measurement techniques limits future studies of the comprehensive role of ATP.

The Luciferin-luciferase method for measuring ATP content is well known for its high sensitivity and has been widely applied for ATP analysis (Rong, Gourine et al. 2003). However, it is only feasible to apply this method for ATP measurement in solution (Brown and Dale 2002). Recently, amperometric ATP biosensors were developed to detect ATP using multi-enzymatic reactions (Katsu, Yang et al. 1994; Compagnone and Guilbault 1997; Kueng, Kranz et al. 2004; Llaudet, Hatz et al. 2005). The biosensor containing glucose oxidase and hexokinase was able to determine ATP concentration in the presence of glucose with a detection sensitivity of 10 nM (Kueng, Kranz et al. 2004). In that biosensor, glucose was catalyzed by hexokinase in the presence of ATP, which reduced the production of hydrogen dioxide from oxidation of glucose by glucose oxidase. Recent studies developed amperometric ATP biosensor based on sequential enzymatic reactions of glycerol kinase (GK) and glycerol 3-phosphate oxidase (G3POX), which broke down ATP and produced hydrogen dioxide (Katsu, Yang et al. 1994; Llaudet, Hatz et al. 2005). In those biosensors, ATP concentration was determined by measuring electrical current using a polarized platinum electrode which oxidized hydrogen dioxide to oxygen and water. However, since those amperometric biosensors can be affected by many other compounds that naturally exist in biological tissues such as ascorbate and glucose (Kueng, Kranz et al. 2004; Llaudet, Hatz et al. 2005), it could potentially be problematic if they are used for in-vivo measurements. To avoid this problem, in this study, an optical ATP biosensor was developed using an optical oxygen sensing technique, based on fluorescence quenching of excited ruthenium complexes, which determined changes in oxygen concentration during enzymatic ATP breakdown. A

compensation method was also developed to enable the new ATP optical biosensor to determine ATP concentration at different oxygen levels after calibration tests.

4.2 EXPERIMENTS

4.2.1 *Materials*

Tetramethoxysilane (TMOS), methyltrimethoxysilane (Me-TriMOS), GK, G3POX, poly (ethylene glycol) (PEG), glycerol and Tris (4, 7-diphenyl-1, 10-phenanthroline) - ruthenium (II) bis (hexafluorophosphate) complex were obtained from Sigma (St. Louis, MO, USA).

Adenosine 5'-triphosphate sodium salt purchased from Sigma (St. Louis, MO, USA) was used for making standard solution. Cyanoacrylate glue was obtained from Pacer Technology (Rancho Cucamonga, CA, USA). NeoFox® phase measurement systems were purchased from Ocean Optic Co. (Dunedin, FL, USA). L-ascorbic acid was purchased from Sigma (St. Louis, MO, USA).

4.2.2 *Fabrication of ATP optical sensor*

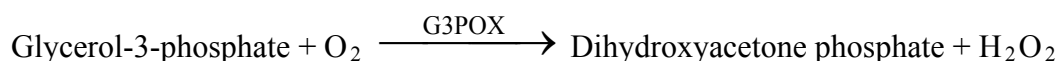
(a) Chemical mechanism

The mechanism of the ATP optical biosensor developed in this study was based on the following sequence of enzymatic reactions (Murphy and Galley 1994):

Equation 2: Enzymatic Reaction 1



Equation 3: Enzymatic Reaction 2



As shown in these enzymatic reactions, ATP can be catalyzed by GK to ADP in the presence of glycerol and yields glycerol-3-phosphate which is further oxidized into dihydroxyacetone phosphate by G3POX. During the second chemical reaction, oxygen is consumed. Therefore, the ATP concentration can be determined by measuring changes in oxygen concentration.

(b) Design of the ATP optical sensor

The ATP biosensor was fabricated by coating two sol-gel layers on the tip of an optical fiber (Figure4-1). In the first layer (i.e., oxygen sensing layer), ruthenium complexes were entrapped in silicate matrix which was fixed to the end of the optical fiber using cyanoacrylate glue. This layer was used to detect change in oxygen concentration. On top of the first layer, a layer of silicate matrix containing G3POX and GK was coated (i.e., enzyme layer), yielding the ATP optical biosensor. Glycerol and PEG were also included in the silicate matrix to stabilize the activity of the enzymes (Llaudet, Hatz et al. 2005).

During the measurement, a semi-permeable silicate matrix allowed ATP to diffuse into the enzyme layer and induce enzymatic reactions described in the reactions Equation 2 and Equation 3. Due to chemical reactions, changes in the oxygen concentration in the silicate matrix can alter the quenching of ruthenium complexes and thus change the decay time of fluorescence emission (Lippitsch, Pusterhofer et al. 1988; Lakowicz 2006). A NeoFox® phase measurement system was used to determine the decay time of fluorescence emission of ruthenium complexes in this study. The precision of decay time measurement is 0.000084 μ s. To test and calibrate the ATP sensor, a linear relationship between the inverse of decay time and the standard ATP concentration was examined (see the section on calibration test).

(c) Preparation of the oxygen sensing layer

The oxygen sensing layer was prepared based on a modified version of the protocols previously described in literature (McEvoy, McDonagh et al. 1996; McNamara, Li et al. 1998; Xiong, Xu et al. 2010). Briefly, a silicate solution was made by mixing 7 μ l of Me-TriMOS, 13 μ l of TMOS, 60 μ l of de-ionized water and 1 μ l of 40 mM HCl. The ratio of the reagents is essential for coating pore size and morphology. Then the silicate solution was sonicated for at least 15 minutes and stirred for 1 hour. These processes are critical to yield a firm and crack-free coating layer. A solution of ruthenium complexes was made by dissolving ruthenium complexes in methanol (5.4 μ g/ μ l). This ruthenium complex solution was mixed with equal amounts of the silicate solution and phosphate buffer solution (PBS) at pH 7.5.

Immediately after applying a very thin layer of cyanoacrylate glue on the end of the optical fiber, one microliter of the ruthenium complex-silicate mixture was spread on the top of the cyanoacrylate glue layer. Cyanoacrylate glue was used to provide a firm adhesion of the ruthenium complex-silicate layer on the optical fiber and prevent detachment of the coating during measurement. The coated optical fiber was left in ambient conditions for 10 minutes before being stored at 4°C overnight. Once the coating became solid, the probe was ready for coating the second enzyme layer or was used for measurement of oxygen concentration.

(d) Preparation of the enzyme layer

Similar to the oxygen sensing layer, a silicate solution was prepared as described in the previous section and used to entrap enzymes in the second layer (Figure 4-1). GK and G3POX were dissolved in PBS with a supplement of PEG and glycerol. The enzyme concentration depends on the ATP concentration range to be measured, varying from 500-1500 units/ml of each.

PEG is well known for its ability to form crosslinks (Kulkarni, Hukkeri et al. 2005) which help to immobilize enzymes and maintain enzymatic activities. The silicate solution and the enzyme solution were then mixed at a 1:1 ratio. One microliter of the enzyme-silicate mixture was immediately spread on top of the oxygen sensing layer to complete the ATP biosensor. The biosensor was ready for ATP measurement after overnight storage in a 4°C environment away from light. To maintain enzymatic activity, the biosensor was stored in PBS with 2mM glycerol after re-hydration.

4.2.3 Calibration test of the ATP sensor

Oxygen sensing is based on the fluorescence quenching of ruthenium complex in the presence of oxygen which can be described by the Stern-Volmer equation:

Equation 4: Stern-Volmer equation

$$\frac{\tau_0}{\tau} - 1 = K_{sv}[O_2] \quad (1)$$

Where τ_0 and τ are the decay times in the absence and presence of oxygen, respectively, K_{sv} is the Stern-Volmer quenching constant, and $[O_2]$ is the oxygen concentration. The decrease in the oxygen concentration ($\Delta [O_2]$) due to the enzymatic reactions was assumed to be linearly proportional to the ATP concentration ($[ATP]$):

Equation 5: Relationship between oxygen concentration and ATP concentration

$$\Delta[O_2] = k[ATP] \quad (2)$$

Here k is the enzymatic reaction parameter which is a function of initial oxygen level and enzyme concentration.

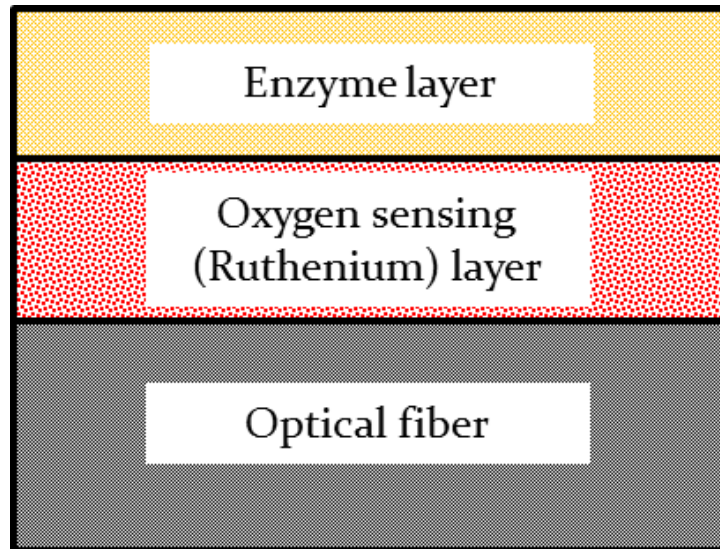


Figure 4-1: Cross sectional view of the ATP sensor

In the presence of ATP, the quenching of ruthenium complex in the coating can be described by Equation 6: Ruthenium quenching in the presence of ATP

$$\frac{\tau_0}{\tau} - 1 = K_{sv}([O_2] - \Delta[O_2]) \quad (3)$$

When the reference oxygen level ($[O_2]$) and the enzyme concentration in the coating remain constant, the enzymatic reaction parameter k can be assumed to be a constant.

Based on Equation 6, a linear relationship between the inverse of decay time and the ATP concentration can be derived as:

Equation 7: Relationship between ATP concentration and decay time

$$[ATP] = A \frac{1}{\tau} + B \quad (4)$$

Where $A = -\frac{\tau_0}{K_{sv}k}$ and $B = \frac{1}{K_{sv}k} + \frac{1}{k}[O_2]$.

In the calibration test, the ATP biosensor was connected to the NeoFox phase measurement system which determined the decay time of fluorescence emission at the wavelength of 600 nm by exciting ruthenium complexes with an impulse light (44 kHz) at the wavelength of 465 nm (Figure 4-2). The resolution of decay time measurement was 10⁻⁴ sec. The biosensor was immersed in the PBS containing 2mM glycerol in a beaker. A magnetic stirring bar was used to stir the solution to distribute all solutes uniformly. After a reference decay time was established, a stock ATP solution of 1mM was added to achieve designated ATP concentrations in the PBS. The decay time was measured for individual ATP concentrations to determine the linear relationship described in Equation 7. The stability of the ATP sensor was also studied. The responses of three sensors to zero and 200 μ M ATP were measured for five consecutive days.

The sensors were stored in PBS contain 2 mM glycerol at 4°C between measurements. The stability of the ATP sensor was analyzed by comparing the difference in the inverse of decay time between the responses to zero and 200 μM ATP.

The stability of the ATP sensor was also studied. The responses of three sensors to zero and 200 μM ATP were measured for five consecutive days. The sensors were stored in PBS contain 2 mM glycerol at 4°C between measurements. The stability of the ATP sensor was analyzed by comparing the difference in the inverse of decay time between the responses to zero and 200 μM ATP.

4.2.4 Examination of the effects of pH on the ATP biosensor

pH in biological tissues may be different from that in the in-vitro calibration condition. This difference may affect the in-situ measurement of the biosensor. Therefore, it is necessary to either calibrate the biosensor under the same conditions as biological tissues or develop a method to compensate for the possible effect that might be introduced by the difference in pH. In this study, the effect of pH on the biosensor measurement was examined by adding an acidic solution to alter the pH in the PBS solution during the calibration test described in the previous section. Then, the measurements of the ATP biosensor at different pH was recorded and normalized for comparison.

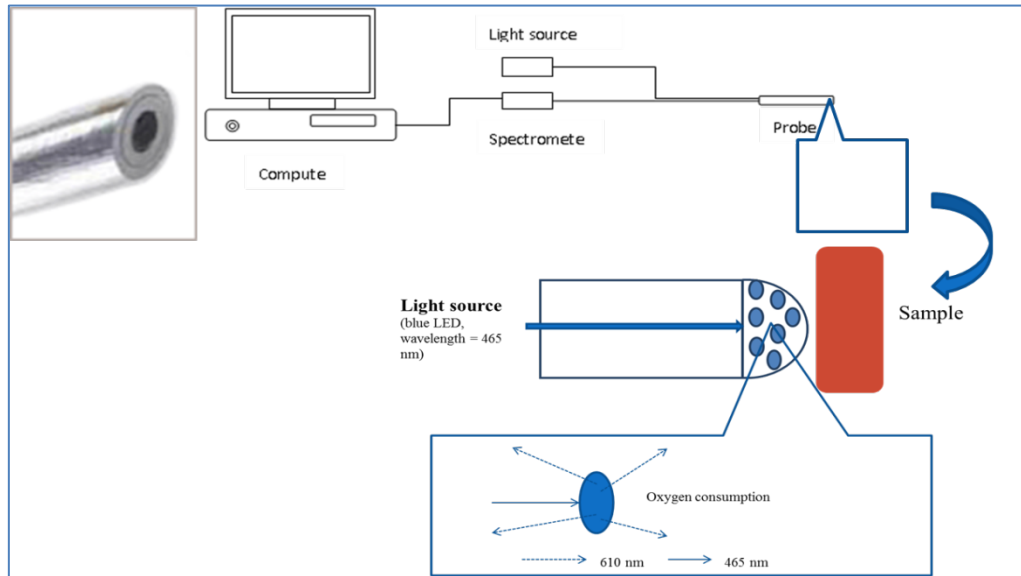


Figure 4-2: Mechanism of optical biosensor system.

4.2.5 Examination of the effects of ADP, AMP, adenosine, and ascorbate on the ATP biosensor

Extracellular ATP is often hydrolyzed into ADP, AMP, or adenosine by ectonucleotidases (Meghji, Pearson et al. 1992). Those adenine nucleotides may coexist with ATP in biological tissues. In addition, previous studies showed that ascorbate affects ATP measurement of amperometric biosensors (Katsu, Yang et al. 1994; Kueng, Kranz et al. 2004; Llaudet, Hatz et al. 2005). Therefore, the effects of ADP, AMP, adenosine and ascorbate on the ATP biosensor were examined on three sensors in this study.

4.2.6 Compensation of the ATP biosensor under different oxygen levels

As described in Equation 7, a linear relationship between the inverse of decay time and the ATP concentration can be established at the same initial oxygen level. Due to differences in tissue material properties, tissue oxygenation varies among different biological tissues. In order to measure ATP concentration under different oxygen levels, a compensation method was developed based on the following mathematical background. It was assumed that the chemical reaction parameter k in Equation 7 is a function of the oxygen level $[O_2]$:

Equation 8: Relationship between k and oxygen level

$$k = C[O_2] + D \quad (5)$$

Here C and D are the material constants. After K_{sv} , τ_0 , C , and D are experimentally determined, Equation 7 can be used to determine the ATP concentration (i.e., $[ATP]$) based on the measurements of the oxygen level (i.e., $[O_2]$) and the delay time (i.e., τ). To test this compensation method, K_{sv} , τ_0 , C , and D for the ATP biosensor were determined from two calibration tests conducted at the oxygen levels of 10% and 20%.

Experimental data obtained from another calibration test at the oxygen level of 15% were used to verify the compensation method. An oxygen regulated incubator was used to provide desired oxygen conditions.

4.2.7 In situ measurement of extracellular ATP in porcine intervertebral disc

To verify the ability of the ATP biosensor for measuring tissue ATP concentration, a tissue measurement experiment was conducted. Porcine NP tissue was obtained from 8-12 month old pig and NP tissue was extracted. This NP tissue was frozen for one day and then immersed into PBS overnight to make sure all ATP was released into the solution. Then this NP tissue was washed three times using PBS and transferred into another PBS solution containing 200 μ M ATP. After one hour the tissue was taken out and placed in a petri dish, the ATP sensor was inserted to measure the ATP concentration. The measurement was compared with the real ATP concentration to verify the ability of the sensor for tissue measurement. We found that our sensor has the ability to accurately measure tissue ATP content: the measured ATP contents are $103\% \pm 4.1\%$ to the real ATP content (n=3).

To test the capability of the ATP biosensor to measure ATP levels in biological tissue; the measurement of extracellular ATP was performed on lumbar intervertebral discs of 12 month-old pigs obtained within 3 hours of sacrifice. Functional spinal units (FSUs) were isolated as described in our previous study (Fernando, Czamanski et al. 2011). The harvested FSUs were then placed and cultured in custom built chambers overnight at 37°C with continuous circulation of culture medium. After overnight culture, a transversal cut was made at the mid-disc height of the FSUs and the nucleus pulposus region was exposed to the ambient condition (20% oxygen level). In order to avoid temperature effect, the ATP measurement was performed using the

ATP biosensor when the temperature of the tissues was reduced to the same level as the calibration test of the sensors (i.e., ambient temperature). The temperature of tissues was monitored using a thermometer. An extra sensor was prepared without the second enzyme layer for determining in-situ oxygen level at the same locations. Calibration of the sensors was performed at the oxygen levels of 10% and 20%. In addition, based on our pilot study, the decay time returned to original value at zero ATP level after the sensors were washed in PBS solution with stirring for 10 minutes between measurements. This was applied to prevent carry over effect.

4.3 RESULTS

4.3.1 *Calibration test of the ATP biosensor*

In the calibration test, when ATP diffused into the enzyme layer of the biosensor, catalysis of ATP decreased local oxygen concentration and thus increased the decay time of fluorescence emitted by the ruthenium complexes. Typical response and calibration curve of the ATP biosensor for different ATP concentrations are shown in Figure 4-3. The rising part of the decay time in the response curve of the ATP biosensor reflected diffusion of ATP into the enzyme layer and initiation of the chemical reactions which reduced the local oxygen partial pressure to a certain level (Figure 4-3a). The inverse of decay time was linearly proportional to the ATP concentration (Figure 4-3b) as described in Equation 7. As shown in Figure 4-3b, the calibration was performed 3 times within 6 hours and small standard deviations indicated the sensor had a good repeatability. By changing the concentration of enzymes, the ATP sensor can be used for different measuring ranges. Based on our experiments, the ATP biosensor had a low detecting limit of 10^{-3} mM (Figure 4-4a) and saturated at 1.5 mM (Figure 4-4b).

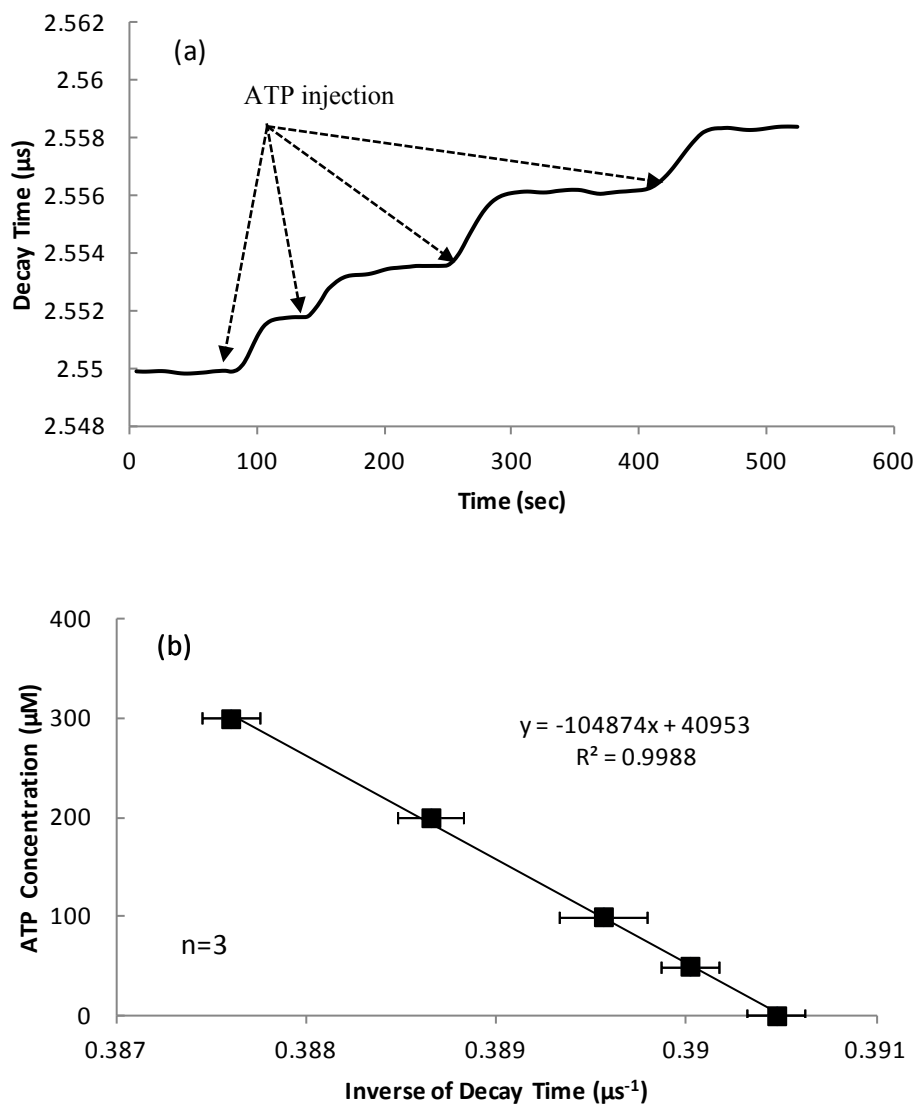


Figure 4-3: (a) A typical decay time curve of the ATP sensor in response to the ATP concentrations of 50, 100, 200, and 300 μM and (b) the corresponding calibration curve (mean values \pm standard deviation).

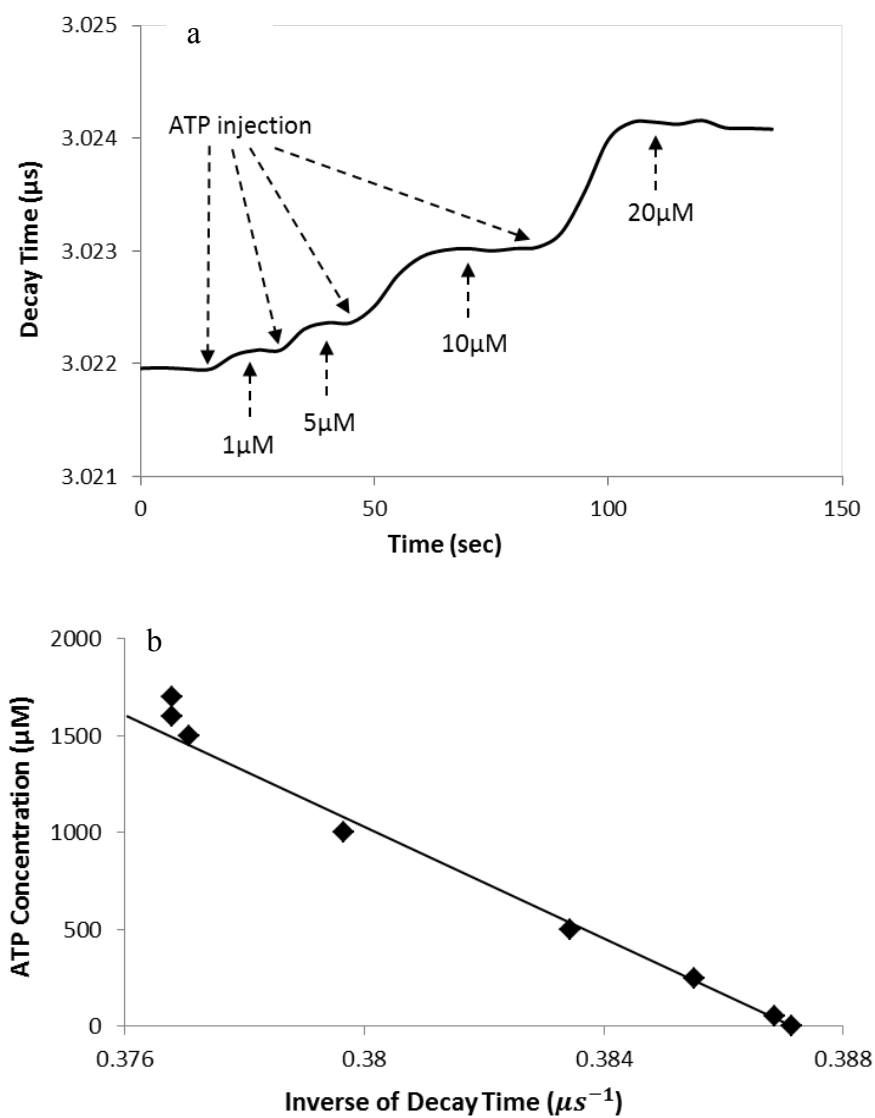


Figure 4-4: (a) A typical sensor response at low ATP levels (1, 5, 10 and 20 μM) and (b) a representative calibration curve showing a linear relationship between the inverse of decay time and the ATP concentration up to 1.5 mM.

4.3.2 The effects of ADP, AMP, adenosine, ascorbate and pH on the ATP biosensor

To examine the effect of ADP, AMP, and adenosine, three ATP biosensors were first equilibrated in the PBS solution without ATP and other adenine nucleotides and then a stock solution of ADP, AMP, or adenosine was added to a final concentration of 200 mM in the PBS and the decay time was recorded. It was found that the ATP biosensors developed in this study exhibited no responses to adenosine, AMP and ADP (Figure 4-5). Similarly, ascorbate (400 μ M) did not exhibit any effect on the ATP biosensors (data not shown).

For the pH test, the responses of three ATP biosensors were tested at the ATP concentration of 100 μ M. The values of pH were chosen based on pH in the normal organism tissues which mostly varies from 6.5-7.5 (Gerweck and Seetharaman 1996). No significant effects of pH were found on the ATP biosensors (Figure 4-6). This is consistent with the previous study (Llaudet, Hatz et al. 2005).

4.3.3 Compensation of the ATP biosensor under different oxygen levels

A linear relationship between the parameter k and the oxygen concentration was found between 10% and 20% oxygen levels (Figure 4-7b) as described in Equation 8. Furthermore, the errors in the ATP measurement by the compensation method for the oxygen level of 15% were found to be less than 5% at different ATP levels (Figure 4-8).

4.3.4 Sensor stability

The responses of three sensors to 200 μM ATP solution were examined for five consecutive days. The signal strength of fluorescence, which is defined as the difference between the inverse of decay times measured at 0 and 200 μM ATP, gradually decreased and fell to about 65% at day 5 compared to day 1 (Figure 4-9). This may mainly attribute to the diffuse out of enzyme loosely entrapped at the top of the coating layer (Kueng, Kranz et al. 2004).

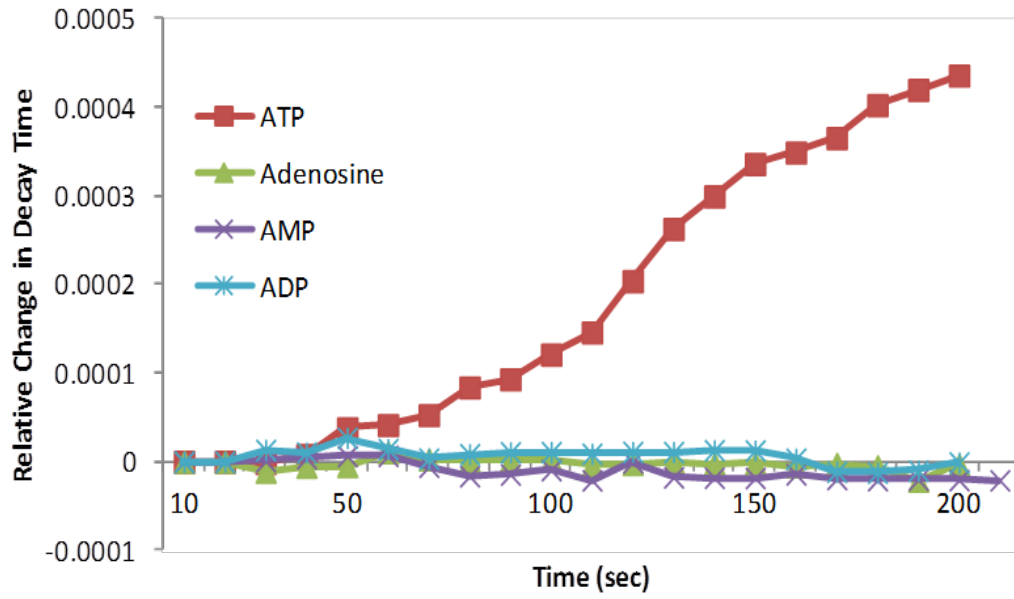


Figure 4-5: The typical reaction of the ATP sensor to ADP, AMP and adenosine of 200 μM compared to ATP of 100 μM .

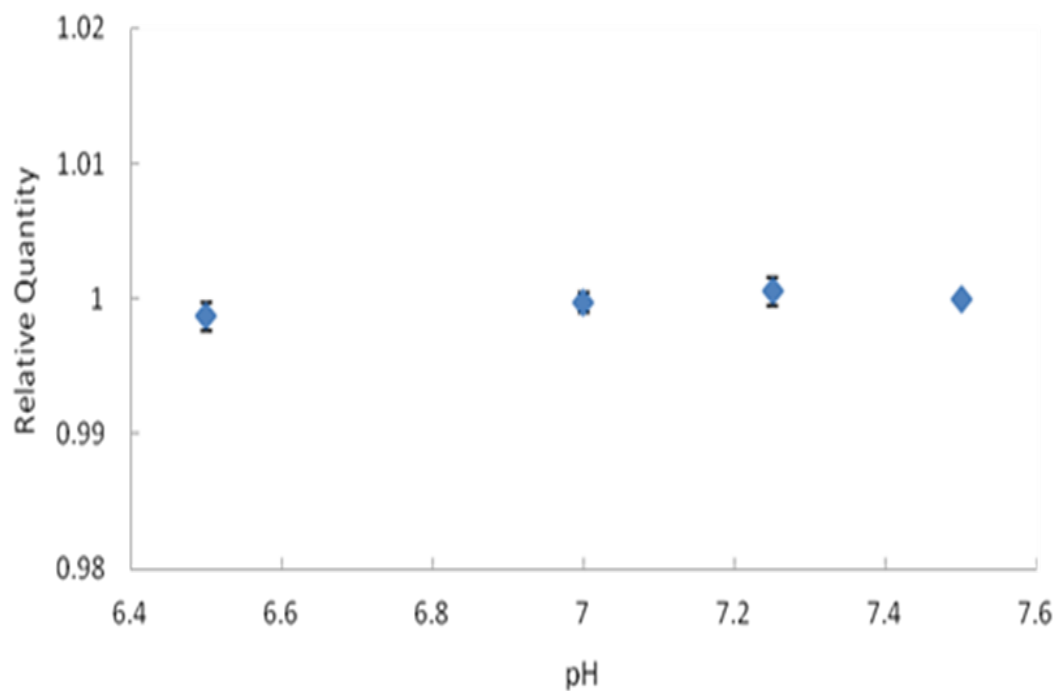


Figure 4-6: Normalized signal of the ATP sensor in response to 100 μ M ATP at different pH conditions (n=3). The data were normalized to the response at pH 7.5 and are expressed as mean values \pm standard deviation.

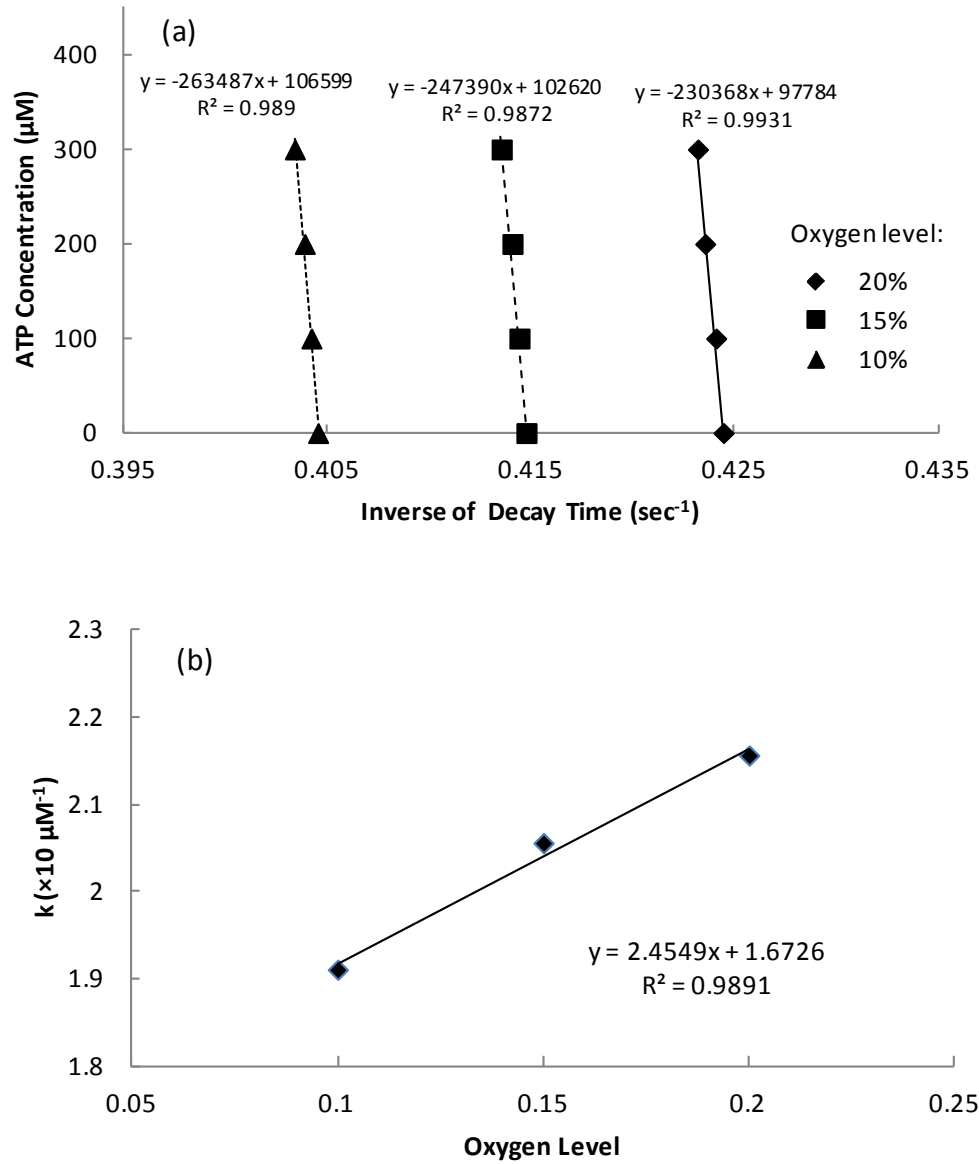


Figure 4-7: (a) Typical calibration curves obtained at different oxygen concentration and (b) the corresponding linear relationship between the parameter k and oxygen concentration.

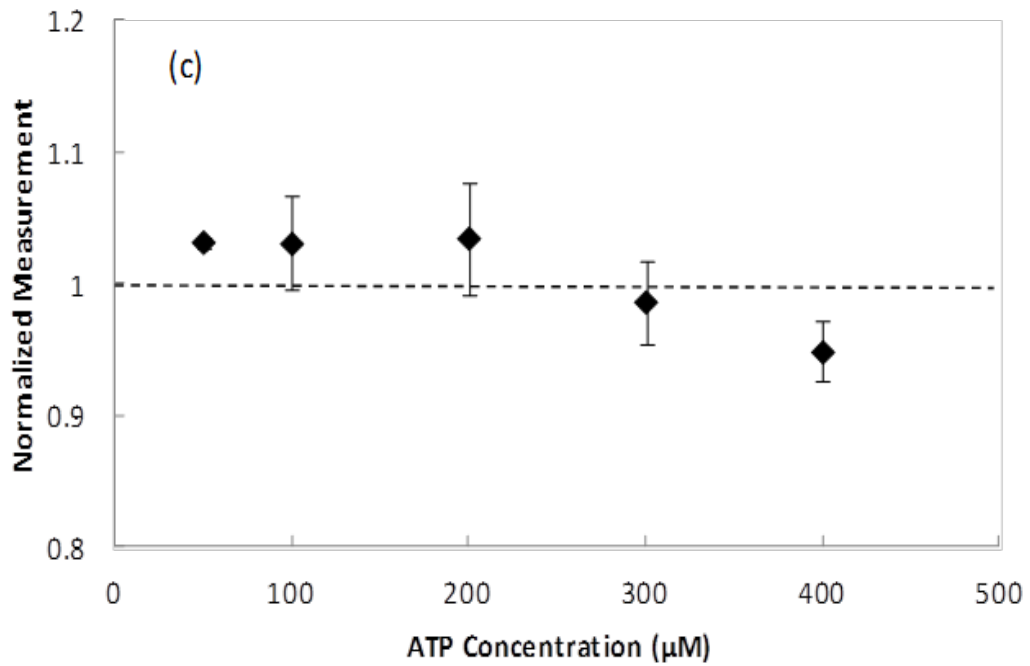


Figure 4-8: Accuracy of the oxygen compensation method on determination of ATP concentration at 15% oxygen level using the parameters obtained from the calibration tests at 10% and 20% oxygen levels ($n=3$). The data were normalized to the corresponding ATP concentration and expressed as mean values \pm standard deviation.

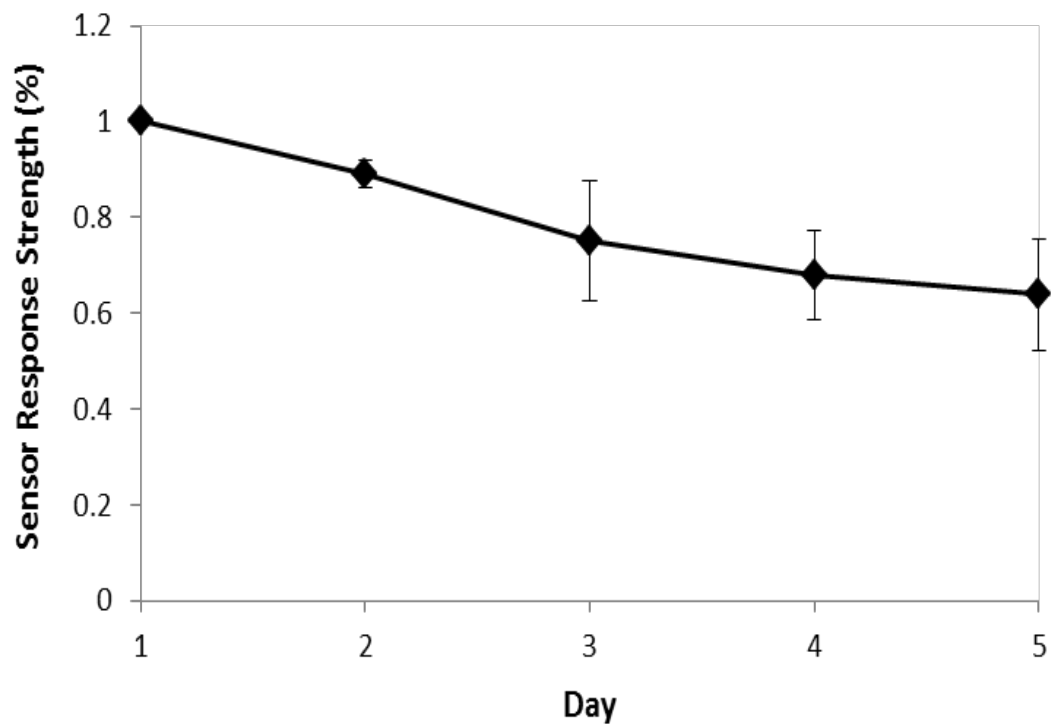


Figure 4-9: Stability of the ATP biosensor. The signal strength of fluorescence is defined as the difference between the inverse of decay times measured at 0 and 200 μM ATP. The data are expressed as mean values \pm standard deviation.

4.3.5 Measurement of extracellular ATP in porcine intervertebral disc

To verify the ability of the ATP biosensor for measuring tissue ATP concentration, a tissue measurement experiment was conducted. Porcine NP tissue was obtained from 8-12 month old pig and NP tissue was extracted. This NP tissue was frozen for one day and then immersed into PBS overnight to make sure all ATP was released into the solution. Then this NP tissue was washed three times using PBS and transferred into another PBS solution containing 200 μM ATP. After one hour the tissue was taken out and placed in a petri dish, the ATP sensor was inserted to measure the ATP concentration. The measurement was compared with the real ATP concentration to verify the ability of the sensor for tissue measurement. We found that our sensor has the ability to accurately measure tissue ATP content: the measured ATP contents are $103\% \pm 4.1\%$ to the real ATP content ($n=3$).

Typical responses of the oxygen and ATP sensors during the extracellular ATP measurement in the nucleus pulposus region of the porcine intervertebral disc were shown in Figure 4-10. After the tissue was exposed to the ambient condition (i.e., 20% oxygen) for a certain time (about 10 min), the oxygen level was still less than the ambient oxygen level (20%) shown in Figure 4-10. The differences in oxygen measurement between the ATP and oxygen sensors indicated oxygen consumption by enzymatic ATP breakdown and were used to determine ATP concentration using Equation 5 with k determined from the calibration tests at 10% and 20% oxygen levels. The extracellular ATP concentration in the nucleus pulposus region of the porcine intervertebral disc was $190 \pm 30 \mu\text{M}$ ($n=3$).

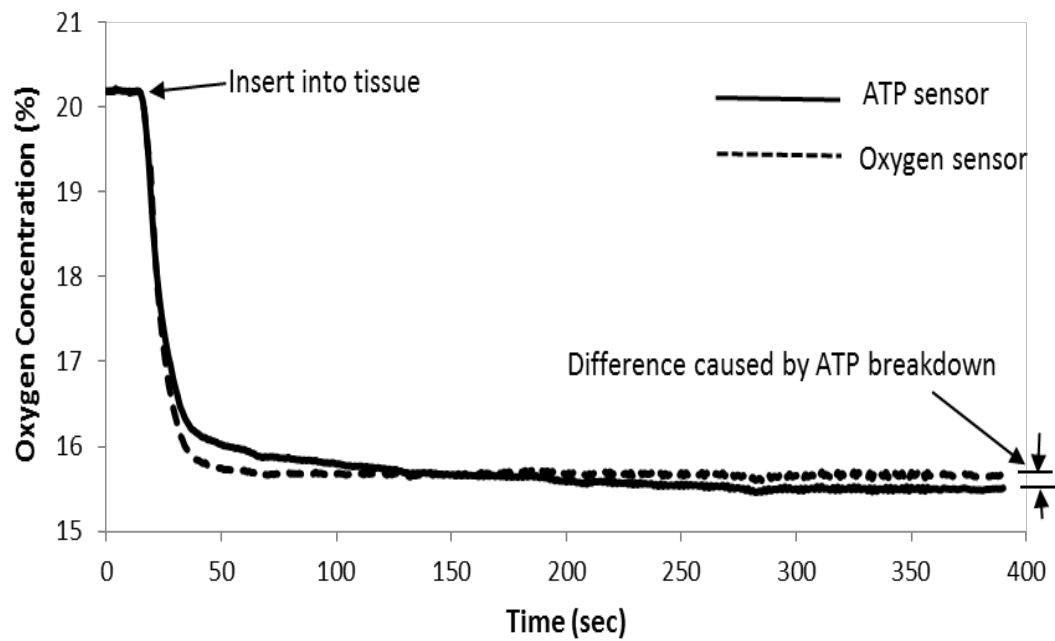


Figure 4-10: Typical responses of the oxygen and ATP sensors during the extracellular ATP measurement in the porcine intervertebral disc.

4.4 DISCUSSION

This study successfully developed a new optical biosensor for in-situ ATP measurement, which was demonstrated by the calibration test and the extracellular ATP measurement in the porcine intervertebral disc.

The optical ATP biosensor utilizes the principle of fluorescence emission of ruthenium complexes which does not exhibit any common electro active interferences by naturally occurring compounds (e.g., ascorbate) as described in previous studies of amperometric biosensors (Katsu, Yang et al. 1994; Kueng, Kranz et al. 2004; Llaudet, Hatz et al. 2005). Therefore, the optical ATP biosensor provides a good alternative method for ATP measurements especially for in-vivo and in-situ measurements.

When the optical ATP biosensor is immersed in a solution containing certain ATP levels, ATP diffuses into the coating layer through the microspores and is catalyzed by enzymes. The process of diffusion is driven by a concentration gradient. Since the concentration gradient is determined by normalizing the concentration difference between the solution and the enzyme layer of the ATP biosensor by the thickness of coating, the response time of the biosensor inversely depends on the coating thickness. Therefore, the response of the ATP biosensor can be further improved by decreasing the thickness of coating. Furthermore, since the rate of oxygen consumption in the enzymatic reactions depends on the concentration of enzymes, the sensitivity of the ATP biosensor can be enhanced by increasing the enzyme concentration in the coating layer.

In the extracellular ATP measurement of porcine intervertebral discs, the oxygen level in the tissue still remained low (Figure 6) after the temperature of the tissue was equilibrated with the ambient condition (i.e., 25°C and 20% oxygen level). It suggested that the oxygen solubility in biological tissues is different from the

condition in the calibration test. Therefore, the oxygen compensation method established in the study is a key component for precise in-situ ATP measurement. By using this method, the optical ATP biosensor was able to determine the extracellular ATP content in the intervertebral disc.

The ambient air temperature for calibration is often around 25 °C and the body temperature is around 37 °C. Since the principle of oxygen sensing using ruthenium complexes involves energy transfer, previous studies have demonstrated that Stern-Volmer quenching constant (K_{sv}) and τ_0 are dependent on temperature (Lakowicz 2006; Morris, Roach et al. 2007). In addition, the enzyme activities could be affected by temperature. Therefore, the temperature effects on k , τ_0 and K_{sv} need to be compensated if the temperature at the measurement sites is different from that in the calibration test.

Luciferin-luciferase assay has long been used for determining the extracellular ATP content (Leach 1981). This method has many advantages such as ability to detect ATP at low concentration (Spielmann, Jacob-Müller et al. 1981). However, Luciferin-luciferase assay also requires strict conditions and operations and many factors can cause contamination to the assay which limits its application in in-vivo/in situ measurements. Additionally, Luciferin-luciferase assay is not feasible for real time monitoring ATP content change (Lundin 2000). Electrochemical ATP sensors with high sensitivity were developed by other researchers (Kueng, Kranz et al. 2004; Llaudet, Hatz et al. 2005). However, these sensors measured ATP by detecting current produced during chemical reaction and thus can be affected by other charged molecules such as ascorbic acid and urinate (Miele and Fillenz 1996). For example, ascorbate has a concentration range of 200-400 mM in human tissue and can generate up to 100 nA of current when using an electrode with 0.5 mm length and 50

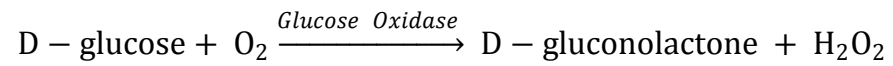
μm diameter (Rice 2000; Llaudet, Hatz et al. 2005). In addition, the chemical reaction required in electrochemical ATP sensors may be affected by substances in body tissues. For instance, the ATP sensor developed by Kueng et al. requires glucose to be present at a known concentration. In human tissues, however, glucose content varies from different tissue and at different time points during a day (Maggs, Jacob et al. 1995; Daly, Vale et al. 1998). These factors make electrochemical ATP sensors difficult to be used for *in vivo/in situ* ATP measurement. The design of our sensor, however, has advantages in *in vivo/in situ* ATP measurement and potential for real time monitoring changes in ATP level. Furthermore, it was reported that that extracellular ATP concentration can reach several hundred micro molar at tumor interstitium (Pellegatti, Raffaghello et al. 2008), while extracellular ATP concentrations are around 4 mM in rabbit central nervous system during systematic inflammatory response (Gourine, Dale et al. 2007). Therefore, the new ATP sensor developed in our study can be used to monitor ATP level in those in-vivo conditions.

A new optical ATP biosensor was successfully developed with less chemical interference. The compensation method was also established to enable the new biosensor to detect ATP at different oxygen levels. This study demonstrated that the newly developed optical biosensor is feasible for in-situ extracellular ATP measurement.

4.5 OTHER OPTICAL SENSORS

Other optical sensors including oxygen sensor and glucose sensor were fabricated using similar mechanism with ATP sensor described above. Only the coating layer containing Ruthenium complex is applied to optical fiber to fabricate oxygen sensor; the coating layer is modified to be able to sustain under direct contact with tissues. G3POX and GK was replaced by glucose oxidase (Sigma Aldrich, St. Louis, MO,

USA) to yield glucose sensors as described by previous literatures (Wolfbeis, Oehme et al. 2000; Endo, Yonemori et al. 2006). These sensors were also used to measure oxygen content and glucose content distribution in IVD as shown in Chapter 5. The enzyme catalyzed reaction of glucose oxidation is as following:



A typical decay time- time reaction of optical glucose sensor is shown in Figure 4-11. A typical calibration of $1/\tau$ versus glucose concentration of this optical glucose sensor is also shown in Figure 4-12.

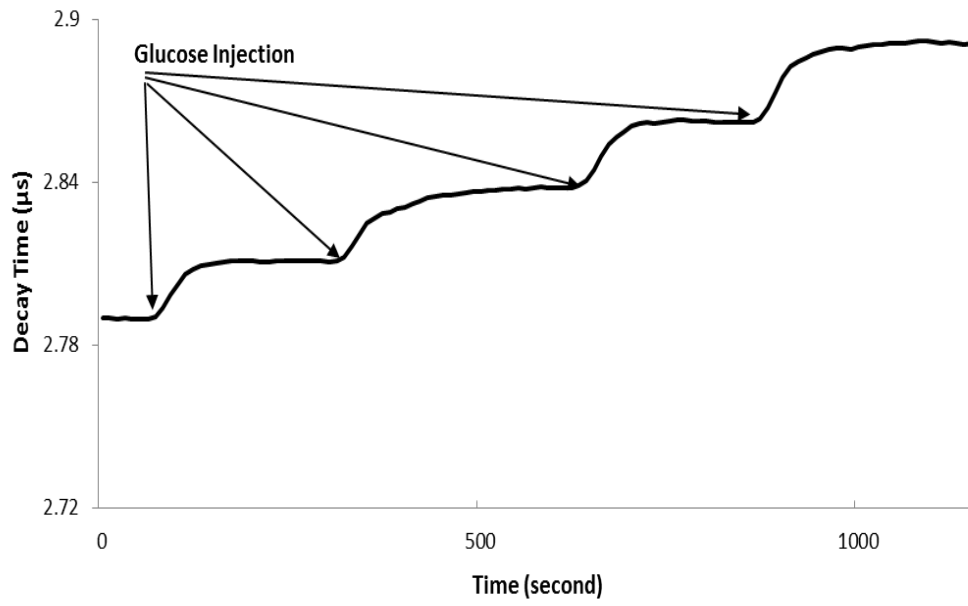


Figure 4-11: A typical response of glucose sensor to 0.05, 0.1, 0.15 and 0.2 g/L glucose solutions.

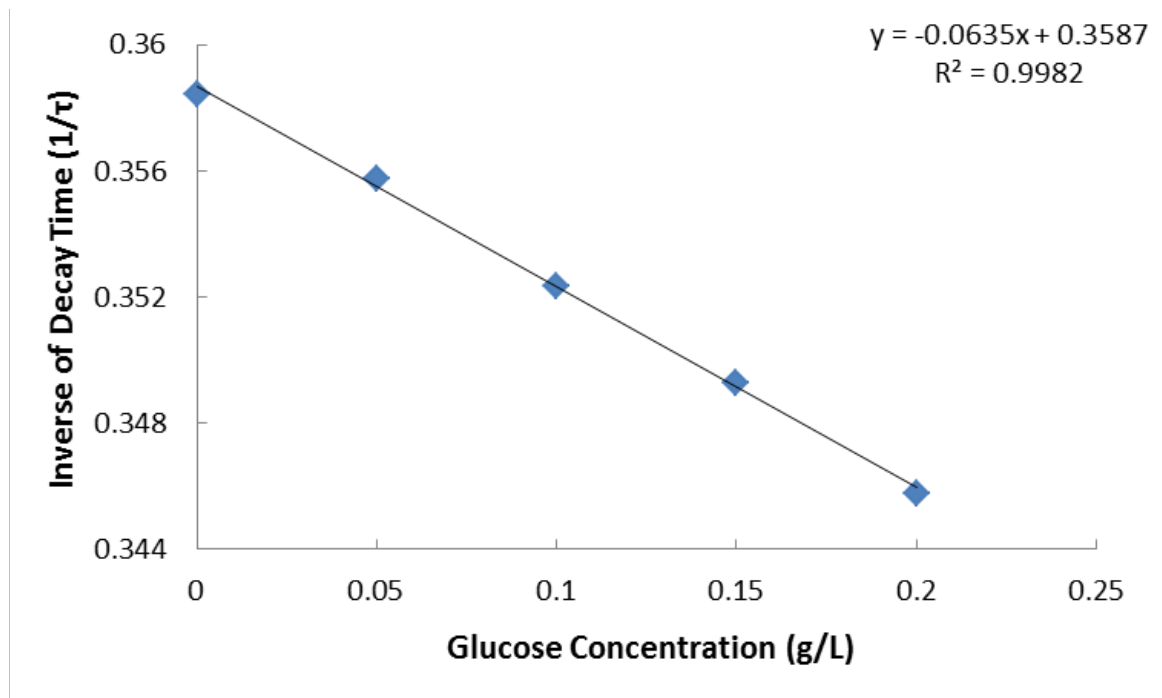


Figure 4-12: A typical calibration curve of a glucose optical sensor.

CHAPTER 5 ENERGY METABOLISM OF IVD UNDER COMPRESSIONS

5.1 INTRODUCTORY REMARKS

There are many reasons for people to miss work; one of the leading contributors is low back pain (LBP), which is believed to affect 80% of the population at some point during their lifetime. Suffering from back pain is the chief complaint of 5% of people who visit the doctor in the US (2008). The total medical cost related to low back pain in the US exceeds 100 billion dollars every year (Willis 2009). Many factors were discovered to contribute to LBP. While the exact cause of LBP remains to be clarified, recent studies revealed that intervertebral disc degeneration is closely related to LBP (Luoma, Riihimaki et al. 2000; Roberts 2003). Aging, nutrition supply, mechanical factors and many other aspects contribute to disc degeneration, however, the pathology of disc degeneration is not yet determined (Hadjipavlou, Tzermiadianos et al. 2008; Kandel, Roberts et al. 2008; Adams, Dolan et al. 2009).

IVD is a strong yet deformable tissue that lies between vertebrae and is important for the whole spine structure. Cells only form 1% of the disc volume, however, they play crucial roles in maintaining disc integrity and health by producing ECM components and the chemicals responsible for breaking down the matrix (Bibby, Jones et al. 2001). These processes are highly energy demanding (Im, Freshwater et al. 1976; Hirschberg, Robbins et al. 1998; Prydz and Dalen 2000). Cells consume large amount of adenosine triphosphate (ATP), which is the main cell energy source and generated via glycolysis and mitochondrial respiration with the consumption of glucose and oxygen. IVDs are under daily cycling mechanical loading *in vivo*; it is reported that mechanical loading can alter transport of oxygen and glucose and release

in the IVD and production of ATP and ECM synthesis of IVD cells *in vitro* (Ohshima, Urban et al. 1995; Huang and Gu 2008; Korecki, Kuo et al. 2009; Fernando, Czamanski et al. 2011; Salvatierra, Yuan et al. 2011). This may indicate the change of overall energy production within the IVD when subjected to mechanical loading. IVD is the biggest avascular cartilaginous tissue in the human body and IVD becomes avascular a few years after the fetal stage, the nutrients supply of IVD is mainly by diffusion, which is not a very efficient transport mechanism and can be hindered by many factors (Urban, Smith et al. 2004); such as endplate calcification and change of proteoglycan content (Grunhagen, Shirazi-Adl et al. 2011). When this transport mechanism is interrupted, the consequence is insufficient nutrient supply which causes decreased energy production and is the main contributing factor in disc degeneration (Urban, Smith et al. 2004; Smith, Nerurkar et al. 2011).

In addition to the important role of intracellular ATP as cellular energy currency, cells constantly release ATP which can regulate cell metabolism, survival, and growth through the purinergic signaling pathway (Burnstock 2006). Hydrolysis of extracellular ATP produces adenosine diphosphate (ADP) and adenosine which can modulate diverse cellular actions via purinergic P2Y and P1 receptors, respectively (Burnstock 2006; Jacobson and Gao 2006), while it also releases inorganic pyrophosphate and phosphate which are strongly associated with mineral crystal formation or tissue calcification (Ryan, Kurup et al. 1992; Johnson and Terkeltaub 2005). Due to the avascular nature of the IVD, ATP and its derivatives may accumulate extracellularly within the disc and be able to influence the biological function of the IVD.

Our recent studies showed that mechanical loading can promote ATP production and release of IVD cells in a 3-dimensional agarose gel model, while cells from two

different anatomical regions, annulus fibrosus (AF) and nucleus pulposus (NP), exhibited different energy metabolism (Fernando, Czamanski et al. 2011; Salvatierra, Yuan et al. 2011). However, the *in vivo* environment involves the cell-ECM interaction, a variety of mechanical events (e.g., tensile/compressive stress and hydrostatic pressure), compression-dependent transport properties, and inhomogeneous distribution of nutrients (Yao and Gu 2007; Huang and Gu 2008). Therefore, the objective of our study is to investigate the energy metabolism in the AF and NP region of the IVD under mechanical loading.

5.2 MATERIALS AND METHODS

Lumbar spines of 4–8 month-old pigs were obtained within 2 hours of sacrifice. Functional spinal units (FSUs) were isolated from lumbar region of the spine by making parallel transverse cuts through the vertebrae. The bone part of the vertebrae was removed till the endplate was disclosed. The FSUs were placed in custom made compression chambers and cultured in high glucose Dulbecco's Modified Eagle Medium (DMEM, Invitrogen Corp., Carlsbad, CA, USA) containing 10% fetal bovine serum (FBS, Invitrogen Corp, Carlsbad, CA, USA) and 1% antibiotic-antimitotic (Invitrogen Corp, Carlsbad, CA, USA) in an incubator at 37°C overnight. The medium was continuously circulated at 0.37ml/min, which is about twice the rate of blood flow to the disc *in vivo*. For the whole disc compression test, the disc height was measured at 3 locations on the disc surface and then divided in to 5 groups. A custom made bioreactor with circulating culture medium was developed to conduct all compression experiments (Figure 5-1). For static compression groups, the discs were subjected to 10% compressive strain for 2 hours and 1 hour, respectively; for dynamic compression groups, the discs were placed under 1 Hz and 0.1 Hz of sinusoidal compression with 10% maximum strain for 1 hour. The control group was left

undisturbed in the incubator for the duration of the experiment. After the experiment, a transverse cut was made on each unit to expose the AF and NP. The pH value of NP region was detected using pH meter from Cole-Palmar Co. (Vernon Hills, IL, USA). Extracellular ATP concentrations were measured using custom made optical ATP sensor (Wang, Huang et al. 2013). The tissue samples (~10 mm³) were then harvested from the locations shown in Figure 5-2. The samples obtained from AF and NP regions were used to determine the lactate, ATP, and DNA contents. ATP and lactate were released from tissue samples using perchloric acid treatment (Leach 1981) and then determined using the Luciferin-luciferase method (Sigma, St. Louis, MO, USA) and an enzymatic assay (Sigma, St. Louis, MO, USA), respectively.

Cell viability was determined using LIVE/DEAD® Cell Viability Assay (Invitrogen, Carlsbad, CA, USA). DNA content of each harvested sample was determined using a Qubit™ fluorometer and Quant-iT dsDNA HS Assay Kit (Invitrogen Corp., Carlsbad, CA). The lactate and ATP contents were normalized by the DNA content. A one-way ANOVA followed by Tukey test was performed to examine differences in ATP and lactate contents between AF and NP regions and experimental groups of each region using SPSS software (IBM, Armonk, NY, USA).

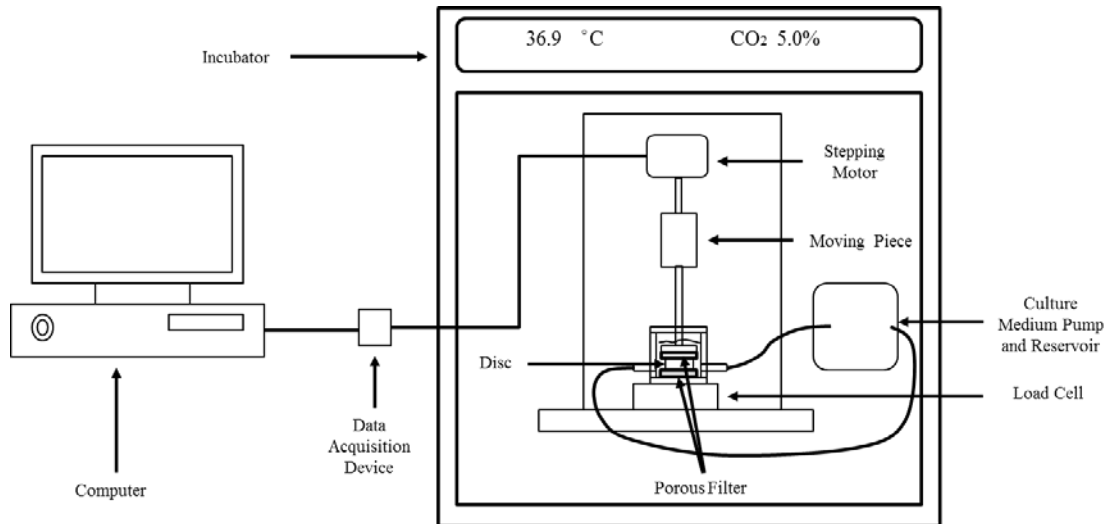


Figure 5-1: Bioreactor system for whole disc loading experiments

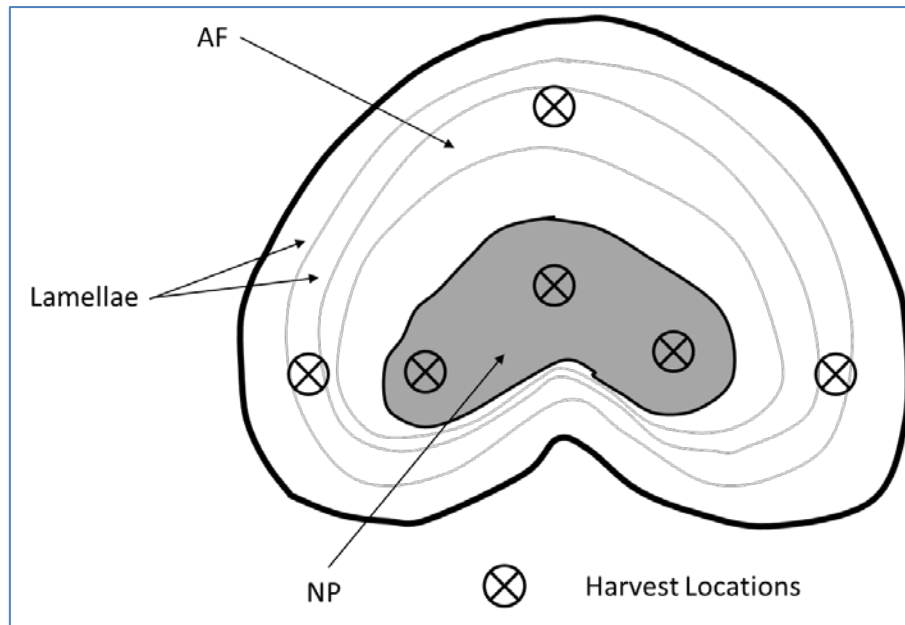


Figure 5-2: Harvest locations of AF and NP from IVD



Figure 5-3: Actual harvest locations of IVD and porcine IVD dimension

5.3 RESULTS

The live/dead cell staining showed a high cell viability after compression experiments with the AF and NP regions having the cell viability of $88.0\% \pm 3.3\%$ and $84.5\% \pm 2.5\%$, respectively (Figure 5-4).

5.3.1 *Effects of static compression*

Static compression significantly increased lactate accumulation in both AF and NP regions after 1 hour, whereas lactate accumulation was reduced to a non-significant level in the AF and NP regions compared to the non-loading group (Figure 5-5). Accordingly, pH was significantly decreased in both AF and NP regions one hour after application of static compression, whereas after 2 hours of compression, a significant difference in pH was only seen in the AF region, but not in the NP region (Figure 5-6). Total ATP content in all static compression groups was significantly increased (Figure 5-7). In addition, the 1 hour compression group exhibited higher ATP content than the 2 hour compression group for the NP region (Figure 5-7).

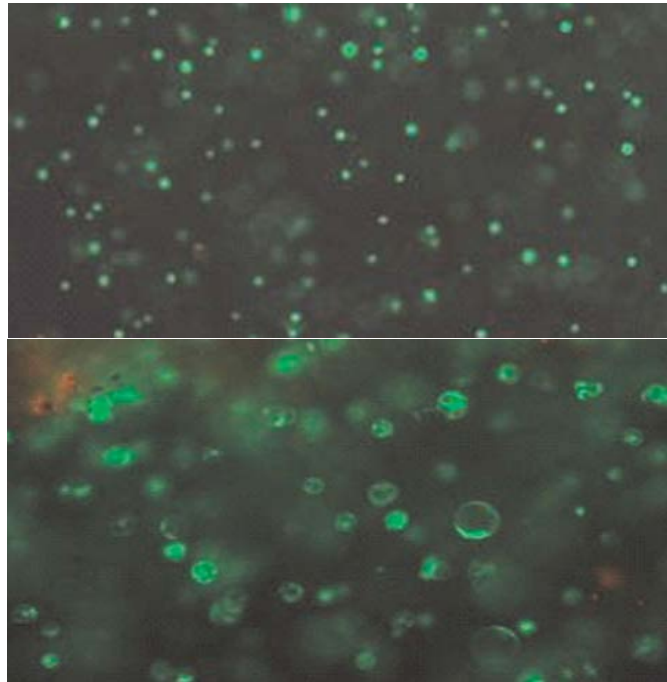


Figure 5-4: Cell viability stain of AF (up) and NP (down) tissues. Green indicates live cells while red indicated dead cells.

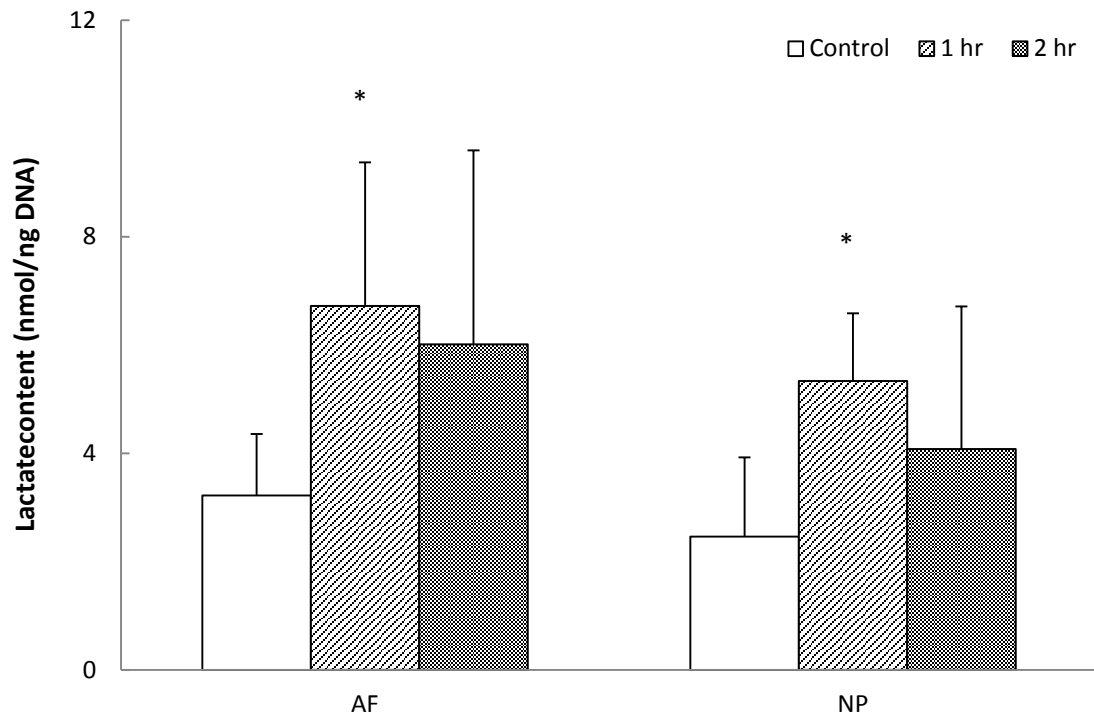


Figure 5-5: Effects of static loadings on lactate content (n=6), *: significantly different from the control group (p<0.05);

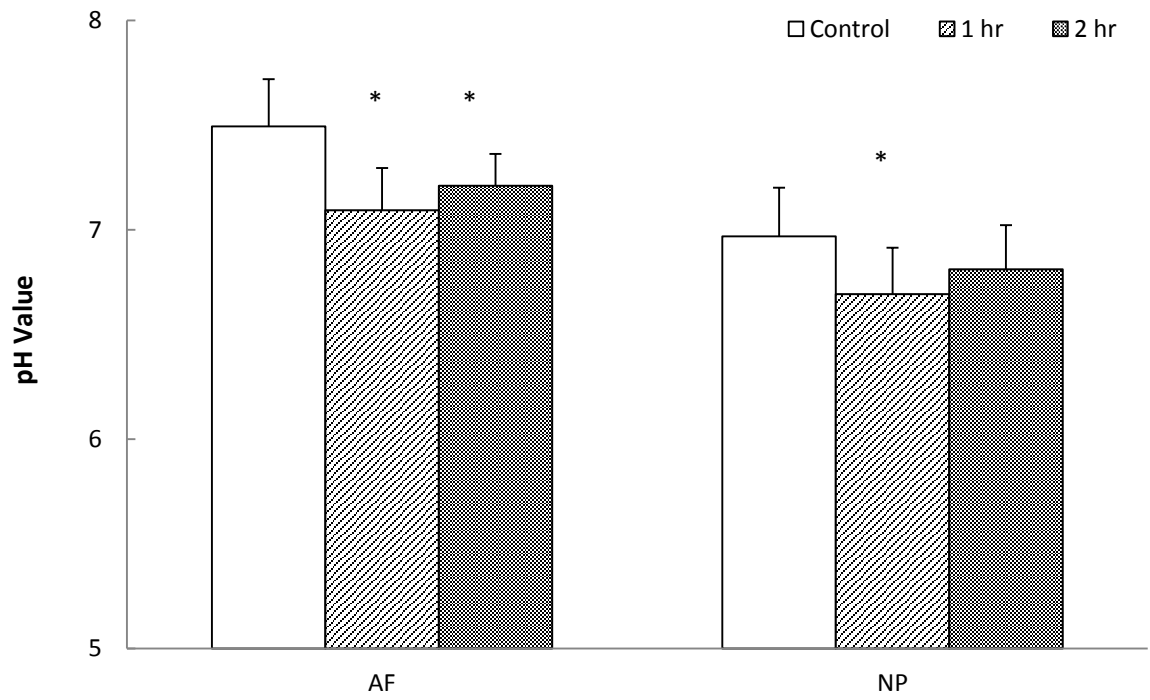


Figure 5-6: Effects of static loadings on pH value (n=8), *: significantly different from the control group (p<0.05).

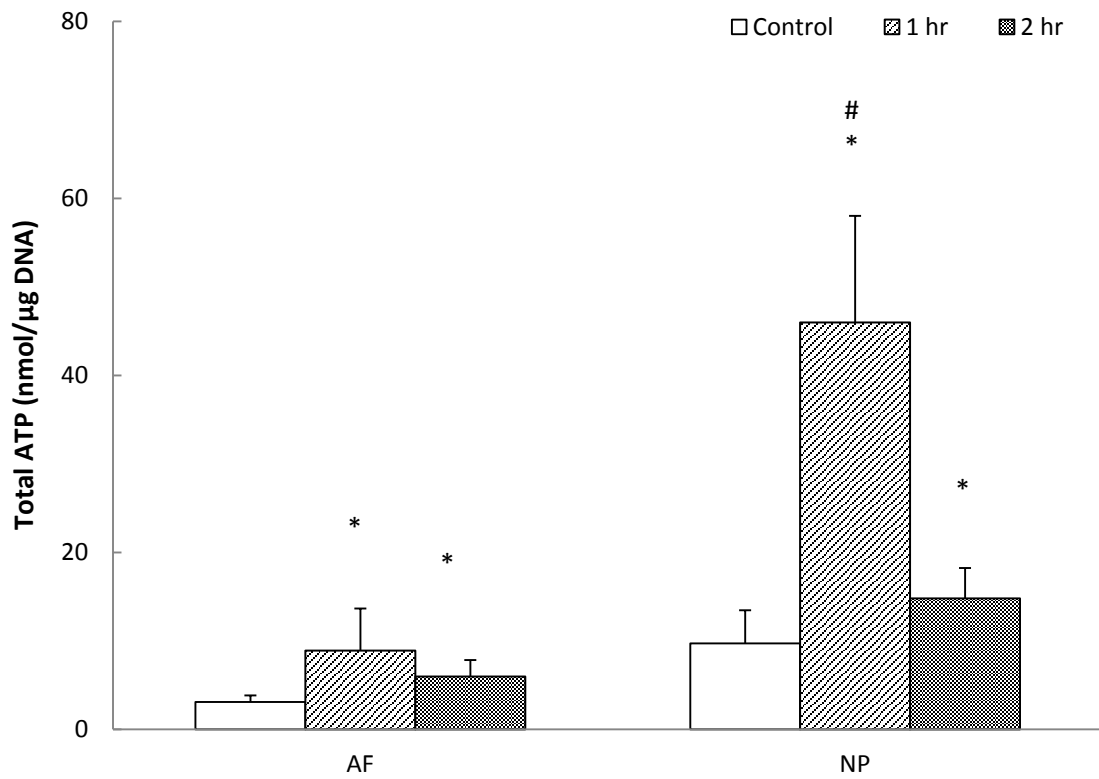


Figure 5-7: Effects of static loadings on total ATP content (n=8). *: significantly different from the control group ($p < 0.05$); #: significantly different from the other groups ($p < 0.05$).

5.3.2 *Effects of dynamic compression*

Only dynamic compression of 1 Hz significantly increased lactate accumulation (Figure 5-8). However, all dynamic loading conditions significantly decreased pH and increased total ATP content in both AF and NP regions (Figure 5-9 & 5-10). In addition, frequency-dependent differences were found in lactate accumulation and total ATP content. Lactate accumulation was significantly higher in the 1Hz compression group than the 0.1 Hz and static (0 Hz) compression groups (Figure 5-8) for both AF and NP regions. The total ATP content was significantly higher in the 0.1 Hz compression than the 1 Hz and static (0 Hz) compression groups for the AF region, while the 1 Hz compression group exhibited significantly lower ATP content than the 0.1 Hz and static (0 Hz) compression groups for the NP region (Figure 5-10).

5.3.3 *Comparison between AF and NP regions*

Under all loading conditions, the NP region exhibited significantly lower pH values and higher total ATP contents than AF (Figure 5-11 and Figure 5-12). There were no significant differences in lactate accumulation between the AF and NP regions for all loading conditions.

5.3.4 *Extracellular ATP content in the NP region*

A high level of extracellular ATP content was measured at the NP region ($165.3 \pm 40.8 \mu\text{M}$). Under both static and dynamic compression, the extracellular ATP content was significantly reduced in the NP region (Figure 5-13).

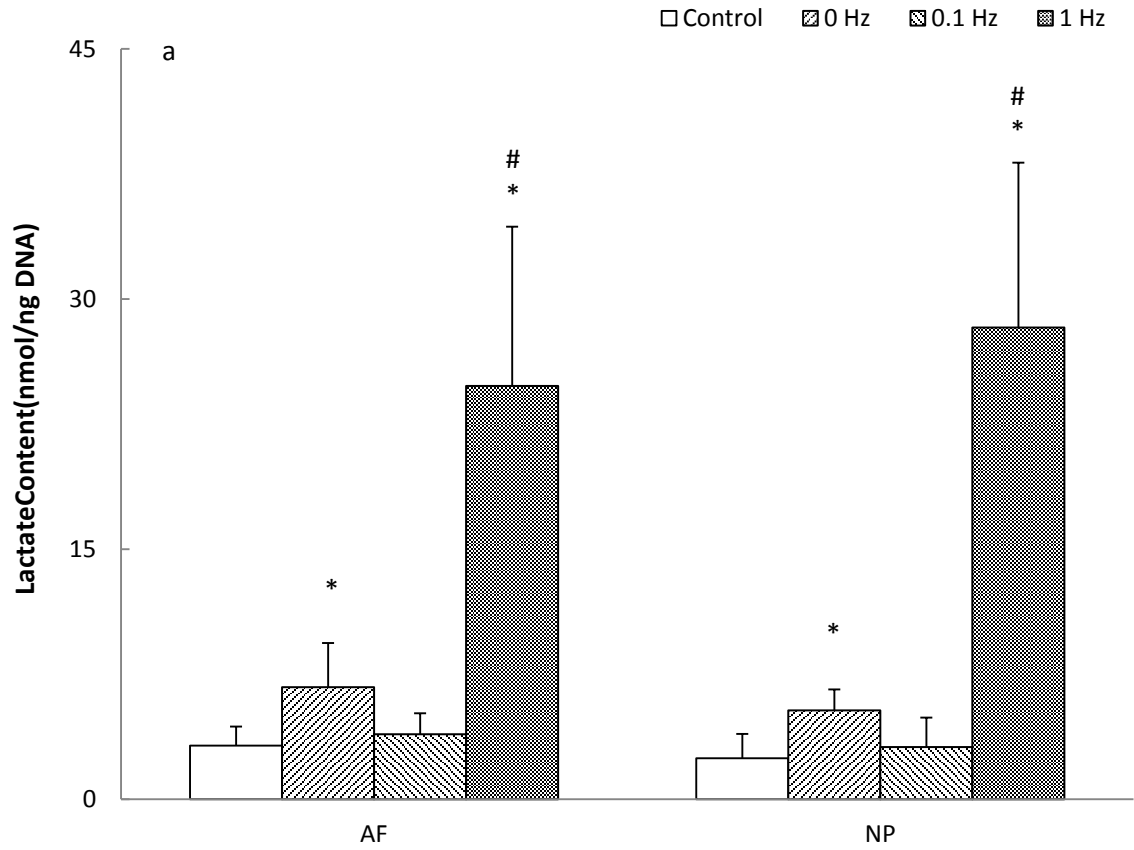


Figure 5-8: Effects of dynamic loadings on lactate accumulation (n=6). Static compression represents as 0 Hz. *: significantly different from the control group (p<0.05); #: significantly different from the other groups (p<0.05).

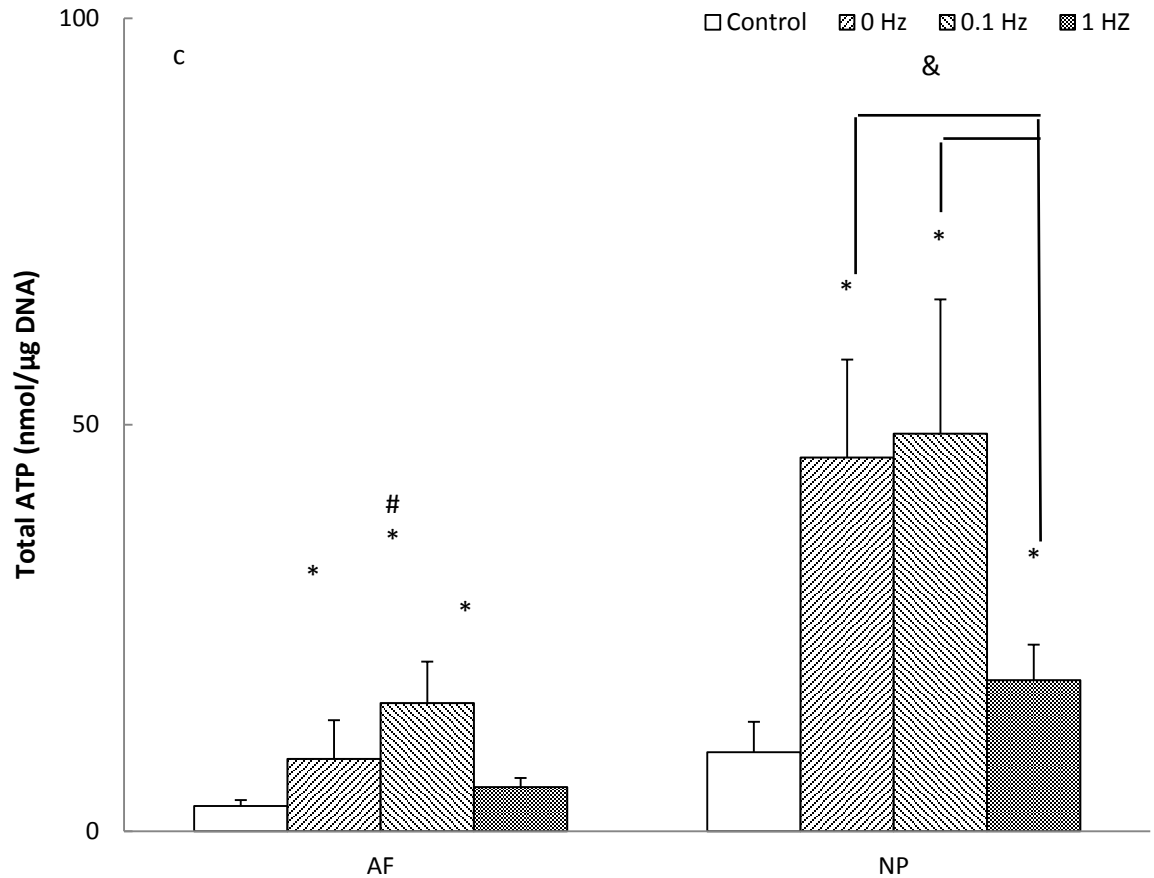


Figure 5-9: Effects of dynamic loadings on total ATP (n=8). Static compression represents as 0 Hz. *: significantly different from the control group ($p<0.05$); #: significantly different from the other groups ($p<0.05$); & significant difference between two groups ($p<0.05$).

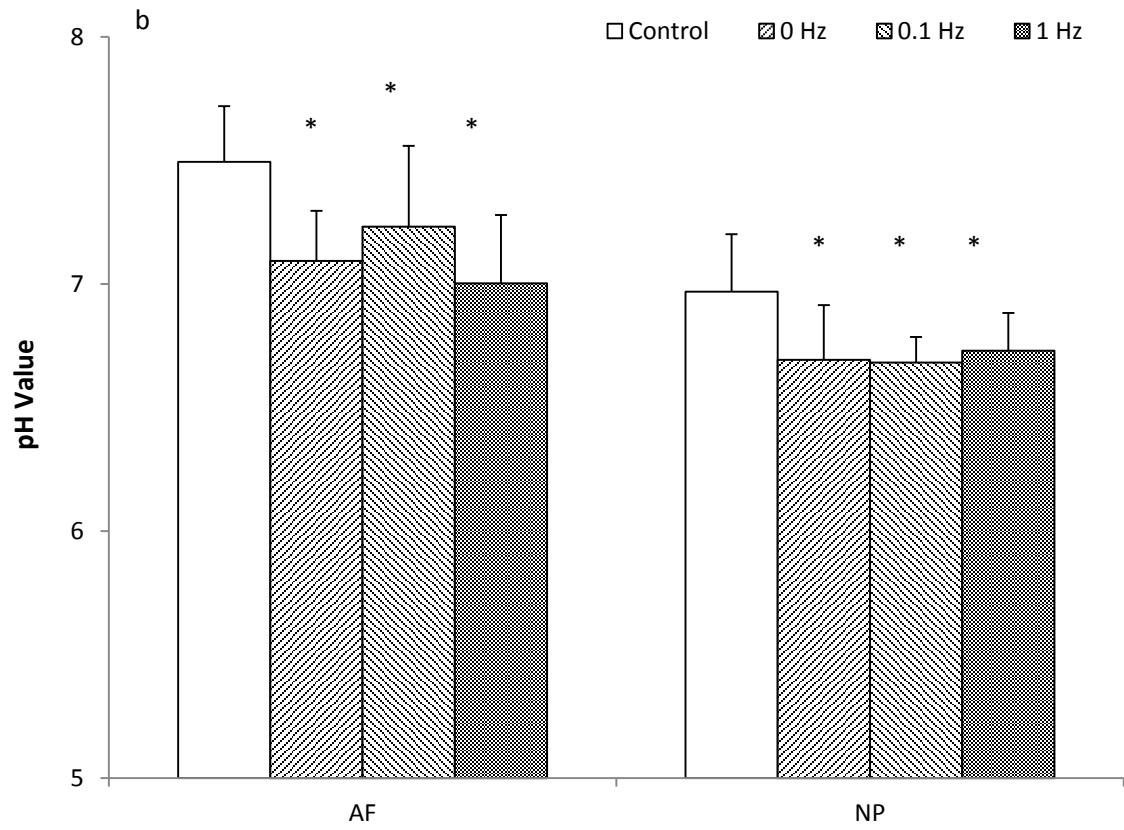


Figure 5-10: Effects of dynamic loadings on pH value (n=8). *: significantly different from the control group ($p < 0.05$).

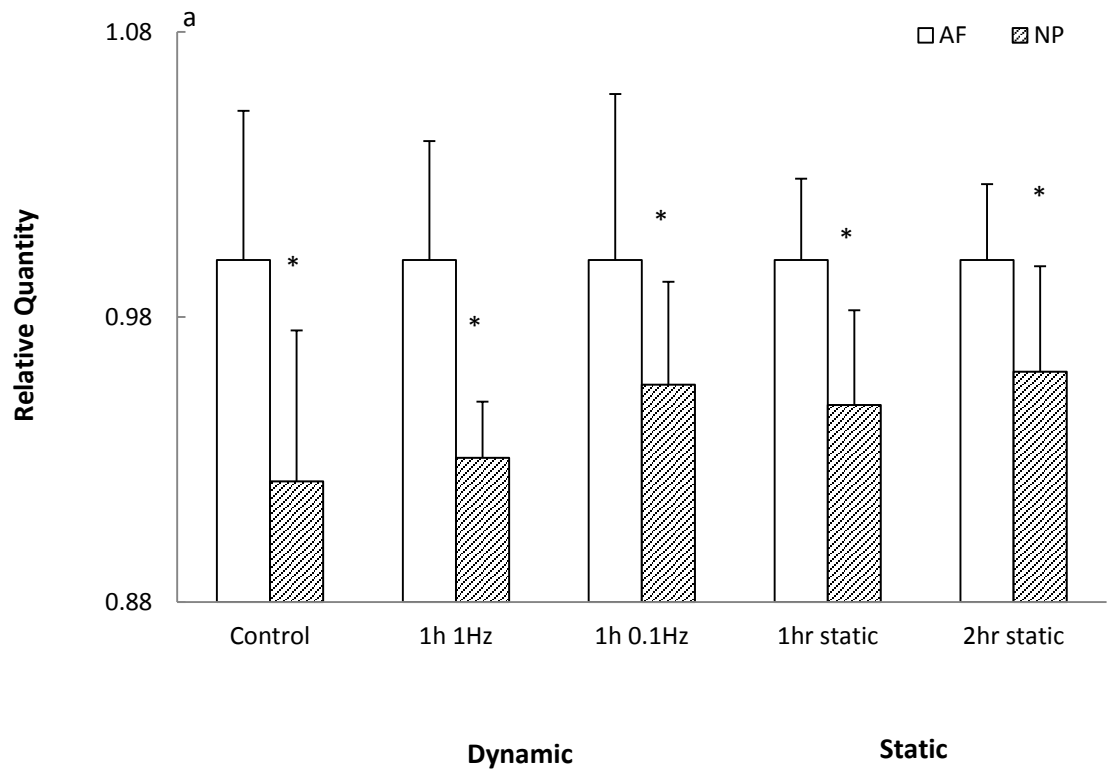


Figure 5-11: Comparison of pH between the AF and NP regions (n=7). *: significantly different from the control group (p<0.05).

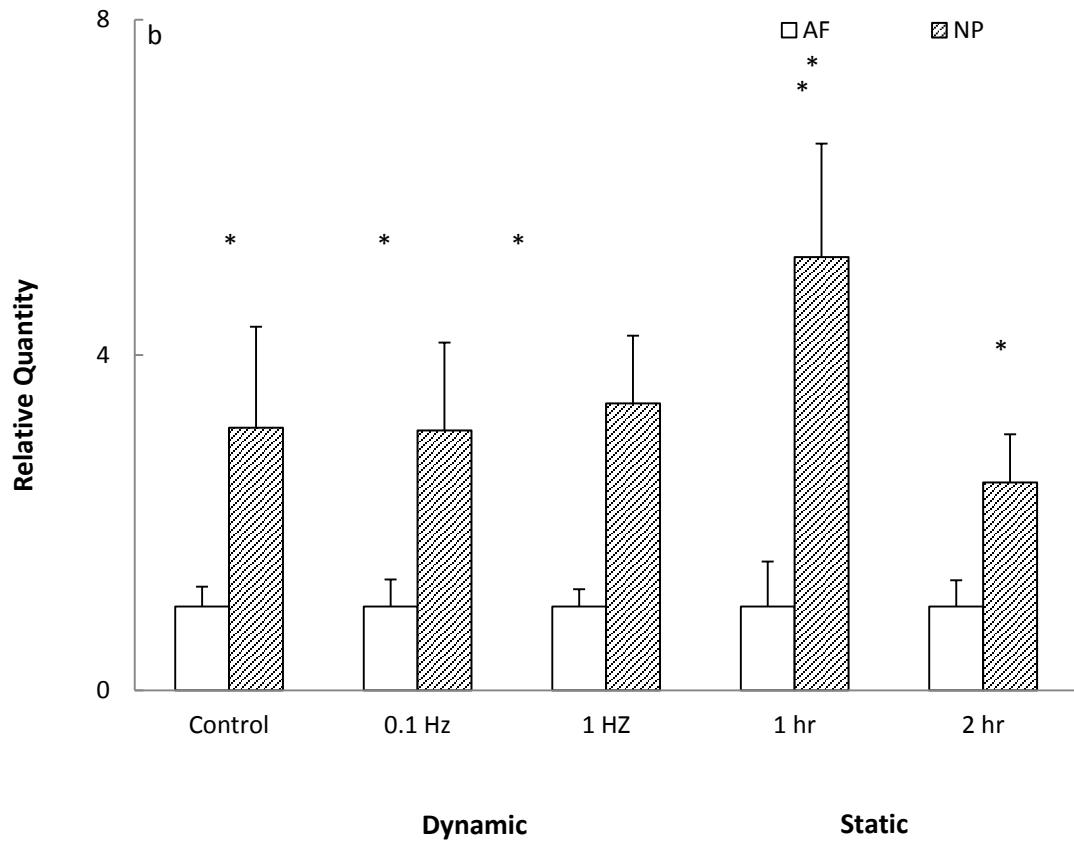


Figure 5-12: Comparison of total ATP content between the AF and NP regions (n=8).
*: significantly different from the control group (p<0.05).

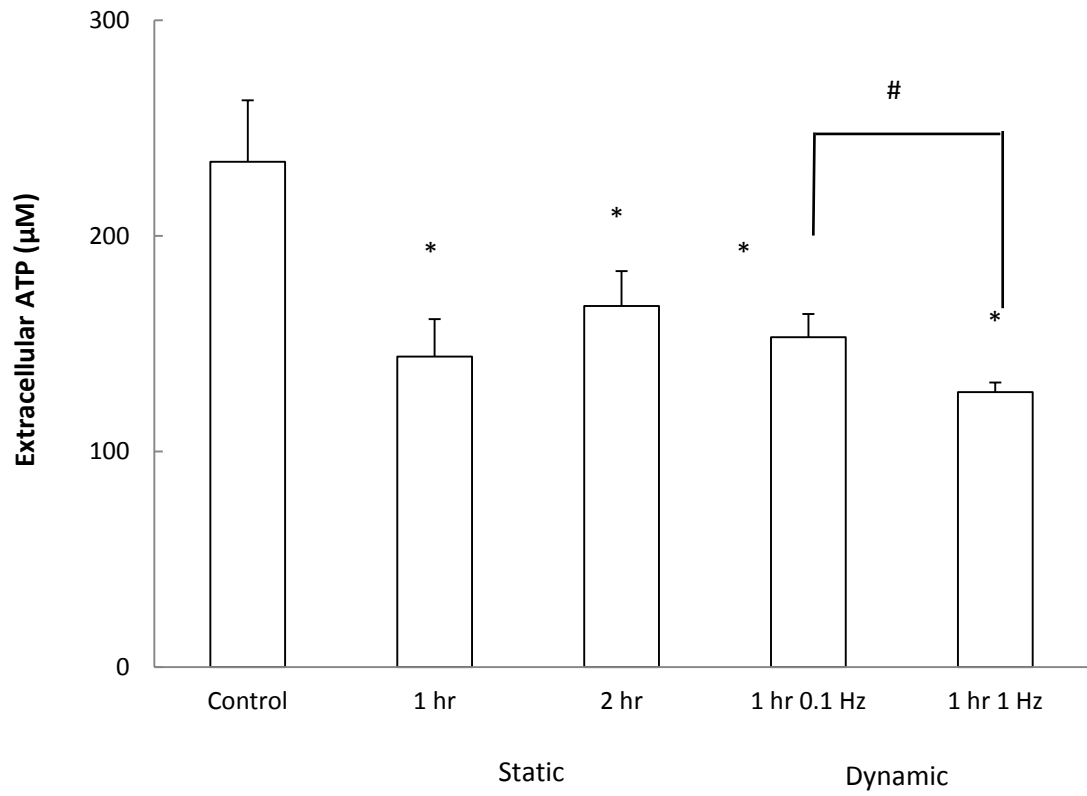


Figure 5-13: Effects of static and dynamic compression on extracellular ATP content in the NP regions (n=5). *: significantly different from the control group ($p<0.05$); # significant difference between two groups ($p<0.05$).

5.4 DISCUSSION

ECM synthesis is an ATP demanding process, especially proteoglycan synthesis in which ATP serves not only as an energy source, but also as a building block in the formation of UDP-sugars and 3'-phosphoadenosine 5'-phosphosulphate (PAPS) (Hirschberg, Robbins et al. 1998; Prydz and Dalen 2000). Because of limited nutrient supply to the IVD, ATP production could be a restrictive factor for maintaining normal ECM synthesis of IVD cells. Furthermore, the IVD is subjected to a variety of mechanical loading, including compression, during spine motion. Compressive loading has been shown to up-regulate ECM gene expression of IVD cells (Chen, Yan et al. 2004; MacLean, Lee et al. 2004; Korecki, Kuo et al. 2009). However, whether up-regulation of gene expressions can increase ECM production may still depend on adequate ATP supply. Although our recent studies showed that both static and dynamic compressions promote energy production of IVD cells in an in-vitro 3-dimensional agarose gel model (Fernando, Czamanski et al. 2011; Salvatierra, Yuan et al. 2011), some *in vivo* environmental factors were not taken into account, such as cell-ECM interaction and complex mechanical stimuli. Therefore, this study investigated energy metabolism inside the IVD under compression. To our knowledge, this is the first study to demonstrate that mechanical compression affects in-situ energy metabolism in the IVD.

Static compression significantly increased total ATP content and lactate accumulation in both the AF and NP regions (Figure 3), suggesting that static compression promotes glycolysis and consequently increases ATP production in both NP and AF cells. This finding is supported by our previous study which showed that static compression promoted ATP production of AF cells in agarose culture (Fernando, Czamanski et al. 2011). A decrease in solute diffusivity (or tissue

permeability) caused by static compression (Huang and Gu 2008) may also facilitate extracellular lactate accumulation. Furthermore, a decrease in pH caused by static compression in both anatomical regions (Figure 3) may result from the increase in lactate accumulation.

Similarly, 1 Hz dynamic compression significantly increased total ATP content and lactate accumulation in both the AF and NP regions (Figure 4). It is in concurrence with our previous study and suggests that dynamic compression can promote ATP production of AF and NP cells via glycolysis (Fernando, Czamanski et al. 2011). Another factor for increasing ATP production could be an increase in transport of nutrients by dynamic compression (Huang and Gu 2008). In addition, higher lactate accumulation caused by dynamic compression may result in reduction of pH as seen in this study (Figure 4). Furthermore, compared to the other compression groups, significantly higher lactate accumulation found in the 1Hz compression group (Figure 4) suggests that more ATP may be produced in the 1 Hz dynamic compression group. However, significantly lower total ATP content found in 1 Hz dynamic compression group suggests that the 1 Hz dynamic compression group may exhibit higher cellular ATP consumption. These findings also indicate that dynamic compression of 1 Hz promotes energy-demanding cellular activities, such as ECM production (Korecki, Kuo et al. 2009).

Fluid pressurization occurs in the disc, especially in the NP region, when the IVD is subjected to compressive loading (Yao and Gu 2007). Since hydrostatic pressure has been shown to modulate cellular ECM biosynthesis (Ishihara, McNally et al. 1996; Handa, Ishihara et al. 1997), cellular ATP metabolism may be affected by hydrostatic pressure. In the static compression test, when a constant displacement is applied to the IVD, hydrostatic pressure reaches a peak and then gradually reduces to a lower

equilibrium level (Yao and Gu 2007). A statistically significant difference in total ATP content between the one and two-hour static compression groups seen in the NP region could be due to the effect of the time-dependent hydrostatic pressure. In addition, the finding that static compression significantly increased total ATP content in the NP region is not consistent with our previous study (Fernando, Czamanski et al. 2011) which found static compression exhibited no significant effect on ATP production of NP cells in the 3-dimensional agarose model. Since little fluid pressurization occurs in agarose gel under compression due to its high hydraulic permeability (Huang, Hagar et al. 2004), hydrostatic pressure induced in the IVD under static compression is a potential factor causing changes in the total ATP content of the NP region. Furthermore, solute transport and hydrostatic pressure in cartilaginous tissue under dynamic loading depend on loading frequency (Yao and Gu 2004). This could be the reason for the frequency-dependent differences seen in this study. Therefore, the effects of hydrostatic pressure on ATP metabolism of IVD cells needs to be further investigated.

Since both static and dynamic compressions can promote ATP release from IVD cells (Fernando, Czamanski et al. 2011; Salvatierra, Yuan et al. 2011), it is expected that extracellular ATP accumulation occurs in the IVD under compression, especially static compression, which can reduce transport rate of solutes in the IVD (Huang and Gu 2008). However, this study found that both static and dynamic compressions significantly reduced extracellular ATP content in the NP region, suggesting that compressive loading promotes hydrolysis of ATP in the NP region. In addition, high extracellular ATP concentration was detected in the NP region ($\sim 165 \mu\text{M}$). This high extracellular ATP level could be due to the avascular nature of the IVD and the high content of proteoglycans which can inhibit ATP hydrolysis (Vieira, Rocha et al. 2001).

Since extracellular ATP can mediate a wide variety of biological responses via purinergic receptors (Burnstock 2006), a high extracellular ATP level may influence NP metabolism. Furthermore, as described before, compressive loading may promote extracellular ATP hydrolysis, which may result in increases in the extracellular contents of adenine derivatives (i.e., ADP, AMP and adenosine), PPi, and Pi. Since ADP and adenosine can regulate different cellular activities via P2 and P1 purinergic receptors (Burnstock 2006; Jacobson and Gao 2006), increases in their extracellular concentrations may also have biological effects on NP cells. Due to the capability of PPi and Pi to regulate crystal formation and tissue calcification (Ryan, Kurup et al. 1992; Johnson and Terkeltaub 2005), increases in the extracellular concentrations of PPi and Pi in the NP region may contribute to endplate calcification which occurs in aged discs and reduces nutrient supply to the IVD (Grunhagen, Shirazi-Adl et al. 2011). Taken all together, the findings in this study suggest that ATP metabolism may play an important role in maintaining normal biological function of the IVD, while compression-regulated ATP (intracellular and extracellular) metabolism may be a novel mechanobiological pathway for regulating the biological activities of the IVD.

Compared to AF cells, a significantly higher ATP content found in NP cells suggests cellular metabolism in NP cells is more active. This result is consistent with our previous studies (Fernando, Czamanski et al. 2011; Salvatierra, Yuan et al. 2011). In addition, since the concentrations of glucose and oxygen are lower in the NP region than the AF region (Huang and Gu 2008), similar lactate accumulation found in the NP and AF regions suggests that NP cells maintain high ATP content by producing ATP via mitochondrial respiration, which is more efficient in ATP production than glycolysis.

In summary, this study demonstrated that static and dynamic loading increased the

total ATP and lactate contents in the IVD, suggesting that compression can cause an increase in ATP production by promoting glycolysis. Compressive compression can also reduce pH in the IVD due to high lactate accumulation. Due to the capability of ATP to regulate a variety of cellular activities, high extracellular ATP content found in the NP region exhibited and regulated by compression may influence the normal biological function of the IVD. The findings in this study suggest that compression-mediated ATP metabolism could be a novel mechanobiological pathway for regulating the biological activities of the IVD.

However, whether up-regulation of gene expressions can increase ECM production may still depend on adequate ATP supply. Although our recent studies showed that both static and dynamic compressive loading promotes energy production of IVD cells in an in-vitro 3-dimensional agarose gel model (Fernando, Czamanski et al. 2011; Salvatierra, Yuan et al. 2011), the *in vivo* environmental factors were not taken into account, such as cell-ECM interaction, compression-dependent transport properties, and differences in mechanical stimuli. Therefore, this study investigated energy metabolism inside the IVD under compression. To our knowledge, this is the first study to demonstrate that mechanical compression affects in-situ energy metabolism in the IVD.

Static compressive loading significantly increased total ATP content and lactate accumulation in both AF and NP region (Figure 5-5 & Figure 5-7), suggesting that static compression promoted glycolysis and consequently increased ATP production in both NP and AF cells. This finding is supported by our previous study which showed that static compressive loadings promoted ATP production of AF cells in agarose culture (Fernando, Czamanski et al. 2011). A decrease in solute diffusivity (or tissue permeability) caused by static compression (Huang and Gu 2008) may also

facilitate extracellular lactate accumulation. Furthermore, a decrease in pH found caused by static compression in both anatomical regions (Figure 5-5-Figure 5-7) may result from the increase in lactate accumulation.

Similarly, 1 Hz dynamic loading significantly increased total ATP and lactate accumulation in both AF and NP regions (Figure 5-8 and Figure 5-9). It is in concurrence with our previous study and suggests that dynamic loading can promote ATP production of AF and NP cells via glycolysis (Fernando, Czamanski et al. 2011). Another factor for increasing ATP production could be an increase in transport of nutrients by dynamic loading (Huang and Gu 2008). In addition, higher lactate accumulation caused by dynamic loading may result in reduction in pH as seen in this study (Figure 5-8 and Figure 5-10). Furthermore, compared to the static compression group, significantly higher lactate accumulation found in the 1Hz loading group (Figure 5-8) suggests more ATP was produced in the dynamic loading group. However, no significant difference found in the ATP content between the static and 1 Hz dynamic loading groups suggests that 1 Hz dynamic loading increases ATP consumption. It also indicates that dynamic loading of 1 Hz promotes energy-demanding cellular activities, such as ECM production (Korecki, Kuo et al. 2009).

Fluid pressurization occurs in the disc, especially NP region, when the IVD is subjected to compressive loading (Yao and Gu 2007). Since hydrostatic pressure has been shown to modulate cellular ECM biosynthesis (Ishihara, McNally et al. 1996; Handa, Ishihara et al. 1997), cellular ATP metabolism may be affected by hydrostatic pressure. In the static compression test, when a constant displacement is applied to the IVD, hydrostatic pressure reaches a peak and then gradually reduces to an equilibrium level (Yao and Gu 2007). Significant difference in the ATP content between the one and two-hour static loading groups seen in the NP region could be due to the effect of

the time-dependent hydrostatic pressure. In addition, the finding that static compression significantly increased the ATP content in the NP region is not consistent with our previous study (Fernando, Czamanski et al. 2011) which found static compression exhibited no significant effect on ATP production of NP cells in 3-dimensional agarose model. Since little fluid pressurization occurs in agarose gel under compression due to its high hydraulic permeability (Huang, Hagar et al. 2004), hydrostatic pressure induced in the IVD under static compression may be the main factor causing changes in ATP content of NP region. Furthermore, solute transport and hydrostatic pressure in cartilaginous tissue under dynamic loading depend on loading frequency (Yao and Gu 2004). This could be the reason for the frequency-dependent differences seen in this study. Therefore, the effects of hydrostatic pressure on ATP metabolism of IVD cells needs to be further investigated.

Since both static and dynamic compression can promote ATP release from IVD cells (Fernando, Czamanski et al. 2011; Salvatierra, Yuan et al. 2011), it was expected that extracellular ATP accumulation occurs in the IVD under compression, especially static compression which can reduce transport of solutes in the IVD (Huang and Gu 2008). However, this study found that both static and dynamic loading significantly reduced extracellular ATP content in the NP region, suggesting that compressive loading promotes hydrolysis of ATP in the NP region. In addition, high extracellular ATP concentration is detected in NP region ($\sim 165 \mu\text{M}$). This high extracellular ATP accumulation could be due to the avascular nature of IVD and the high content of proteoglycans which can inhibit ATP hydrolysis (Vieira, Rocha et al. 2001). Since extracellular ATP can mediate a wide variety of biological responses via purinergic receptors (Burnstock 2006), high extracellular ATP level may influence NP metabolism. Furthermore, as described before, compressive loading may promote

extracellular ATP hydrolysis, which can result in increases in the extracellular contents of adenine derivatives (i.e., ADP, AMP, and adenosine), PPi, and Pi. Since ADP and adenosine can regulate different cellular activities via P2 and P1 purinergic receptors (Burnstock 2006; Jacobson and Gao 2006), increases in their extracellular concentrations may also have biological effects on NP cells. Due to the capability of PPi and Pi to regulate crystal formation and tissue calcification (Ryan, Kurup et al. 1992; Johnson and Terkeltaub 2005), increases in the extracellular concentrations of PPi and Pi in the NP region may contribute to endplate calcification which occurs in aged discs and reduces nutrient supply to the IVD (Grunhagen, Shirazi-Adl et al. 2011). Taken all together, the findings in this study suggest that ATP may play an important role in maintaining normal biological function of the IVD, while compression-regulated ATP (intracellular and extracellular) metabolism may be a novel mechanobiological pathway for regulation of IVD metabolism.

Compared to AF cells, a significantly higher ATP content found in NP cells suggests cellular metabolism in NP cells is more active. It is consistent with our previous studies (Fernando, Czamanski et al. 2011; Salvatierra, Yuan et al. 2011). In addition, since the concentrations of glucose and oxygen are lower in the NP region than the AF region (Huang and Gu 2008), similar lactate accumulation found in the NP and AF regions suggests that NP cells maintain high ATP content by producing ATP via mitochondrial respiration, which is more efficient in ATP production than glycolysis.

In summary, this study demonstrated that static and dynamic loading promoted ATP production and lactate accumulation in the IVD, suggesting that compression can increase in ATP production by promoting glycolysis. Compressive loading can reduce pH in the IVD due to high lactate accumulation. This study also found that the

NP region exhibited high extracellular ATP content which was reduced by compressive loading. The findings suggest that compression-mediated ATP metabolism could be a novel mechanobiological pathway which regulates IVD metabolism.

Low pH was detected in this study especially in NP region after compressive loads (~6.5). It has been shown that low pH can affect many activities of the IVD such as cell viability and protein synthesis rate (Ohshima and Urban 1992; Bibby and Urban 2004). This acidic low pH environment was believed to be fatal for cells (Staub, Baethmann et al. 1990); however, previous studies about IVD cells have shown that decreased cell viability under low pH is also time dependent, which is to say that IVD cells can survive for a short period of time under low pH environment (Liang, Li et al. 2012). Another study also showed that IVD cells cultured in low glucose (0.5 mM) low pH (6.2) conditions for 24 hours have decreased cell viability, from 100% at the beginning to 95% at the end of the experiment (Bibby and Urban 2004). Therefore the low pH (as low as 6.5) condition found in NP region from our study is toxic, but cells can manage to maintain short-term viability under such environment.

A possible limit of this study is that the experimental environment has a different oxygen contents (20%) comparing with *in vivo* (as low as 1% in central NP region) (Bartels, Fairbank et al. 1998). Cells are believed to utilize glycolysis for the production of ATP under anoxic environments (Romano and Conway 1996). However, glycolysis was observed for IVD cells *in vitro* which has a culture environment with plenty of oxygen supply (Guehring, Wilde et al. 2009; Fernando, Czamanski et al. 2011; Salvatierra, Yuan et al. 2011). These studies have shown that results obtained from high oxygen contents environments can provide valuable information to explain the responses of cells at *in vivo* conditions.

5.5 OTHER MEASUREMENTS

Oxygen and glucose distributions in IVDs were also measured using custom-made optical sensors described previously in this dissertation.

A needle type oxygen sensor was inserted from outer AF till reach NP and a caliper was used to record inserting depth. After the measurement the disc was cut transversally and the measurements were corresponded with locations. The result is presented in Figure 5-14. Our finding is consistent with previous researches (Bartels, Fairbank et al. 1998).

Glucose profiles were measured using glucose sensor described in Chapter 4. IVDs were cultured in high glucose (4.5 g/L D-glucose) and low glucose (1 g/L D-glucose) Dulbecco's Modified Eagle Medium (DMEM, Invitrogen Corp., Carlsbad, CA, USA) containing 10% fetal bovine serum (FBS, Invitrogen Corp, Carlsbad, CA, USA) and 1% antibiotic-antimitotic (Invitrogen Corp, Carlsbad, CA, USA). No significant difference was found in glucose content between the measurement locations in the AF and NP regions when the IVD was cultured in high glucose DMEM. However, AF had higher glucose concentration than NP when low glucose DMEM was used for disc culture (Figure 5-15). This measurement is consistent with previous study (Jackson, Huang et al. 2011).

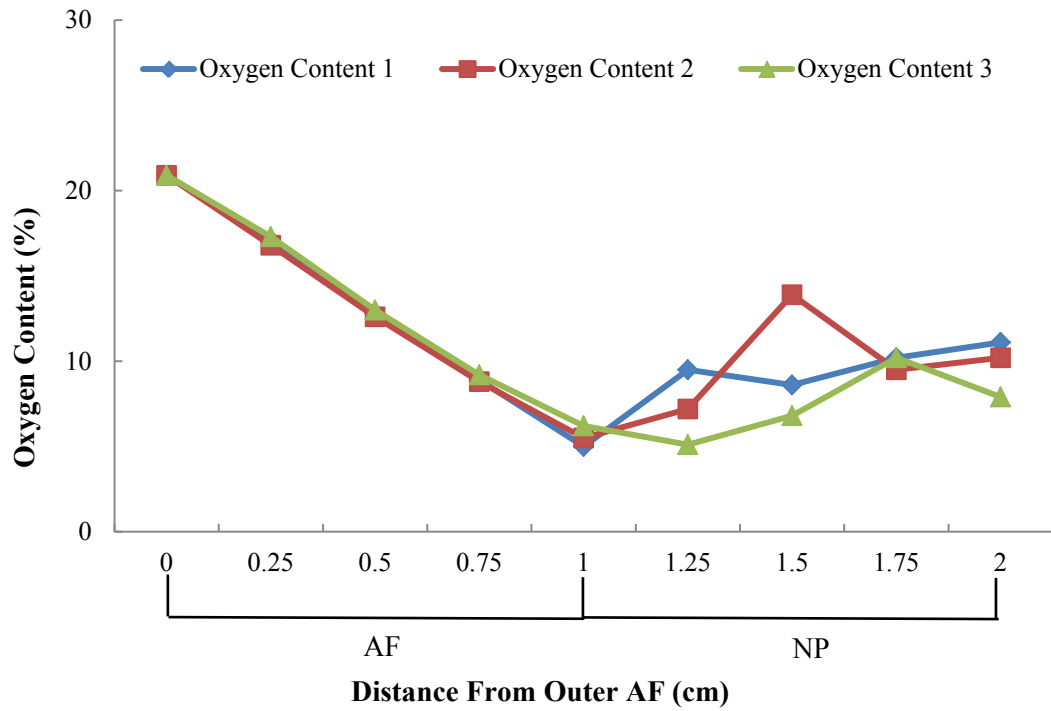


Figure 5-14: Oxygen profiles measured in the IVD using a needle type optical oxygen sensor.

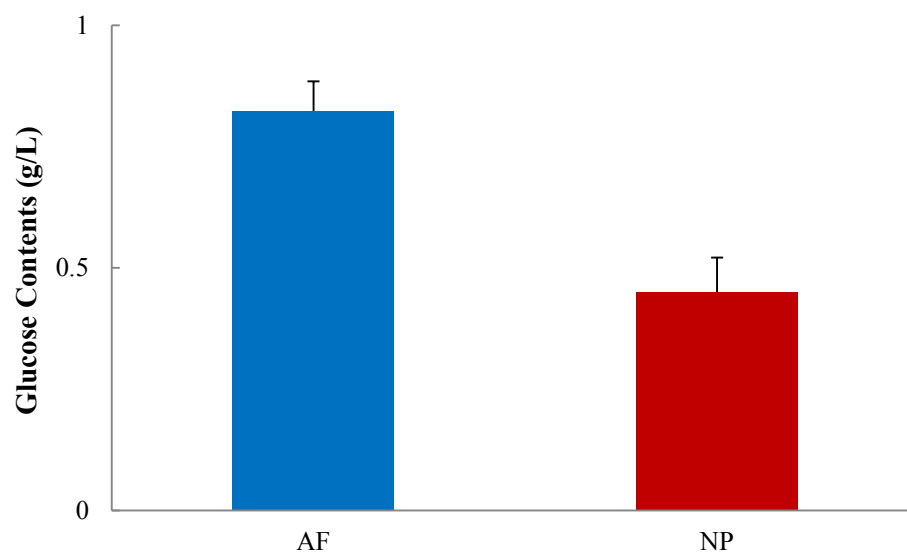


Figure 5-15: Glucose contents of AF and NP under low glucose DMEM culture.

CHAPTER 6 CONCLUSION AND RECOMMENDATIONS

6.1 SUMMARY AND CONCLUDING REMARKS

Low back pain is a big social burden which affects 80% of people in USA at certain time point during their lives and cost numerous societal resources. Each year more than 50 billion US dollars are spent for low back pain in United States (Borenstein, Calin et al. 2012). Although it is not very well studied yet, intervertebral disc degeneration was revealed to be a possible cause of low back pain (Cox 2011). IVD is the biggest avascular tissue in human body, the pathway of nutrient supply is through peripheral blood vessels. For NP cells the distance to closest blood vessel can be as far as 20mm, which makes the environment of NP cells one of the worst in human body with regards to having a very poor nutrient supply (Grunhagen, Shirazi-Adl et al. 2011). Cells play pivotal roles in IVDs by synthesizing and breaking down ECM to maintain a favorable environment for tissue functions, however these activities are high energy commanding (Urban and Roberts 2003; Bibby, Jones et al. 2005). Thus nutrient supply can be a limit factor for cells to maintain ECM integrity. Previous researches showed that mechanical loadings can affect cell energy metabolism (Lee, Wilkins et al. 2002; Fernando, Czamanski et al. 2011; Salvatierra, Yuan et al. 2011). However, there are more mechanical events inside IVDs when mechanical loadings are applied, such as hydrostatic pressure, cell-ECM interaction, etc. All of these have been showed to affect ECM synthesis of IVD cells (Ishihara, McNally et al. 1996; Setton and Chen 2006; Korecki, Kuo et al. 2009). Therefore it is essential to study the energy metabolism of IVD under mechanical loadings, especially compression which is the most common mechanical loading.

Hence, the main objectives of this dissertation were threefold: (1) To design and build a novel bioreactor system for whole IVD disc culture and perform static and dynamic compression studies; (2) To develop novel optical sensors to detect glucose and ATP contents and (3) To investigate the effects of static and dynamic compressions on energy metabolism of IVD. Three studies were carried out to achieve the following specific aims: (1) A bioreactor system were built to perform both static and dynamic compressive loadings with attached culture medium circulation and loading force detecting and recording devices (Chapter 3); (2) An optical fiber based ATP sensor was fabricated using sol-gel entrapping enzyme technique (Chapter 4) and (3) the changes on lactate accumulation, pH value, total ATP and extracellular ATP were measured in the porcine IVD under static and dynamic compression. Measurements of oxygen tension and glucose distribution were also performed (Chapter 5). The important findings from these studies are discussed as following.

6.1.1 Optical fiber based ATP sensor

A novel optical fiber based ATP sensor was fabricated. Two layers of sol-gel coating layers were applied to the end of optical fiber, the first layer contained Ruthenium complex which can be excited by blue light (465 nm wave length) and emits red light (610 nm wave length); this red light can be absorbed by oxygen molecules without radiation, thus quench the signal and increase decay time (τ).

The second layer entraps two enzymes: glycerol kinase and glycerol 3-phosphate, which can catalyze the oxidization of ATP and consume oxygen. Reverse of decay time ($1/\tau$) has a linear relationship with oxygen concentration. Therefore ATP content can be detected by measuring the change of decay time.

This sensor has a broad detecting range from 10^{-3} mM to 1.5 mM and is not affected by physiological pH value change or ATP derivatives such as ADP, AMP and adenosine (Wang, Huang et al. 2013). Since this sensor measures the change of oxygen partial pressure at the local micro-environment of coating layers, we also developed a compensation method for different environmental oxygen contents.

Oxygen sensor was fabricated by coating the first layer only as subscribed above; glucose sensor was developed by the same method, only replace the enzymes glycerol kinase and glycerol 3-phosphate to glucose oxidase. Oxygen sensors and glucose sensors all have robust performance and are suitable for physiological tissue *in situ* measurements.

6.1.2 Effects of static and dynamic compressions on IVD energy metabolism

Five (5) groups of static and dynamic compressive loadings were performed: control group without any mechanical loadings (0 Hz 0 hour group), 1 hour static compression group (0 Hz 1 hour group), 2 hour static compression group (0 Hz 2 hour group), 1 hour 0.1 Hz group and 1 hour 1 Hz group. 10% strain was applied to compressive groups.

A transversal cut was applied to the disc after experiment; lactate accumulation and total ATP contents were measured using corresponding assays. Extracellular ATP

contents at NP region were detected using ATP sensors described earlier (Wang, Huang et al. 2013). Oxygen distribution inside of IVD and glucose contents at AF and NP regions were also measured using custom made sensors.

We discovered that both static and dynamic loadings tend to increase lactate accumulation in AF and NP regions; and significantly decrease the pH value; total ATP contents were significantly increased in both AF and NP regions, these suggests that mechanical loadings promote ATP production via glycolysis which produces lactate, causes the decrease in pH value. However, we also detected significant decrease of extracellular ATP in NP region, this may due to the increase of ATP hydrolysis induced by mechanical loadings. The measured high extracellular ATP contents in NP region ($\sim 160 \mu\text{M}$) also reveal certain pivotal environmental condition for NP cells.

In summary, this study helps us to better understand the energy metabolism of IVD under compressive mechanical loadings, which is essential to better understand disc degeneration and low back pain and may also be beneficial for future endeavor on disc regeneration.

6.2 RECOMMENDATION FOR FUTURE STUDIES

The overall objective of this study was to elucidate energy metabolism of IVD under compressive loading. Although valuable insights of energy metabolism changes induced by compressions were provided in this dissertation, there are still many important works left to finish under this big frame. Therefore recommendations of future work are described as following. Compression experiments reveals that lactate accumulation in both AF and NP region were promoted by compressive loadings and cause a significant

decrease in pH (to as low as 6.5). This creates a harsh environment for IVD cells, especially NP cells, which are surrounded by dense AF tissue and up to 20 mm away from nearest blood supply (Moore 2006). How IVD cells survive and maintain activities under such difficult conditions remains an enigma. Therefore a study about IVD cell response and activities at low pH environment should be conducted.

It was also found that NP region maintains high extracellular ATP contents (~160 μM); this may reveal a vital condition for NP cells to survive in the harsh mechanical and biochemical conditions and maintain their normal biological function (e.g., ECM biosynthesis) and notochordal phenotype. Effects of high extracellular ATP on NP cells could also be studied. Our study showed that extracellular ATP contents were significantly decreased for all compression groups. This indicates that compressions may promote ATP hydrolysis and thus increase local concentrations of adenine derivatives (i.e., ADP, AMP and adenosine) and phosphate. This should be elucidated by future works on measuring changes in the contents of ADP, AMP and adenosine of NP region under compressive loading. Calcium has a high concentration in cartilage but is mostly bound in proteoglycan as part of the anionic groups and hence not available for precipitation. Phosphate can replace calcium by a ion-exchange effect and thus increase endplate calcification (Hunter 1987). Therefore the relation of compressive loadings on IVD, hydrolysis of ATP and endplate calcification should be further studied. Other products of ATP hydrolysis include ADP, AMP and adenosine.

Adenosine may also play a very important role on protecting notochordal cells which was reported to protect the NP from degradation (Erwin, Islam et al. 2011). A future

study should be carried out to investigate the effects of adenosine on preventing IVD cells degeneration.

A discrepancy between this study and previous agarose model study about effects of static compression on IVD ATP production was mentioned in Chapter 5. As discussed in that chapter, this may due to the hydrostatic pressure inside IVD tissue. Thus a future study should be conducted to investigate the effect of hydrostatic pressure on ATP metabolism of IVD cells, especially on NP cells which undergo high hydrostatic pressure during static and dynamic compressions.

Glycolysis produces lactate and less ATP than mitochondrial respiration and is likely the dominant energy production method for NP which has limited oxygen supply. It is essential to solve the problem of nutrition supply for NP cells to acquire enough energy to maintain extracellular matrix integrity, which is essential to prevent degradation of IVDs (Urban and Roberts 2003). Inability of NP to maintain integrity of ECM will cause the IVDs to lose their mechanical properties and further lead to disc degeneration (Roughley 2004). Therefore, works should be carried out in investigating the effect of promoting nutrient supply to NP on retarding or even inverting disc degeneration.

In summary, the recommended studies would extend the accomplishment of the studies in this dissertation and help to achieve the long term goal which is to elucidate the pathophysiology of disc degeneration and low back pain, and develop treatment to retard or repair disc degeneration and cure low back pain.

REFERENCES

- (2008). The Burden of Musculoskeletal Diseases in the United States. A. A. o. O. Surgeons: 21-53.
- (2008). Low Back Pain Fact Sheet. NIH.
- Adam, M. and Z. Deyl (1984). "Degenerated annulus fibrosus of the intervertebral disc contains collagen type II." Ann Rheum Dis **43**(2): 258-263.
- Adams, M. A., P. Dolan, et al. (2009). "The internal mechanical functioning of intervertebral discs and articular cartilage, and its relevance to matrix biology." Matrix Biol **28**(7): 384-389.
- Adams, M. A., M. Stefanakis, et al. (2010). "Healing of a painful intervertebral disc should not be confused with reversing disc degeneration: Implications for physical therapies for discogenic back pain." Clinical Biomechanics **25**(10): 961-971.
- Aguiar, D. J., S. L. Johnson, et al. (1999). "Notochordal cells interact with nucleus pulposus cells: regulation of proteoglycan synthesis." Exp Cell Res **246**(1): 129-137.
- Bartels, E. M., J. C. Fairbank, et al. (1998). "Oxygen and lactate concentrations measured in vivo in the intervertebral discs of patients with scoliosis and back pain." Spine (Phila Pa 1976) **23**(1): 1-7; discussion 8.
- Bartels, E. M., J. C. T. Fairbank, et al. (1998). "Oxygen and lactate concentrations measured in vivo in the intervertebral discs of patients with scoliosis and back pain." Spine (Phila Pa 1976) **23**(1): 1-7.
- Benneker, L. M., P. F. Heini, et al. (2005). "2004 Young Investigator Award Winner: vertebral endplate marrow contact channel occlusions and intervertebral disc degeneration." Spine (Phila Pa 1976) **30**(2): 167-173.
- Benz, R. and F. Conti (1986). "Effects of hydrostatic pressure on lipid bilayer membranes. I. Influence on membrane thickness and activation volumes of lipophilic ion transport." Biophys J **50**(1): 91-98.

- Berg, J. M., J. L. Tymoczko, et al. (2012). Biochemistry. New York, W.H. Freeman.
- Bibby, S. R., D. A. Jones, et al. (2001). "The pathophysiology of the intervertebral disc." Joint Bone Spine **68**(6): 537-542.
- Bibby, S. R. and J. P. Urban (2004). "Effect of nutrient deprivation on the viability of intervertebral disc cells." Eur Spine J **13**(8): 695-701.
- Bibby, S. R. S., D. A. Jones, et al. (2005). "Metabolism of the intervertebral disc: Effects of low levels of oxygen, glucose, and pH on rates of energy metabolism of bovine nucleus pulposus cells." Spine (Phila Pa 1976) **30**(5): 487-496.
- Boos, N., A. Wallin, et al. (1993). "Quantitative MR imaging of lumbar intervertebral disks and vertebral bodies: influence of diurnal water content variations." Radiology **188**(2): 351-354.
- Borenstein, D. G., A. Calin, et al. (2012). Fast facts : low back pain. Abingdon, Oxford, Health Press.
- Bron, J. L., M. N. Helder, et al. (2009). "Repair, regenerative and supportive therapies of the annulus fibrosus: achievements and challenges." Eur Spine J **18**(3): 301-313.
- Brown, P. and N. Dale (2002). "Spike-independent release of ATP from *Xenopus* spinal neurons evoked by activation of glutamate receptors." J Physiol **540**(Pt 3): 851-860.
- Burnstock, G. (2000). "P2X receptors in sensory neurones." Br J Anaesth **84**(4): 476-488.
- Burnstock, G. (2006). "Pathophysiology and therapeutic potential of purinergic signaling." Pharmacological Reviews **58**(1): 58-86.
- Bush, K. T., S. H. Keller, et al. (2000). "Genesis and reversal of the ischemic phenotype in epithelial cells." J Clin Invest **106**(5): 621-626.
- Chen, J., W. Yan, et al. (2004). "Static compression induces zonal-specific changes in gene expression for extracellular matrix and cytoskeletal proteins in intervertebral disc cells in vitro." Matrix Biol **22**(7): 573-583.

- Chen, J., W. Yan, et al. (2004). "Static compression induces zonal-specific changes in gene expression for extracellular matrix and cytoskeletal proteins in intervertebral disc cells in vitro." Matrix Biology **22**(7): 573-583.
- Chowdhury, T. T. and M. M. Knight (2006). "Purinergic pathway suppresses the release of .NO and stimulates proteoglycan synthesis in chondrocyte/agarose constructs subjected to dynamic compression." J Cell Physiol **209**(3): 845-853.
- Cockayne, D. A., S. G. Hamilton, et al. (2000). "Urinary bladder hyporeflexia and reduced pain-related behaviour in P2X(3)-deficient mice." Nature **407**(6807): 1011-1015.
- Compagnone, D. and G. G. Guilbault (1997). "Glucose oxidase/hexokinase electrode for the determination of ATP." Analytica Chimica Acta **340**(1-3): 109-113.
- Cook, S. P., L. Vulchanova, et al. (1997). "Distinct ATP receptors on pain-sensing and stretch-sensing neurons." Nature **387**(6632): 505-508.
- Cook, S. P., L. Vulchanova, et al. (1997). "Distinct ATP receptors on pain-sensing and stretch-sensing neurons." Nature **387**(6632): 505-508.
- Costi, J. J., I. A. Stokes, et al. (2008). "Frequency-dependent behavior of the intervertebral disc in response to each of six degree of freedom dynamic loading: solid phase and fluid phase contributions." Spine (Phila Pa 1976) **33**(16): 1731-1738.
- Cox, J. M. (2011). Low back pain : mechanism, diagnosis, treatment. Philadelphia, Wolters Kluwer/Lippincott Williams & Wilkins Health.
- Daly, M. E., C. Vale, et al. (1998). "Acute effects on insulin sensitivity and diurnal metabolic profiles of a high-sucrose compared with a high-starch diet." Am J Clin Nutr **67**(6): 1186-1196.
- Deyo, R. A. (1998). "Low-back pain." Sci Am **279**(2): 48-53.
- Endo, H., Y. Yonemori, et al. (2006). "A needle-type optical enzyme sensor system for determining glucose levels in fish blood." Analytica Chimica Acta **573-574**(0): 117-124.
- Erwin, W. M., D. Islam, et al. (2011). "Notochordal cells protect nucleus pulposus cells from degradation and apoptosis: implications for the mechanisms of intervertebral disc degeneration." Arthritis Res Ther **13**(6): R215.

- Eyre, D. M., H. (1977). "Quantitative analysis of types I and II collagens in human intervertebral discs at various ages." Biochim Biophys Acta **492**(1): 29-42.
- Eyre, D. R., Benya, P., Buckwalter, J., Caterson, B., Heinegard, D., Oegema, T., Pearce, R., Pope, M., Urban, J. (1989). Intervertebral disk: Basic science perspectives. New Perspectives on Low Back Pain. J. W. Frymoyer, Gordon, S. L. Park Ridge, IL, American Academy of Orthopaedic Surgeons: 147-207.
- Felix, R. and H. Fleisch (1976). "Pyrophosphatase and ATPase of isolated cartilage matrix vesicles." Calcif Tissue Res **22**(1): 1-7.
- Ferguson, S. J. and T. Steffen (2003). "Biomechanics of the aging spine." Eur Spine J **12 Suppl 2**: S97-S103.
- Fernando, H. N., J. Czamanski, et al. (2011). "Mechanical loading affects the energy metabolism of intervertebral disc cells." J Orthop Res **29**(11): 1634-1641.
- Fernando, H. N., J. Czamanski, et al. (2011). "Mechanical Loading Affects the Energy Metabolism of Intervertebral Disc Cells." Journal of Orthopaedic Research **29**(11): 1634-1641.
- Gerweck, L. E. and K. Seetharaman (1996). "Cellular pH gradient in tumor versus normal tissue: Potential exploitation for the treatment of cancer." Cancer Research **56**(6): 1194-1198.
- Golub, E. E. (2011). "Biom mineralization and matrix vesicles in biology and pathology." Semin Immunopathol **33**(5): 409-417.
- Gourine, A. V., N. Dale, et al. (2007). "Release of ATP in the central nervous system during systemic inflammation: real-time measurement in the hypothalamus of conscious rabbits." Journal of Physiology-London **585**(1): 305-316.
- Gruber, H. E. and E. N. Hanley, Jr. (1998). "Analysis of aging and degeneration of the human intervertebral disc. Comparison of surgical specimens with normal controls." Spine (Phila Pa 1976) **23**(7): 751-757.
- Grunhagen, T., A. Shirazi-Adl, et al. (2011). "Intervertebral disk nutrition: a review of factors influencing concentrations of nutrients and metabolites." Orthop Clin North Am **42**(4): 465-477, vii.

- Gu, W. Y., X. G. Mao, et al. (1999). "The anisotropic hydraulic permeability of human lumbar annulus fibrosus. Influence of age, degeneration, direction, and water content." Spine (Phila Pa 1976) **24**(23): 2449-2455.
- Guehring, T., G. Wilde, et al. (2009). "Notochordal intervertebral disc cells: sensitivity to nutrient deprivation." Arthritis Rheum **60**(4): 1026-1034.
- Guiot, B. H. and R. G. Fessler (2000). "Molecular Biology of Degenerative Disc Disease." Neurosurgery **47**(5): 1034-1040.
- Hadjipavlou, A. G., M. N. Tzermiadianos, et al. (2008). "The pathophysiology of disc degeneration: a critical review." J Bone Joint Surg Br **90**(10): 1261-1270.
- Hall, A. C. (1999). "Differential effects of hydrostatic pressure on cation transport pathways of isolated articular chondrocytes." J Cell Physiol **178**(2): 197-204.
- Hall, A. C., J. P. Urban, et al. (1991). "The effects of hydrostatic pressure on matrix synthesis in articular cartilage." J Orthop Res **9**(1): 1-10.
- Handa, T., H. Ishihara, et al. (1997). "Effects of hydrostatic pressure on matrix synthesis and matrix metalloproteinase production in the human lumbar intervertebral disc." Spine (Phila Pa 1976) **22**(10): 1085-1091.
- Hay, E. D. (1991). Cell biology of extracellular matrix. New York, Plenum Press.
- Hendry, N. G. (1958). "The hydration of the nucleus pulposus and its relation to intervertebral disc derangement." J Bone Joint Surg Br **40-B**(1): 132-144.
- Hickey, D. S. and D. W. Hukins (1980). "Relation between the structure of the annulus fibrosus and the function and failure of the intervertebral disc." Spine (Phila Pa 1976) **5**(2): 106-116.
- Hirschberg, C. B., P. W. Robbins, et al. (1998). "Transporters of nucleotide sugars, ATP, and nucleotide sulfate in the endoplasmic reticulum and Golgi apparatus." Annu Rev Biochem **67**: 49-69.
- Holguin, N., J. Muir, et al. (2007). Mechanical vibrations reduce the Intervertebral Disc swelling and muscle atrophy from Bed Rest. Bioengineering Conference, 2007. NEBC '07. IEEE 33rd Annual Northeast.

- Hsu, H. H. and H. C. Anderson (1996). "Evidence of the presence of a specific ATPase responsible for ATP-initiated calcification by matrix vesicles isolated from cartilage and bone." J Biol Chem **271**(42): 26383-26388.
- Hsu, H. H., N. P. Camacho, et al. (1999). "Further characterization of ATP-initiated calcification by matrix vesicles isolated from rachitic rat cartilage. Membrane perturbation by detergents and deposition of calcium pyrophosphate by rachitic matrix vesicles." Biochim Biophys Acta **1416**(1-2): 320-332.
- Huang, C. Y. and W. Y. Gu (2008). "Effects of mechanical compression on metabolism and distribution of oxygen and lactate in intervertebral disc." J Biomech **41**(6): 1184-1196.
- Huang, C. Y., K. L. Hagar, et al. (2004). "Effects of cyclic compressive loading on chondrogenesis of rabbit bone-marrow derived mesenchymal stem cells." Stem Cells **22**(3): 313-323.
- Humzah, M. D. and R. W. Soames (1988). "Human intervertebral disc: structure and function." Anat Rec **220**(4): 337-356.
- Hunter, G. K. (1987). "An ion-exchange mechanism of cartilage calcification." Connect Tissue Res **16**(2): 111-120.
- Hutton, W. C., W. A. Elmer, et al. (1999). "The effect of hydrostatic pressure on intervertebral disc metabolism." Spine (Phila Pa 1976) **24**(15): 1507-1515.
- Iatridis, J. C., J. J. MacLean, et al. (2007). "Measurements of proteoglycan and water content distribution in human lumbar intervertebral discs." Spine (Phila Pa 1976) **32**(14): 1493-1497.
- Iatridis, J. C., P. L. Mente, et al. (1999). "Compression-induced changes in intervertebral disc properties in a rat tail model." Spine (Phila Pa 1976) **24**(10): 996-1002.
- Im, M. J. C., M. F. Freshwater, et al. (1976). "Enzyme-Activities in Granulation Tissue - Energy for Collagen-Synthesis." Journal of Surgical Research **20**(2): 121-125.
- Ishihara, H., D. S. McNally, et al. (1996). "Effects of hydrostatic pressure on matrix synthesis in different regions of the intervertebral disk." J Appl Physiol **80**(3): 839-846.

- Jackson, A. R., C. Y. Huang, et al. (2011). "Effect of endplate calcification and mechanical deformation on the distribution of glucose in intervertebral disc: a 3D finite element study." Comput Methods Biomech Biomed Engin **14**(2): 195-204.
- Jacobson, K. A. and Z. G. Gao (2006). "Adenosine receptors as therapeutic targets." Nature Reviews Drug Discovery **5**(3): 247-264.
- Johnson, K. and R. Terkeltaub (2005). "Inorganic pyrophosphate (PPI) in pathologic calcification of articular cartilage." Frontiers in Bioscience **10**: 988-997.
- Johnstone, B., J. P. G. Urban, et al. (1992). "The Fluid Content of the Human Intervertebral-Disk - Comparison between Fluid Content and Swelling Pressure Profiles of Disks Removed at Surgery and Those Taken Postmortem." Spine (Phila Pa 1976) **17**(4): 412-416.
- Kandel, R., S. Roberts, et al. (2008). "Tissue engineering and the intervertebral disc: the challenges." Eur Spine J **17 Suppl 4**: 480-491.
- Katsu, T., X. R. Yang, et al. (1994). "Amperometric Biosensor for Adenosine-5'-Triphosphate Based on a Platinum-Dispersed Carbon-Paste Enzyme Electrode." Analytical Letters **27**(7): 1215-1224.
- Knowles, J. R. (1980). "Enzyme-catalyzed phosphoryl transfer reactions." Annu Rev Biochem **49**: 877-919.
- Korecki, C. L., C. K. Kuo, et al. (2009). "Intervertebral Disc Cell Response to Dynamic Compression Is Age and Frequency Dependent." Journal of Orthopaedic Research **27**(6): 800-806.
- Kraemer, J., D. Kolditz, et al. (1985). "Water and Electrolyte Content of Human Intervertebral Disks under Variable Load." Spine (Phila Pa 1976) **10**(1): 69-71.
- Kueng, A., C. Kranz, et al. (2004). "Amperometric ATP biosensor based on polymer entrapped enzymes." Biosensors & Bioelectronics **19**(10): 1301-1307.
- Kulkarni, A. R., V. I. Hukkeri, et al. (2005). "A novel method for the synthesis of the PEG-crosslinked chitosan with a pH-independent swelling behavior." Macromolecular Bioscience **5**(10): 925-928.
- Lakowicz, J. R. (2006). Principles of fluorescence spectroscopy. New York, Springer.

- Leach, F. R. (1981). "ATP determination with firefly luciferase." J. Appl. Biochem **3**(51): 7.
- Lee, R. B. and J. P. Urban (1997). "Evidence for a negative Pasteur effect in articular cartilage." Biochem J **321** (Pt 1): 95-102.
- Lee, R. B., R. J. Wilkins, et al. (2002). "The effect of mechanical stress on cartilage energy metabolism." Biorheology **39**(1-2): 133-143.
- Liang, C., H. Li, et al. (2012). "Responses of human adipose-derived mesenchymal stem cells to chemical microenvironment of the intervertebral disc." J Transl Med **10**: 49.
- Lippitsch, M. E., J. Pusterhofer, et al. (1988). "Fibre-Optic Oxygen Sensor with the Fluorescence Decay Time as the Information Carrier." Analytica Chimica Acta **205**(1-2): 1-6.
- Llaudet, E., S. Hatz, et al. (2005). "Microelectrode biosensor for real-time measurement of ATP in biological tissue." Anal Chem **77**(10): 3267-3273.
- Lodish, H. F. (2013). Molecular cell biology. New York, W.H. Freeman and Co.
- Lohmann, K. (1929). "Über die Pyrophosphatfraktion im Muskel." Naturwissenschaften **17**(31): 624-625.
- Lotz, J. C. and J. R. Chin (2000). "Intervertebral Disc Cell Death Is Dependent on the Magnitude and Duration of Spinal Loading." Spine (Phila Pa 1976) **25**(12): 1477-1483.
- Lundin, A. (2000). Use of firefly luciferase in atp-related assays of biomass, enzymes, and metabolites. Methods in Enzymology, Academic Press. **Volume 305**: 346-370.
- Lundon, K. and K. Bolton (2001). "Structure and function of the lumbar intervertebral disk in health, aging, and pathologic conditions." J Orthop Sports Phys Ther **31**(6): 291-303; discussion 304-296.
- Luoma, K., H. Riihimaki, et al. (2000). "Low back pain in relation to lumbar disc degeneration." Spine (Phila Pa 1976) **25**(4): 487-492.

- Maclean, J. J., C. R. Lee, et al. (2004). "Anabolic and catabolic mRNA levels of the intervertebral disc vary with the magnitude and frequency of in vivo dynamic compression." J Orthop Res **22**(6): 1193-1200.
- MacLean, J. L., C. R. Lee, et al. (2004). "Anabolic and catabolic mRNA levels of the intervertebral disc vary with the magnitude and frequency of in vivo dynamic compression." Journal of Orthopaedic Research **22**(6): 1193-1200.
- Maggs, D. G., R. Jacob, et al. (1995). "Interstitial fluid concentrations of glycerol, glucose, and amino acids in human quadricep muscle and adipose tissue. Evidence for significant lipolysis in skeletal muscle." J Clin Invest **96**(1): 370-377.
- Maldonado, B. A. and T. R. Oegema, Jr. (1992). "Initial characterization of the metabolism of intervertebral disc cells encapsulated in microspheres." J Orthop Res **10**(5): 677-690.
- Marchand, F. and A. M. Ahmed (1990). "Investigation of the laminate structure of lumbar disc annulus fibrosus." Spine (Phila Pa 1976) **15**(5): 402-410.
- Maroudas, A. (1975). "Biophysical chemistry of cartilaginous tissues with special reference to solute and fluid transport." Biorheology **12**(3-4): 233-248.
- McEvoy, A. K., C. M. McDonagh, et al. (1996). "Dissolved oxygen sensor based on fluorescence quenching of oxygen-sensitive ruthenium complexes immobilized in sol-gel-derived porous silica coatings." Analyst **121**(6): 785-788.
- McNamara, K. P., X. P. Li, et al. (1998). "Fiber-optic oxygen sensor based on the fluorescence quenching of tris (5-acrylamido, 1,10 phenanthroline) ruthenium chloride." Analytica Chimica Acta **361**(1-2): 73-83.
- Meghji, P., J. D. Pearson, et al. (1992). "Regulation of extracellular adenosine production by ectonucleotidases of adult rat ventricular myocytes." Am J Physiol **263**(1 Pt 2): H40-47.
- Miele, M. and M. Fillenz (1996). "In vivo determination of extracellular brain ascorbate." J Neurosci Methods **70**(1): 15-19.
- Miller, J. A., C. Schmatz, et al. (1988). "Lumbar disc degeneration: correlation with age, sex, and spine level in 600 autopsy specimens." Spine (Phila Pa 1976) **13**(2): 173-178.

- Moore, R. J. (2006). "The vertebral endplate: disc degeneration, disc regeneration." Eur Spine J **15 Suppl 3**: S333-337.
- Morris, K. J., M. S. Roach, et al. (2007). "Luminescence lifetime standards for the nanosecond to microsecond range and oxygen quenching of ruthenium(II) complexes." Anal Chem **79**(24): 9310-9314.
- Murphy, L. J. and P. T. Galley (1994). "Measurement in-Vitro of Human Plasma Glycerol with a Hydrogen-Peroxide Detecting Microdialysis Enzyme Electrode." Anal Chem **66**(23): 4345-4353.
- N., B. (2005). Clinical Anatomy of the Lumbar Spine and Sacrum. Livingstone, Elsevier Churchill.
- Nerlich, A. G., E. D. Schleicher, et al. (1997). "1997 Volvo Award winner in basic science studies. Immunohistologic markers for age-related changes of human lumbar intervertebral discs." Spine (Phila Pa 1976) **22**(24): 2781-2795.
- North, R. A. (2002). "Molecular physiology of P2X receptors." Physiol Rev **82**(4): 1013-1067.
- O'Halloran, D. M. and A. S. Pandit (2007). "Tissue-engineering approach to regenerating the intervertebral disc." Tissue Eng **13**(8): 1927-1954.
- Oegema, T. R., Jr. (1993). "Biochemistry of the intervertebral disc." Clin Sports Med **12**(3): 419-439.
- Ohshima, H. and J. P. Urban (1992). "The effect of lactate and pH on proteoglycan and protein synthesis rates in the intervertebral disc." Spine (Phila Pa 1976) **17**(9): 1079-1082.
- Ohshima, H., J. P. Urban, et al. (1995). "Effect of static load on matrix synthesis rates in the intervertebral disc measured in vitro by a new perfusion technique." J Orthop Res **13**(1): 22-29.
- Panagiotacopoulos, N. D., M. H. Pope, et al. (1987). "Water-Content in Human Intervertebral Disks .1. Measurement by Magnetic-Resonance Imaging." Spine (Phila Pa 1976) **12**(9): 912-917.
- Panagiotacopoulos, N. D., M. H. Pope, et al. (1987). "Water content in human intervertebral discs. Part I. Measurement by magnetic resonance imaging." Spine (Phila Pa 1976) **12**(9): 912-917.

- Panjabi, M. M., M. H. Krag, et al. (1977). "Effects of preload on load displacement curves of the lumbar spine." Orthop Clin North Am **8**(1): 181-192.
- Pearce, R. H. (1993). Morphologic and Chemical Aspects of Aging. Musculoskeletal Soft-Tissue Aging: Impact on Mobility. D. O. Wood, Goldberg, V. M., Woo, S. L. Rosemont, IL, American Academy of Orthopaedic Surgeons: 363-379.
- Pearce, R. H., B. J. Grimmer, et al. (1987). "Degeneration and the chemical composition of the human lumbar intervertebral disc." Journal of Orthopaedic Research **5**(2): 198-205.
- Pellegatti, P., L. Raffaghello, et al. (2008). "Increased Level of Extracellular ATP at Tumor Sites: In Vivo Imaging with Plasma Membrane Luciferase." Plos One **3**(7).
- Peng, B. H., Shuxun; Shi, Qi and Jia, Lianshun (2001). "The relationship between cartilage end-plate calcification and disc degenerat ion: an experimental study." Chinese Medical Journal **114**(3): 308-312
- Prydz, K. and K. T. Dalen (2000). "Synthesis and sorting of proteoglycans - Commentary." Journal of Cell Science **113**(2): 193-205.
- Przedborski, S. and M. Vila (2001). "MPTP: a review of its mechanisms of neurotoxicity." Clinical Neuroscience Research **1**(6): 407-418.
- Raj, P. P. (2008). "Intervertebral disc: anatomy-physiology-pathophysiology-treatment." Pain Pract **8**(1): 18-44.
- Rice, M. E. (2000). "Ascorbate regulation and its neuroprotective role in the brain." Trends Neurosci **23**(5): 209-216.
- Roberts, J. P. U. S. (2003). "Degeneration of the intervertebral disc." Arthritis Res Ther **5**: 120-130.
- Roberts, S., S. Ayad, et al. (1991). "Immunolocalisation of type VI collagen in the intervertebral disc." Ann Rheum Dis **50**(11): 787-791.
- Romano, A. H. and T. Conway (1996). "Evolution of carbohydrate metabolic pathways." Res Microbiol **147**(6-7): 448-455.

- Rong, W. F., A. V. Gourine, et al. (2003). "Pivotal role of nucleotide P2X(2) receptor subunit of the ATP-gated ion channel mediating ventilatory responses to hypoxia." Journal of Neuroscience **23**(36): 11315-11321.
- Roughley, P. J. (2004). "Biology of intervertebral disc aging and degeneration: involvement of the extracellular matrix." Spine (Phila Pa 1976) **29**(23): 2691-2699.
- Ryan, L. M., I. V. Kurup, et al. (1992). "Atp-Induced Chondrocalcinosis." Arthritis and Rheumatism **35**(12): 1520-1525.
- Salvatierra, J. C., T. Y. Yuan, et al. (2011). "Difference in Energy Metabolism of Annulus Fibrosus and Nucleus Pulposus Cells of the Intervertebral Disc." Cell Mol Bioeng **4**(2): 302-310.
- Schneider, S. W., M. E. Egan, et al. (1999). "Continuous detection of extracellular ATP on living cells by using atomic force microscopy." Proc Natl Acad Sci U S A **96**(21): 12180-12185.
- Seminario-Vidal, L., E. R. Lazarowski, et al. (2009). "Assessment of extracellular ATP concentrations." Methods Mol Biol **574**: 25-36.
- Setton, L. A. and J. Chen (2006). "Mechanobiology of the Intervertebral Disc and Relevance to Disc Degeneration." The Journal of Bone & Joint Surgery **88**(suppl_2): 52-57.
- Siegel, G. J. (1999). Basic neurochemistry : molecular, cellular, and medical aspects. Philadelphia, Lippincott Williams & Wilkins.
- Silva, E. A. and D. J. Mooney (2004). "Synthetic extracellular matrices for tissue engineering and regeneration." Curr Top Dev Biol **64**: 181-205.
- Smith, L. J., N. L. Nerurkar, et al. (2011). "Degeneration and regeneration of the intervertebral disc: lessons from development." Disease Models & Mechanisms **4**(1): 31-41.
- Souslova, V., P. Cesare, et al. (2000). "Warm-coding deficits and aberrant inflammatory pain in mice lacking P2X(3) receptors." Nature **407**(6807): 1015-1017.

- Spielmann, H., U. Jacob-Müller, et al. (1981). "Simple assay of 0.1–1.0 pmol of ATP, ADP, and AMP in single somatic cells using purified luciferin luciferase." Analytical Biochemistry **113**(1): 172-178.
- Staub, F., A. Baethmann, et al. (1990). "Effects of lactacidosis on glial cell volume and viability." J Cereb Blood Flow Metab **10**(6): 866-876.
- Stephan, S., W. E. Johnson, et al. (2011). "The influence of nutrient supply and cell density on the growth and survival of intervertebral disc cells in 3D culture." Eur Cell Mater **22**: 97-108.
- Takagi, M., K.-I. Ohara, et al. (1995). "Effect of hydrostatic pressure on hybridoma cell metabolism." Journal of Fermentation and Bioengineering **80**(6): 619-621.
- Trautmann, A. (2009). "Extracellular ATP in the immune system: more than just a "danger signal"." Sci Signal **2**(56): pe6.
- Trout, J. J., J. A. Buckwalter, et al. (1982). "Ultrastructure of the human intervertebral disc. I. Changes in notochordal cells with age." Tissue Cell **14**(2): 359-369.
- Urban, J. P., S. Holm, et al. (1982). "Nutrition of the intervertebral disc: effect of fluid flow on solute transport." Clin Orthop Relat Res(170): 296-302.
- Urban, J. P. and A. Maroudas (1981). "Swelling of the intervertebral disc in vitro." Connect Tissue Res **9**(1): 1-10.
- Urban, J. P. and J. F. McMullin (1988). "Swelling pressure of the lumbar intervertebral discs: influence of age, spinal level, composition, and degeneration." Spine (Phila Pa 1976) **13**(2): 179-187.
- Urban, J. P. and S. Roberts (1995). "Development and degeneration of the intervertebral discs." Mol Med Today **1**(7): 329-335.
- Urban, J. P., S. Smith, et al. (2004). "Nutrition of the intervertebral disc." Spine (Phila Pa 1976) **29**(23): 2700-2709.
- Urban, J. P. G. and S. Roberts (2003). "Degeneration of the intervertebral disc." Arthritis Research & Therapy **5**(3): 120-130.
- Urban, J. P. G., S. Smith, et al. (2004). "Nutrition of the intervertebral disc." Spine (Phila Pa 1976) **29**(23): 2700-2709.

- Urban, M. R., J. C. T. Fairbank, et al. (2001). "Intervertebral Disc Composition in Neuromuscular Scoliosis: Changes in Cell Density and Glycosaminoglycan Concentration at the Curve Apex." Spine (Phila Pa 1976) **26**(6): 610-617.
- Vieira, V. P., J. B. T. Rocha, et al. (2001). "Heparin and chondroitin sulfate inhibit adenine nucleotide hydrolysis in liver and kidney membrane enriched fractions." International Journal of Biochemistry & Cell Biology **33**(12): 1193-1201.
- Vlaskovska, M., L. Kasakov, et al. (2001). "P2X(3) knock-out mice reveal a major sensory role for urothelially released ATP." Journal of Neuroscience **21**(15): 5670-5677.
- Walker, M. H. and D. G. Anderson (2004). "Molecular basis of intervertebral disc degeneration." Spine J **4**(6 Suppl): 158S-166S.
- Walsh, A. J. and J. C. Lotz (2004). "Biological response of the intervertebral disc to dynamic loading." J Biomech **37**(3): 329-337.
- Wang, C., C. Y. C. Huang, et al. (2013). "Optical ATP biosensor for extracellular ATP measurement." Biosensors and Bioelectronics **43**(0): 355-361.
- Willis, W. T. C. D. R. (2009). "Estimating Cost of Care for Patients With Acute Low Back Pain: A Retrospective Review of Patient Records." The Journal of the American Osteopathic Association **109**(4): 229-233.
- Wolfbeis, O. S., I. Oehme, et al. (2000). "Sol-gel based glucose biosensors employing optical oxygen transducers, and a method for compensating for variable oxygen background." Biosensors and Bioelectronics **15**(1-2): 69-76.
- Wu, J. J., D. R. Eyre, et al. (1987). "Type VI collagen of the intervertebral disc. Biochemical and electron-microscopic characterization of the native protein." Biochem J **248**(2): 373-381.
- Xiong, Y., J. Xu, et al. (2010). "Fiber-optic fluorescence sensor for dissolved oxygen detection based on fluorinated xerogel immobilized with ruthenium (II) complex." Journal of Sol-Gel Science and Technology **53**(2): 441-447.
- Yao, H. and W. Y. Gu (2004). "Physical signals and solute transport in cartilage under dynamic unconfined compression: finite element analysis." Ann Biomed Eng **32**(3): 380-390.

Yao, H. and W. Y. Gu (2007). "Three-dimensional inhomogeneous triphasic finite-element analysis of physical signals and solute transport in human intervertebral disc under axial compression." J Biomech **40**(9): 2071-2077.

